Tycho-Gaia and beyond: Combining data for precision astrometry

Michalik, Daniel

2015

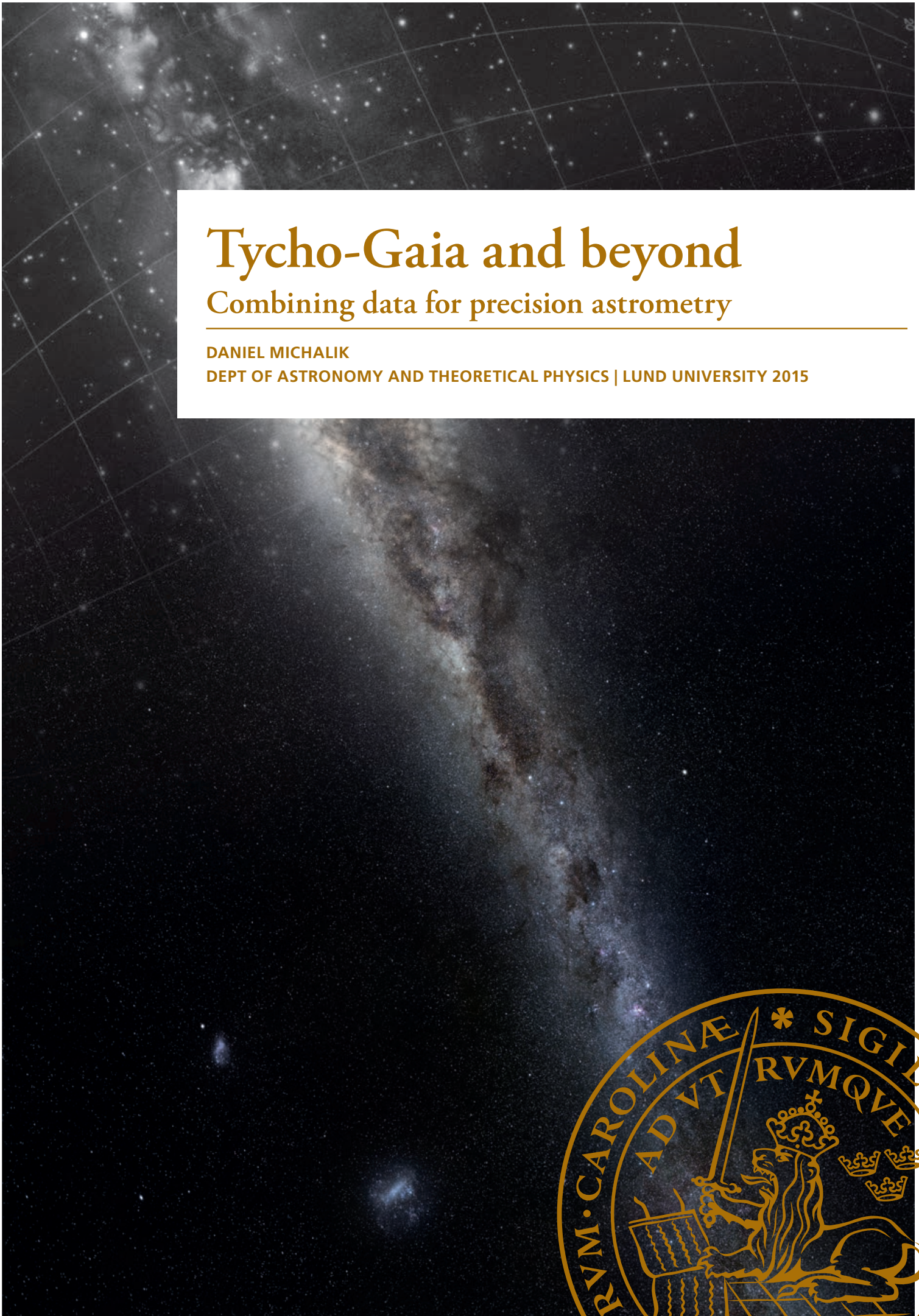

Tycho-Gaia and beyond

Combining data for precision astrometry

DANIEL MICHALIK
DEPT OF ASTRONOMY AND THEORETICAL PHYSICS | LUND UNIVERSITY 2015

Tycho-Gaia and beyond
Combining data for precision astrometry

Tycho-Gaia and beyond

Combining data for precision astrometry

by Daniel Michalik

LUND
UNIVERSITY

Thesis for the degree of Doctor of Philosophy
Thesis advisors: David Hobbs, Lennart Lindegren, Uwe Lammers
Faculty opponent: Coryn Bailer-Jones

To be presented, with the permission of the Faculty of Science of Lund University, for public criticism in the Lundmark lecture hall (Lundmarksalen) at the Department of Astronomy and Theoretical Physics on Saturday, the 28th of November 2015 at 14:00.

Organization
LUND UNIVERSITY

Department of Astronomy and Theoretical Physics
Box 43
SE–221 00 LUND
Sweden

Author(s)
Daniel Michalik

Document name
DOCTORAL DISSERTATION

Date of disputation
2015-11-28

Sponsoring organization

Title and subtitle
Tycho-Gaia and beyond: Combining data for precision astrometry

Abstract
Astrometry aims at producing a three-dimensional map of positions and motions of stars and other celestial bodies in a consistent coordinate system covering the whole sky. This is best done from space, which provides a way of scanning the entire sky by a single instrument in a thermally stable environment. Space astrometry was pioneered by the Hipparcos satellite (1989–1993), and the successor mission Gaia began nominal operations in mid-2014.

Determining a good astrometric solution for a star, i.e., all five astrometric parameters for its position, parallax and proper motion, requires a certain minimum stretch of observational data. The conditions for a good solution might not be met in the early phases of a space mission, for stars at the detection limit, or for transient objects such as supernovae. If the available observations are too few or do not span a sufficiently long time interval, additional constraints could be added to reduce the degrees of freedom of the mathematical problem. An example is the assumption that parallax and proper motion are exactly zero. Alternatively one can add prior information to lift the parameter degeneracy, at the cost of losing independence to external data.

This doctoral thesis discusses the incorporation of prior information in an astrometric solution of Gaia data, with the aim to improve our understanding of these data early in the mission. Prior information is taken from the Hipparcos and Tycho-2 catalogues as well as a Galactic model. The influence of a prior on the astrometric solution is discussed in detail and the feasibility of joint solutions is demonstrated through simulations of various combination scenarios.

One major result of the research work presented is the development and demonstration, through simulations, of a Tycho-Gaia Astrometric Solution (TGAS). Applied to real Gaia data it would allow us to obtain a full astrometric solution one year earlier than originally foreseen, with the additional benefit of long-baseline proper motion results.

Key words
astrometry, catalogue combination, detection of exo-planets, Gaia, joint solution, map of the Milky Way, positions, parallaxes, proper motions, Tycho-Gaia Astrometric Solution, Hundred Thousand Proper Motion project

Classification system and/or index terms (if any)

Supplementary bibliographical information

Language
English

ISSN and key title

ISBN
978-91-7623-546-1 (print)
978-91-7623-547-8 (pdf)

Recipient's notes

Number of pages
108

Price

Security classification

Signature _____ Date 2015-10-26

Tycho-Gaia and beyond

Combining data for precision astrometry

by Daniel Michalik

LUND
UNIVERSITY

A doctoral thesis at a university in Sweden takes either the form of a single, cohesive research study (monograph) or a summary of research papers (compilation thesis), which the doctoral student has written alone or together with one or several other author(s).

In the latter case the thesis consists of two parts. An introductory text puts the research work into context and summarizes the main points of the papers. Then, the research publications themselves are reproduced, together with a description of the individual contributions of the authors. The research papers may either have been already published or are manuscripts at various stages (in press, submitted, or in draft).

Cover illustration front: The Milky Way as seen from Earth, composed from two images.
Top: Lund Observatory Milky Way Panorama (1955, hand-drawn, Martin and Tatjana Kesküla)
Bottom: ESO Milky Way Panorama (2009, composite photograph, Serge Brunier)

Cover illustration back: Simulated Gaia astrometry of the Tycho-2 stars (Fig. 2 from Paper IV)

Funding information: The thesis work was financially supported by the European Space Agency, the Royal Physiographic Society of Lund, the Royal Swedish Academy of Sciences, and the Swedish National Space Board.

Faculty of Science, Department of Astronomy and Theoretical Physics

ISBN: 978-91-7623-546-1 (print)
ISBN: 978-91-7623-547-8 (pdf)
Series: LUNFD6/(NFAS-1048)/1-108/(2015)

Printed in Sweden by Media-Tryck, Lund University, Lund 2015

Dedicated to my siblings
Susanna – Matze – Johannes

Contents

List of publications

This thesis is based on the following publications, referred to by their Roman numerals:

I **Combining and Comparing Astrometric Data from Different Epochs: A Case Study with Hipparcos and Nano-JASMINE**

D. Michalik, L. Lindegren, D. Hobbs, U. Lammers, Y. Yamada (2012)
ASP Conference Series, Vol. 461, pp. 549–552

II **Improving distance estimates to nearby bright stars: Combining astrometric data from Hipparcos, Nano-JASMINE and Gaia**

D. Michalik, L. Lindegren, D. Hobbs, U. Lammers, Y. Yamada (2013)
IAU Symposium, Volume 289, pp. 414–417

III **Joint astrometric solution of Hipparcos and Gaia. A recipe for the Hundred Thousand Proper Motions project**

D. Michalik, L. Lindegren, D. Hobbs, U. Lammers (2014)
Astronomy & Astrophysics, Volume 571, A85, pp. 1–15

IV **The Tycho-Gaia astrometric solution. How to get 2.5 million parallaxes with less than one year of Gaia data**

D. Michalik, L. Lindegren, D. Hobbs (2015a)
Astronomy & Astrophysics, Volume 574, A115, pp. 1–8

V **Gaia astrometry for stars with too few observations. A Bayesian approach**

D. Michalik, L. Lindegren, D. Hobbs, A. G. Butkevich (2015b)
Astronomy & Astrophysics, Volume 583, A68, pp. 1–10

VI **Quasars can be used to verify the parallax zero-point of the Tycho-Gaia Astrometric Solution**

D. Michalik, L. Lindegren (2015)
Astronomy & Astrophysics, accepted October 2015, in press, 4 pages

Acknowledgements

My PhD student time in Lund was an interesting, rewarding, and sometimes challenging journey. I am lucky to have had the loving and caring support from friends and family throughout it and am grateful to all the wonderful people, who stood with me through the ups and downs of learning about research. Your support was invaluable.

This research project started one year before the PhD studies with a traineeship at the European Space Agency's centre in Madrid, Spain. This offered me the unique chance of becoming part of the Gaia core data processing team. Uwe, your exceptional mentorship and professional advice were invaluable for my development, and your efforts in shaping my career and finding the best-suited place for my research – and the funding for it – were most appreciated. You warned me that it wouldn't always be easy (and there was certainly some truth to that). Yet, it was an incredibly rewarding and fascinating time. Once in Lund I felt immediately welcome, and received nothing but excellent supervision. Lennart, you shared your tremendous expertise and immense experience with me. I learned so much from your friendly and focused work attitude, your patient explanations, and your constructive feedback. David, your understanding of the Gaia mission, its data, the simulations, and your kind help with so many details in my projects were indispensable. Thanks to all three of you for your guidance and support!

Sweden and Lund felt soon like home, thanks to the wonderful people here who were open and welcoming, and quickly became an important part of my life. Carro, Vidar, Liz, Martin, I share a lot of fantastic memories with you. Berry, one of the first people I met in Lund, I hope we will remain in contact for a long time. Emma, det är väl delvis ditt fel att jag pratar svenska nu! Johanna, really happy we have met – here is to many more festivals and adventures in Gothenburg! My back-then flatmate Chris, I hope you enjoy Canada, and my current flatmate Bert, glad that you are back and that we still have this wonderful fridge arrangement. Helene, you are an irreplaceable part of my life and I am immensely happy to share it with you. Your support with typographical advice, proofreading of my thesis, translations, and your patience with me throughout the final stretches mean a lot.

It is too easy to take a stimulating yet cosy work environment for granted, and to forget that it is the students and staff who shape it. Thank you to my colleagues and friends at Lund Observatory, too many for all to be named individually. Shout-out to the rest of the fabulous group of four, Michiel, Chiara, Alexey, I am glad to have started this great journey with you. Ewa, your friendliness when coming to work at morning was most delightful and made every day a little better! Eva and Mandana, you take such great care of the people in the department. Nils and Johan R., I am very happy you involved and supported me in teaching and telescope observations, I learned so much from it! Nels, I am incredibly sad that I did not know enough Swedish when I had the chance to actually

get to know you. The department still benefits from your clever constructions, and your skills inspired me to improve my own handiness. Sven, you helped me with that, patiently showing me how to fix and develop electronics, and teaching me some basics of soldering after-hours, from which I benefit both at work and at home. Similarly, Torbjörn, you contributed to me refining my practical skills and to gain confidence in setting up, using, and fixing observational equipment. Getting the 101 year old Astrograph telescope back into a usable shape together with you is a precious memory. Hampus, your patient support for my teaching-related (and also after-hours) projects was highly appreciated. In terms of observing I'd like to highlight Petter, Tryggvi, and Ryan, who often organized events and observations with me. Ross and Paul, your professional advice and the occasional beer with you was always great to have, and certainly helped to keep calm, especially at the end. To all the party people at the department, it is truly a blast celebrating the ups and downs of life with you, watching movies, playing ping pong, talking, dancing, and sharing this time.

My research project started with the ESA traineeship in Spain and continued as a split position. Especially during the first two years of my PhD studies I spent a significant fraction working in Spain, and always felt very welcome and at home. Many thanks to my friends in Madrid and my colleagues at ESAC, Marta, Wouter, Ana, Dennis, Paul W., Jorge, Michele, Ranpal, and all the other wonderful people who make ESAC such a great workplace.

Research is greatly facilitated by having competent colleagues and friends in other scientific institutes, such as the Gaia (AGIS) groups at ESAC, at ESTEC, in Dresden, Heidelberg, Nice, and Leiden. Very specifically, thank you for discussions, implementation help, advice, dinners and evenings out in town, to Alcione, Alex (B. and H.!), Alexey, Anthony, Emmanuel J., Gonzalo, Hagen, Hassan, John, Jos, Jose, Mercedes, Sebastian, Wil, and Sergei. Uli, you quickly became my diplomatic and strategic advisor, and always took time for questions and discussions, thank you. Finally, I would like to highlight our Japanese collaborators, in particular Yoshiyuki and Naoteru, who went out of their way to make us feel welcome in Japan. We are always happy to see you in Europe.

Working and studying abroad necessitates big changes. It requires family and friends who understand the situation, and who make an effort in keeping in touch and maintaining communication. I dearly loved having every single visitor, phone call, chat, or email, and the certainty that I am not forgotten far away from home. A shout-out to friends and family from Germany, especially to the people who came over for visits to Spain and Sweden. Peter, Dani, Hildegard, Ulrich, Sophie, Franzi, Anke, Sebastian, Conny, it was fantastic having you here and you are always welcome back!

To my parents Hanni and Wolfgang, and my siblings Susanna and Johannes, the biggest thank you for your continuous support and love. I love you, too. And to my brother Matthias, who inspired me in his love for Scandinavia, with his open mindset, his patience and kindness, and in making bold decisions to follow dreams; You will never be forgotten.

Popular summary in English

Introduction to astrometry

Objectives Astrometry is the research field within astronomy that deals with measuring where stars and other celestial objects are located. This may sound trivial at first, but the immense distances involved make astrometric measurements extremely difficult. One of the aims is to create a three-dimensional map of the stars' positions and motions in our Galaxy, the Milky Way. Think of it as a Galactic census that tells us where each star is, how it moves, and of which type it is, for many millions of stars. Such a catalogue can be used to understand what our Galaxy looks like, how it was formed, and how it will evolve in the future. And that's not all: just like a human census would not only list the adults but also the children, astrometry tries to also find planets and other companions around the stars that it measures. The currently ongoing Gaia mission, for example, is expected to discover tens of thousands of exo-planets (planets not orbiting our Sun, but other stars). Another aim of astrometry is to catalogue asteroids and their orbits in our own solar system – allowing us to keep track of even these small space rocks. Finally, astrometry determines the reference frame on the sky (the coordinate system for all other discoveries), based on a set of far-away bright galaxy cores (*quasars*). This information is, for example, necessary to be able to navigate in space.

Astrometry from space, 2013–2019: Gaia Astrometry is best done from space to avoid the distortions of light caused by the Earth's atmosphere, and to obtain a stable environment for observations. There are of course also ground-based projects, for example using radio telescopes, but for the purpose of this thesis we restrict our view to satellite data. The most recent milestone in astrometry was the 2013 launch of the European satellite *Gaia*. The European Space Agency ESA describes Gaia like this[1]: "Gaia will make the largest, most precise three-dimensional map of our Galaxy by surveying more than a thousand million stars. It is expected to discover hundreds of thousands of new celestial objects, such as exo-planets and brown dwarfs, and observe hundreds of thousands of asteroids within our own Solar System. The mission will also study about 500 000 distant quasars and will provide stringent new tests of Albert Einstein's General Theory of Relativity." Quite an exciting mission to be a part of!

Hipparcos (1989–1993) and the JASMINE satellite series Gaia is already the second space mission dedicated to astrometry, following the pioneering efforts of ESA with the Hipparcos satellite about 25 years ago. Hipparcos determined parallaxes, proper motions, and

[1] `http://www.esa.int/Our_Activities/Space_Science/Gaia_overview`

positions for some 100 000 stars. The spacecraft also employed an auxiliary starmapper instrument for attitude determination of the satellite, which observed the positions – but not the parallaxes and proper motions – of an additional 2.5 million stars, giving the Tycho-2 catalogue. More space astrometry missions are planned for the future. Amongst those are a series of Japanese satellites called Nano-JASMINE, Small-JASMINE, and JASMINE, with the goal of conducting observations in near-infrared wavelengths rather than in visible light. That is beneficial for observing towards the central regions of our Milky Way. Furthermore, the scientific community in Europe is already brainstorming about a successor to Gaia in a few decades time.

Principle of astrometric measurements

Astrometry uses a very simple principle: one measures where a star is seen on the celestial sphere (an imagined far-away shell that carries the stars around the Earth), and repeats these measurements many times over a timespan of years or decades. Imagine an infinitely far away star that does not move: it would always be seen in the same place on the celestial sphere. However, even though stars are very far away they are absolutely not *infinitely* far away, and they do move at an unknown speed and in an unknown direction, and that makes life of an astrometrist more difficult (and more interesting).

Distances to stars and their average position Distances to far away objects of unknown size are hard to measure, and without the distance a perceived speed cannot be translated into the real physical speed of an object either. One possible solution for directly measuring very large distances is to move the observer, and to compare the views from different observing locations. If one, for example, observes clouds from a flying aircraft, nearby clouds can be easily distinguished from distant clouds: neglecting for the time being the motions of the clouds themselves, the forward motion of the aircraft makes the nearby clouds *appear* to move quickly backwards while the distant clouds seem to almost stand still in the background. In astrometry we use our own Earth's motion around the Sun for a similar effect. Really far away stars seem to remain in the same place at all times during the year, while nearby stars seemingly move on elliptical paths. If one measures the size of the displacement one gets an estimation of the distance to the star (see Fig. 1 of the main thesis text). This type of distance determination is called *parallax measurement*. A star's location can then be described by three parameters: two angles to give its average position, and the parallax. The parallax is the (very small) angular displacement, caused by the finite distance to the star from us and the Earth's orbit around the Sun.

Proper motion of stars Stars never stand still but move, typically on a straight line at constant speed relative to the Sun. Therefore, in addition to the apparent displacement

stemming from the parallax, one can observe the star continuously and slowly moving along a line on the celestial sphere. This gives two more parameters to be astrometrically determined, describing the linear changes in stellar position. This is called the *proper motion* parameters. The third component of motion, the change of distance over time, is the so called radial velocity, the motion towards or away from the observer. Its effect is very small from an astrometric point of view, and the radial velocity is instead determined through a spectroscopic analysis of the star's light. Proper motion and parallax taken together cause a star to seemingly follow an elongated spiral track on the sky, with one loop per year of observations. Since all these effects are too small to be seen by the human eye, one needs extremely precise measurements instead.

The research project in a nutshell

In practice one does not observe a single star continuously for many years. Instead many stars are observed repeatedly, by a satellite that continuously scans the sky in all directions. If the satellite observes a star on average every few months, data processing needs to combine all its observations to derive the star's five astrometric parameters for position, parallax, and proper motion. That means reconstructing the perceived spiral paths of the stars on the sky as accurately as possible from their single observations. This requires at least five observations, at different times, for each star, but preferably many more should be acquired. The redundant observations help to better calibrate the instrumentation of the satellite and to determine more accurately its orientation in space (the so-called *spacecraft attitude*). They are also needed to discover, for example, exo-planets, which would otherwise remain undetected. Furthermore, the observations need to span sufficient time. The parallax effect causes an annually repeating elliptical displacement, and proper motion is a linear trend. The two effects can only be disentangled if observations span many months and preferably more than one year. This PhD thesis is part of a study of the data processing strategies of the Gaia mission. It explores how stars with only a few observations can be handled, so that the ambiguity between parallax and proper motion is overcome. In these cases one needs to use additional knowledge (*prior information*) to make the astrometric solution of Gaia possible.

In this thesis six research papers are presented, showing different ways of deriving prior information, and demonstrating the principle of catalogue combination in astrometry in different situations. Papers I and II are case studies which were presented at astronomy conferences. They demonstrate the principle of combining catalogues by directly integrating prior information in the data processing of an astrometry satellite. Paper I shows how Nano-JASMINE's proper motions can be improved through the incorporation of Hipparcos data, and Paper II extends this scenario with a simulated Gaia catalogue providing additional reference points. In subsequent work we focused however on improving early Gaia

datasets. Integrating the Hipparcos data yields updated (long-baseline) proper motions for the approximately 100 000 Hipparcos stars (the *Hundred Thousand Proper Motion project*; HTPM). This scenario is explored in Paper III which also gives a detailed description of the incorporation method and its properties. HTPM has a one significant drawback by not containing a sufficient number of stars for a complete and independent astrometric solution. This limitation leads to systematically wrong estimates of the astrometric results of the HTPM stars. Paper IV shows how this limitation can be eradicated by adding the 2.5 million stars from the Tycho-2 catalogue with their former positions as prior information. This joint *Tycho-Gaia Astrometric Solution* (TGAS) provides enough coverage of the celestial sphere to avoid the bias inherent in the HTPM project; it is one of the major achievements of this thesis work. Finally, we explored the use of generic prior information, that is constraints to the astrometric parameters in the solution based on the expected properties of stars in our Galaxy (Paper V). This method can be applied even to extragalactic sources such as quasars, which allows us to make an independent check of the parallax results in the TGAS project (Paper VI).

More figures related to the research work, and pictures of the satellites, can be found in the conference posters in Appendix A and in the main text of the thesis.

Populärwissenschaftliche Zusammenfassung auf Deutsch

Einführung in die Astrometrie

Ziele Astrometrie ist das Forschungsfeld der Astronomie, das sich mit der Vermessung der Positionen von Sternen und anderen Himmelskörpern beschäftigt. Das klingt zunächst vielleicht trivial, aber die unglaublich großen Entfernungen machen astrometrische Messungen äußerst schwierig. Eins der Ziele ist es, eine dreidimensionale Karte der Stern-Positionen und -Bewegungen in unserer Galaxie, der Milchstraße, zu erstellen. Quasi eine Art galaktischer Volkszählung, die uns sagt wo sich jeder Stern befindet, wie er sich bewegt, und von welchem Typ er ist, für viele Millionen von Sternen. Ein solcher Katalog kann verwendet werden, um zu verstehen wie unsere Galaxie aussieht, wie sie sich gebildet hat, und wie sie sich in Zukunft weiterentwickeln wird. Und das ist noch nicht alles: Genau wie eine menschliche Volkszählung nicht nur die Erwachsenen sondern auch die Kinder auflisten würde, versucht die Astrometrie auch Planeten und andere Begleiter der vermessenen Sterne zu finden. Zum Beispiel wird erwartet, dass die derzeit laufende Gaia-Mission zehntausende von Exo-Planeten (Planeten die nicht um die Sonne, sondern um andere Sterne kreisen) entdecken wird. Ein weiteres Ziel der Astrometrie ist das Katalogisieren von Asteroiden und ihren Bahnen in unserem eigenen Sonnensystem – das gibt uns die Möglichkeit, auch diese kleinen Steine im Weltall im Blick zu behalten. Schlussendlich bestimmt Astrometrie auch einen Referenzrahmen am Himmel (das Koordinatensystem für alle weiteren Entdeckungen), basierend auf weit entfernten leuchtstarken Kernen von Galaxien (genannt *Quasare*). Diese Referenz ist zum Beispiel notwendig um im Weltall navigieren zu können.

Astrometrie vom Weltraum, 2013–2019: Gaia Astrometrie wird am besten vom Weltraum aus betrieben, um den störenden Einfluss der Erdatmosphäre zu vermeiden, und weil der Weltraum eine stabilere Umgebung für Beobachtungen bietet. Es gibt auch erdgebundene Projekte, zum Beispiel unter Verwendung von Radio-Teleskopen, aber in dieser Arbeit beschränken wir unseren Blick auf Satellitendaten. Der jüngste Meilenstein in der Astrometrie war der Raketenstart des europäischen Satelliten *Gaia* Ende 2013. Die europäische Raumfahrtagentur ESA beschreibt die Gaia-Mission etwa so (siehe englische Fassung für das Original-Zitat): „Gaia wird die größte, präziseste dreidimensionale Karte unserer Galaxie erstellen, durch die Vermessung von mehr als einer Milliarde Sterne. Man erwartet, dass Hunderttausende von neuen Himmelskörpern wie zum Beispiel Exo-Planeten und braune Zwergen entdeckt und hunderttausende Asteroiden in unserem Sonnensystem beobachtet werden. Die Gaia-Mission wird auch etwa 500 000 weit entfernte Quasare beobachten und Albert Einsteins Allgemeine Relativitätstheorie neuen, strengen Tests unterwerfen.“ Fantastisch, Teil einer so spannenden Mission zu sein.

Hipparcos (1989–1993) und die JASMINE Satelliten-Reihe Gaia ist bereits die zweite Weltraummission, die ausschließlich der Astrometrie gewidmet ist, und folgt den bahnbrechenden Fortschritten, die ESA mit dem Hipparcos-Satelliten vor etwa 25 Jahren gemacht hat. Hipparcos hat Parallaxen, Eigenbewegungen und Positionen von etwa 100 000 Sternen bestimmt. Der Satellit verfügte außerdem über ein Hilfsinstrument (Englisch: *starmapper*) zur Bestimmung seiner Ausrichtung im Weltall, mit dessen Hilfe die Positionen – nicht aber die Parallaxen und Eigenbewegungen – von weiteren 2,5 Millionen Sternen beobachtet wurden. Dies resultierte in einem Katalog, der Tycho-2 genannt wird. Weitere Astrometrie-Missionen sind für die Zukunft geplant. Unter diesen befinden sich die japanischen Satelliten Nano-JASMINE, Small-JASMINE und JASMINE, die auf Beobachtungen im nahen infraroten Wellenlängenbereich anstelle von sichtbarem Licht ausgerichtet sind. Dies ist besser geeignet, um die zentralen Regionen unserer Milchstraße zu beobachten. Außerdem denkt die wissenschaftliche Gemeinschaft in Europa bereits über einen Gaia-Nachfolger in einigen Jahrzehnten nach.

Prinzip astrometrischer Beobachtungen

Astrometrie nutzt ein sehr einfaches Prinzip aus: Man misst, wo sich ein Stern auf der Himmelskugel (eine gedachte, weit entfernte Kugel um die Erde, auf der die Sterne liegen) befindet und wiederholt die Messungen viele Male über einen Zeitraum von Jahren oder Jahrzehnten. Einen unendlich weit entfernten stillstehenden Stern würde man immer an der gleichen Stelle auf der Himmelskugel sehen. Obwohl doch Sterne sehr weit weg sind, so sind sie doch definitiv nicht *unendlich* weit entfernt und bewegen sich mit einer unbekannten Geschwindigkeit und in eine unbekannte Richtung, und es ist genau das, was den Astrometrikern das Leben schwerer (und interessanter) macht.

Entfernungen zu Sternen und ihre mittlere Position Entfernungen zu weit entfernten Objekten von unbekannter Größe sind schwierig zu messen, und ohne die Entfernung kann man die scheinbare Geschwindigkeit nicht in die reale physikalische Geschwindigkeit eines Objekts übersetzen. Eine mögliche Lösung für die direkte Messungen von sehr großen Entfernungen ist es, den Betrachter zu bewegen und die Ergebnisse von verschiedenen Beobachtungsstellen aus zu vergleichen. Wenn man beispielsweise von einem Flugzeug aus Wolken beobachtet, können Wolken in der Nähe leicht von weit entfernten Wolken unterschieden werden. Unter Vernachlässigung der Bewegungen der Wolken selbst verursacht die Vorwärtsbewegung des Flugzeugs, dass nahe gelegene Wolken sich schnell rückwärts zu bewegen *scheinen*, während weit entfernte Wolken so wirken, als stünden sie stationär im Hintergrund. In der Astrometrie nutzen wir die Umlaufbahn der Erde um die Sonne für einen ähnlichen Effekt. Wirklich weit entfernte Sterne scheinen das ganze Jahr an der gleichen Stelle zu verbleiben, während nahe gelegene Sterne scheinbar elliptischen Bahnen

folgen. Wenn man die Größe der Verschiebung misst, erhält man eine Abschätzung der Entfernung zum Stern (siehe Abbildung *Figure 1* im Hauptteil der Doktorarbeit). Diese Art der Abstandsbestimmung wird als *Parallaxenmessungen* bezeichnet. Eine Stern-Position kann dann durch drei Größenangaben beschrieben werden: zwei Winkel, die die durchschnittliche Sternposition am Himmel angeben, und die Parallaxe. Die Parallaxe ist die (sehr kleine) Winkelverschiebung, die durch die endliche Entfernung des Sterns und den Umlauf der Erde um die Sonne verursacht wird.

Eigenbewegung von Sternen Sterne stehen jedoch nie still, sondern bewegen sich (in der Regel) geradlinig und mit konstanter Geschwindigkeit relativ zur Sonne. Zusätzlich zu der scheinbaren Verschiebung durch den Parallaxen-Effekt kann man also beobachten, wie sich ein Stern langsam und beständig auf einer Linie am Himmel vorwärts bewegt. Dies bedeutet, dass zwei zusätzliche Größen astrometrisch bestimmt werden müssen, und zwar die lineare Veränderung der Sternposition. Diese wird *Eigenbewegung* (Englisch: *proper motion*) genannt. Die dritte Bewegungskomponente, die Abstandsveränderung, ist die sogenannte Radialgeschwindigkeit, also die Bewegung zum Beobachter oder vom Beobachter weg. Ihr Effekt ist aus astrometrischer Sicht vernachlässigbar klein, die Radialgeschwindigkeit wird stattdessen durch eine spektroskopische Untersuchung des Sternlichts bestimmt. Eigenbewegung und Parallaxe zusammengenommen verursachen dass ein Stern scheinbar einer langgezogenen Spirale am Himmel folgt, mit einer Spiralschlinge pro Beobachtungs-Jahr. Da all diese Effekte zu klein sind als dass ein menschliches Auge sie sehen könnte, benötigt man stattdessen hochgenaue Messungen.

Das Forschungsprojekt in Kürze

In der Praxis beobachtet man nicht einen einzelnen Stern für viele Jahre. Stattdessen beobachtet man viele Sterne einen nach dem anderen mit einem Satelliten der kontinuierlich den gesamten Himmel abtastet. Wenn der Satellit einen Stern im Durchschnitt alle paar Monate beobachtet, ist es Aufgabe der Datenverarbeitung alle seine Beobachtungen zu kombinieren, um die fünf astrometrischen Stern-Parameter für Position, Parallaxe und Eigenbewegung abzuleiten. Das bedeutet, die scheinbaren Spiralbahnen der Sterne auf dem Himmel so genau wie möglich aus deren Einzelbeobachtungen zu rekonstruieren. Dies erfordert mindestens fünf Beobachtungen pro Stern, zu verschiedenen Zeitpunkten, deutlich mehr sind jedoch wünschenswert. Die zusätzlichen Beobachtungen helfen, die Instrumentierung des Satelliten besser zu kalibrieren und seine Ausrichtung (Englisch: *spacecraft attitude*) im Weltraum genauer zu bestimmen. Sie werden auch gebraucht, um zum Beispiel Exo-Planeten zu entdecken; diese blieben andernfalls unerkannt. Des Weiteren müssen die Beobachtungen einen genügend langen Zeitraum abdecken. Die Parallaxe bewirkt eine sich jährlich wiederholende elliptische Verschiebung, und die Eigenbewegung ist ein

linearer Trend. Die zwei Effekte können nur voneinander unterschieden werden, wenn sich Beobachtungen über viele Monate erstrecken, am besten sogar über mehr als ein Jahr. Diese Doktorarbeit ist Teil einer Studie der Datenverarbeitungsstrategien für Gaia. Sie erforscht wie Sterne mit nur wenigen Beobachtungen behandelt werden können, damit die Mehrdeutigkeit zwischen Parallaxe und Eigenbewegung überwunden wird. In solchen Fällen muss man zusätzliche Vorab-Informationen (Englisch: *prior information*) verwenden, um die astrometrische Lösung der Gaia-Beobachtungen möglich zu machen.

In dieser Arbeit werden sechs Forschungsartikel vorgestellt, die sich mit verschiedenen Wegen beschäftigen, Vorab-Informationen abzuleiten, und die das Prinzip von astrometrischen Katalogkombination in verschiedenen Situationen demonstrieren. Artikel I und II sind Fallstudien, die auf Astronomiekonferenzen vorgestellt wurden. Sie zeigen das Prinzip der Katalogkombination durch die direkte Integration von Vorab-Informationen in der Datenanalyse eines Astrometrie-Satelliten. Artikel I zeigt, wie Nano-JASMINEs Eigenbewegungen durch die Integration von Hipparcos-Daten verbessert werden können, und Artikel II erweitert das Szenario um einen simulierten Gaia-Katalog, der weitere Referenz-Punkte hinzufügt. Im Weiteren konzentrierten wir uns jedoch auf Verbesserungen der ersten Gaia-Datensätze. Integriert man die Hipparcos-Daten, erhält man aktualisierte (Langzeit-)Eigenbewegungen für die circa 100 000 Hipparcos-Sterne (Englisch: *Hundred Thousand Proper Motion project*, HTPM; zu Deutsch etwa: Das Hunderttausend-Eigenbewegungen-Projekt). Dieses Szenario wird in Artikel III untersucht, welcher im Detail die Integrationsmethode und ihre Eigenschaften beschreibt. HTPM hat einen großen Nachteil: Es enthält nicht genügend Sterne für eine vollständige und unabhängige astrometrische Lösung. Diese Einschränkung verursacht systematische Abweichungen in den Ergebniswerten der HTPM-Sterne. Artikel IV zeigt, wie diese Einschränkung beseitigt werden kann, indem man zusätzlich die 2.5 Millionen Sterne des Tycho-2 Katalogs verwendet, und ihre damaligen Positionen als Vorab-Information hinzufügt. Diese gemeinsame Tycho-Gaia-Lösung (Englisch: *Tycho-Gaia Astrometric Solution*, TGAS) enthält genug Himmelsabdeckung, um die verzerrten Werte in HTPM zu vermeiden; sie stellt eine der wichtigsten Errungenschaften dieser Doktorarbeit dar. Zu guter Letzt erforschten wir die Verwendung generischer Vorab-Informationen, das heißt Beschränkungen der astrometrischen Parameter in der Lösung basierend auf den erwarteten Werten für Sterne in unserer Galaxie (Artikel V). Diese Methode kann auch für extragalaktische Quellen wie Quasare verwendet werden und ermöglicht es, die Parallaxen-Werte im TGAS-Projekt unabhängig zu überprüfen (Artikel VI).

Weitere Abbildungen im Zusammenhang mit der Forschungsarbeit, und Bilder der verwendeten Satelliten, sind auf den Konferenz-Postern im Appendix A sowie im Hauptteil der Doktorarbeit zu finden.

Populärvetenskaplig sammanfattning på svenska

Introduktion till astrometri

Syfte Astrometri är forskningsfältet inom astronomin som behandlar mätningar av var stjärnor och andra himlakroppar befinner sig. Detta låter kanske trivialt, men avstånden det handlar om är oerhört stora, vilket gör astrometriska mätningar ytterst svåra. Ett av syftena är att skapa en tredimensionell karta över stjärnornas positioner och rörelser i vår galax, Vintergatan. Man kan se det som en galaktisk folkräkning, som berättar var varje stjärna befinner sig, hur den rör sig, och vilken typ det är, för miljontals stjärnor. En sådan katalog kan användas för att förstå hur vår galax ser ut, hur den bildats och hur den kommer att utvecklas i framtiden. Men det är inte allt: precis som en folkräkning inte bara skulle förteckna de vuxna utan även barnen, försöker man med astrometri även hitta planeter och andra följeslagare till de uppmätta stjärnora. Det just nu pågående Gaia-projektet, till exempel, förväntas upptäcka tiotusentals exoplaneter (planeter som inte kretsar kring vår sol men kring andra stjärnor). Ett annat syfte med astrometri är att katalogisera asteroider och deras banor i vårt eget solsystem – detta ger oss möjlighet att hålla koll även på dessa små rymdstenar. Slutligen skapar astrometri även en referensram på himlen (ett koordinatsystem för alla andra upptäckter), baserat på ett antal avlägsna ljusa galaxkärnor (*kvasarer*). Denna referensram är till exempel nödvändig för att kunna navigera i rymden.

Astrometri från rymden, 2013–2019: Gaia Astrometri bedrivs bäst från rymden för att undvika störningar från jordens atmosfär och dessutom ger rymden en stabil miljö för observationer. Det finns även markbaserade projekt, till exempel med hjälp av radioteleskop, men i detta arbete begränsar vi oss till satellitdata. Den senaste milstolpen i astrometri var uppskjutningen av den europeiska satelliten *Gaia* i slutet av 2013. Den europeiska rymdorganisationen ESA beskriver Gaias uppdrag så här (se engelsk version för det ursprungliga citatet): ”Gaia kommer att skapa den största, mest exakta, tredimensionella kartan av vår galax genom att mäta mer än en miljard stjärnor. Förväntningarna är att man ska upptäcka hundratusentals nya himlakroppar, som t.ex. exoplaneter och bruna dvärgar, och att hundratusentals asteroider kommer att observeras i vårt solsystem. Gaia kommer även att observera ca 500 000 avlägsna kvasarer och utsätta Albert Einsteins allmänna relativitetsteori för nya, rigorösa tester.” Ett fantastiskt projekt att få vara delaktig i!

Hipparcos (1989–1993) och satellitserien JASMINE Gaia är redan det andra rymdprojektet som helt ägnas åt astrometri, efter de banbrytande framsteg som ESA gjorde med Hipparcos-satelliten för cirka 25 år sedan. Hipparcos fastställde parallaxer, egenrörelser och positioner för cirka 100 000 stjärnor. Satelliten hade ett hjälpinstrument (på engelska: *starmapper*) för bestämning av dess inriktning i rymden, med vars hjälp man mätte positioner – men

inte parallaxer och egenrörelser – för ytterligare 2,5 miljoner stjärnor. Detta resulterade i en katalog som kallas Tycho-2. Fler astrometriprojekt är planerade för framtiden. Bland dem finns de japanska satelliterna Nano-JASMINE, Small-JASMINE, och JASMINE, vars syfte är att genomföra observationer i det nära-infraröda våglängdsområdet, istället för i synligt ljus. Detta är fördelaktigt för att observera de centrala delarna av vår Vintergata. Vidare funderar vetenskapssamfundet i Europa redan på en efterföljare till Gaia under de närmaste decennierna.

Principen för astrometriska mätningar

Astrometri använder sig av en mycket enkel princip: man mäter var en stjärna syns på himmelssfären (ett tänkt skal långt bort, som bär upp stjärnorna kring jorden), och upprepar dessa mätningar många gånger under ett tidsintervall av flera år eller årtionden. Föreställ er en orörlig stjärna oändligt långt bort: den skulle alltid synas på samma ställe på himmelssfären. Men även om stjärnorna är mycket långt borta så är de definitivt inte *oändligt* långt bort, och de rör sig med en okänd hastighet i en okänd riktning, och det är precis detta som gör en astrometrikers liv svårare (och intressantare).

Avstånden till stjärnor och deras genomsnittliga positioner Avstånden till avlägsna objekt av okänd storlek är svåra att mäta, och utan avståndet kan den skenbara hastigheten inte översättas till den verkliga, fysikaliska hastigheten hos objektet. En lösning för att direkt mäta mycket stora avstånd är att flytta observatören och jämföra resultaten från olika platser. Om man exempelvis observerar moln från ett flygplan, kan närbelägna moln lätt skiljas från avlägsna. Vi bortser här från molnens egna rörelser. Flygplanets rörelse framåt gör att de närbelägna molnen *verkar* röra sig snabbt bakåt medan avlägsna moln tycks stå stilla i bakgrunden. I astrometrin använder vi istället vår jords rörelse runt solen för att uppnå en liknande effekt. Stjärnor som befinner sig verkligt långt borta tycks befinna sig på samma plats under hela året, medan mer närbelägna stjärnor ser ut att röra sig i elliptiska banor. Genom att mäta denna förskjutning får man en uppskattning av avståndet till stjärnan (se *Figure 1* i huvuddelen av avhandlingen). Denna slags avståndsbestämning kallas *parallaxmätning*. En stjärnas läge kan då beskrivas med tre storheter: två vinklar som ger stjärnans genomsnittliga position på himlen, och parallaxen. Parallaxen är den (väldigt lilla) vinkelförskjutning som uppstår på grund av stjärnans ändliga avstånd och jordens omlopp kring solen.

Stjärnors egenrörelse Stjärnor står dock inte stilla utan rör sig som regel i en rät linje med konstant hastighet i förhållande till solen. Förutom den skenbara förskjutningen på grund av parallaxeffekten kan man alltså se hur en stjärna rör sig kontinuerligt och långsamt längs en linje på himmelssfären. Detta ger ytterligare två storheter att fastställa astrometriskt,

nämligen de linjära förändringarna i stjärnpositionen. Detta kallas *egenrörelse* (på engelska: *proper motion*). Den tredje rörelsekomponenten, förändringen i avstånd över tiden, är den så kallade radialhastigheten, alltså rörelsen mot eller bort från observatören. Dess effekt är ur astrometrisk synpunkt väldigt liten, och radialhastigheten fastställs istället genom spektroskopisk undersökning av stjärnans ljus. Egenrörelse och parallax tillsammans gör att en stjärna ser ut att följa en utdragen spiral på himlen, med en ögla i spiralslingan för varje år av observationer. Eftersom alla dessa effekter är alltför små för att uppfattas av det mänskliga ögat, krävs i stället extremt noggranna mätningar.

Forskningsprojektet i korthet

I praktiken observerar man inte en enskild stjärna ständigt under många år. Istället observeras många stjärnor vid upprepade tillfällen av en satellit som kontinuerligt avsöker himlen i alla riktningar. Om satelliten observerar en stjärna i genomsnitt varannan månad, ska databehandlingen kombinera alla dessa observationer för att härleda de fem astrometriska parametrarna för stjärnans position, parallax och egenrörelse. Det innebär att stjärnornas skenbara spiralspår på himlen måste rekonstrueras så exakt som möjligt från de enskilda observationerna. Detta kräver minst fem observationer, vid olika tidpunkter, för varje stjärna, men helst betydligt fler. De extra observationerna hjälper till att bättre kalibrera satellitens instrument och mer exakt fastställa dess inriktning i rymden (på engelska: *spacecraft attitude*), men behövs också för att exempelvis upptäcka stjärnor med planeter, som annars inte skulle märkas. Dessutom måste observationerna sträcka sig över tillräckligt lång tid. Parallaxen orsakar en årligen upprepad elliptisk förskjutning, och egenrörelsen en linjär trend. De två effekterna kan bara särskiljas om observationerna spänner över ett antal månader, och helst betydligt mer än ett år. Denna avhandling ingår i en studie av databehandlingsstrategier för Gaia. Den undersöker hur stjärnor med bara ett fåtal observationer kan hanteras, så att mångtydigheten mellan parallax och egenrörelse övervinns. I dessa fall är det nödvändigt att införa viss förhandsinformation (på engelska: *prior information*) för att möjliggöra en astrometrisk lösning av Gaia-observationerna.

I avhandlingen framläggs sex vetenskapliga artiklar som visar på olika sätt att härleda förhandsinformation, och som demonstrerar principen för kombination av astrometriska kataloger i olika situationer. Artikel I och II är fallstudier som presenterats vid astronomiska konferenser. De visar principen för katalogkombination genom direkt inkorporering av förhandsinformation i databehandlingen för en astrometrisatellit. Artikel I visar hur egenrörelser från Nano-JASMINE kan förbättras genom att inkorporera data från Hipparcos, och Artikel II utvidgar detta scenario med en simulerad Gaia-katalog för att lägga till ytterligare referenspunkter. I det fortsatta arbetet fokuserade vi dock på att förbättra tidiga uppsättningar av data från Gaia. Inkorporering av Hipparcos-data ger förbättrade egenrörelser för ca 100 000 Hipparcos-stjärnor (på engelska: *Hundred Thousand Proper Motion project*,

HTPM; på svenska ungefär: ”hundratusen egenrörelser”-projektet). Detta scenario utforskas i Artikel III, som även i detalj beskriver inkorporeringsmetoden och dess egenskaper. HTPM har en betydande nackdel i att inte omfatta ett tillräckligt stort antal stjärnor för en helt oberoende astrometrisk lösning. Denna begränsning leder till systematiska fel i de astrometriska resultaten för HTPM-stjärnorna. Artikel IV visar hur man kan avlägsna denna begränsning genom att även använda de 2,5 miljoner stjärnorna från Tycho-2-katalogen och införa deras dåvarande positioner som förhandsinformation. Denna gemensamma Tycho-Gaia-lösning (på engelska: *Tycho-Gaia Astrometric Solution*, TGAS) ger tillräckligt täckning av himmelssfären för att undvika den inneboende skevheten i HTPM-projektet, och utgör ett av de viktigaste resultaten i denna avhandling. Slutligen har vi utforskat användningen av generisk förhandsinformation, dvs. begränsningar av de astrometriska storheterna i lösningen, baserade på förväntade egenskaper hos stjärnor i vår galax (Artikel V). Den här metoden kan även tillämpas på extragalaktiska objekt som kvasarer, vilket möjliggör en oberoende verifiering av parallaxresultaten i TGAS-projektet (Artikel VI).

Mer grafik relaterad till forskningsarbetet, och bilder av satelliterna, finns i konferansaffischerna i Appendix A samt i huvuddelen av avhandlingen.

Tycho-Gaia and beyond: Combining data for precision astrometry

1 Astrometry – how and why?

1.1 Introduction

Astrometry refers to the precise measurement of the positions and motions of celestial objects (such as planets, asteroids, stars, and galaxies, here-after jointly called *sources*). One repeatedly measures the instantaneous direction towards an object on the celestial sphere and analyses how it changes over time. In the absence of additional perturbations and neglecting the Galactic acceleration, the motion of any object outside of our Solar System can be assumed to be uniform and linear. The motion component towards or away from the observer is called the radial velocity and typically determined through spectroscopy. It is thus neglected for the time being. The component perpendicular to the observation direction is the *proper motion*, and measured by the change in right ascension and declination over time. For a moving observer (say, an observer on the Earth orbiting around the Sun), observations of the actual physical motion of a celestial body are overlaid with the *trigonometric parallax effect*. That is the perceived shift of an object's position at a finite distance seen from different places in the observer's orbit. Seemingly this follows an elliptical displacement over the course of a year, compared to far-away background stars (see Fig. 1). The semi-major axis of the parallax ellipse depends on the size of the observer's orbit and the distance to the star. Together, parallax and proper motion give an apparent spiral path of an object on the sky, and a star's position is given as one point on this path, referring to a specific reference epoch. Together, the two position components, the parallax value, and the two proper motion components form the basic set of five astrometric parameters. Complemented by the spectroscopic radial velocity, they give three-dimensional positions and velocity information, basically a kinematic map of the stellar contents of the Galaxy.

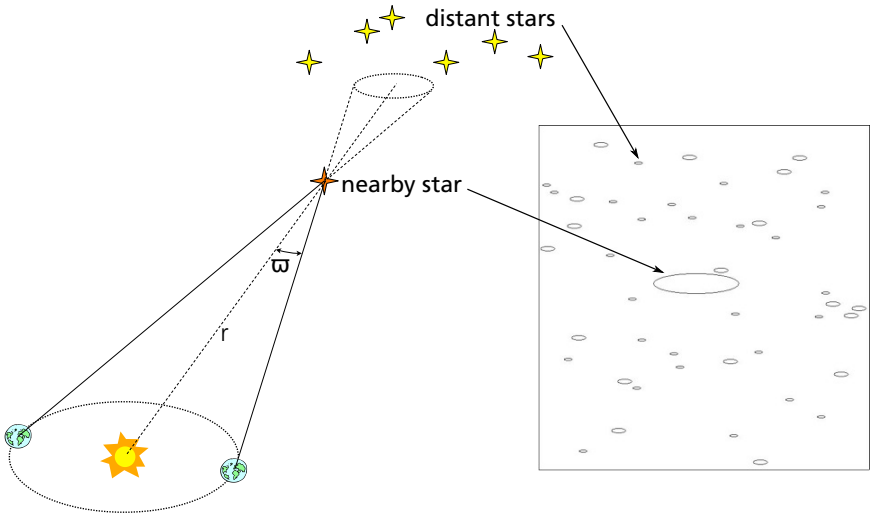

Figure 1: Illustration of the parallax effect. (Figure: Lindegren & Michalik)

1.2 Objectives of astrometry

Astrometric observations provide fundamental data for a wide range of astrophysical studies (for detailed discussions see, e.g., van Altena 2013). Accurate distances and motions of large numbers of stars allow us to derive a better understanding of the structure and kinematics of our Galaxy. Advances in stellar evolution require the determination of intrinsic stellar properties such as luminosity, which relies on accurate distances. Small deviations of the uniform linear motion of a star allow us to detect invisible binary components and exoplanets. Astrometric measurements within our Solar System are used to determine accurate orbits of asteroids (and comets), needed to predict their future positions, e.g. for stellar occultations, and to understand the dynamics of the Solar System. Observations of far-away extra-galactic objects (such as quasars, see Sects. 3.2 and 4.5) define a reference frame for other observations and space navigation. Astrometry also provides a stringent test for general relativistic effects, such as light bending around massive objects. The trigonometric parallaxes are arguably the most important of the astrometric parameters, since they are the only direct way of measuring distances outside of our Solar System. Parallaxes constitute the first rung of the cosmological distance ladder and are used, directly or indirectly, to calibrate further steps, such as distance determination based on main sequence fitting, Cepheids, and RR Lyrae- and Mira-type variables.

1.3 Challenges of modern astrometry

Our Galaxy is at least some 30 kpc across. Galactic research spanning a significant fraction of the whole Galaxy thus corresponds to parallaxes of some 30–100 μas. Determining such small parallaxes to within, say, 10% gives an accuracy requirement of a few up to a few tens of μas. This is extremely difficult to achieve in practice, and requires great care in mission

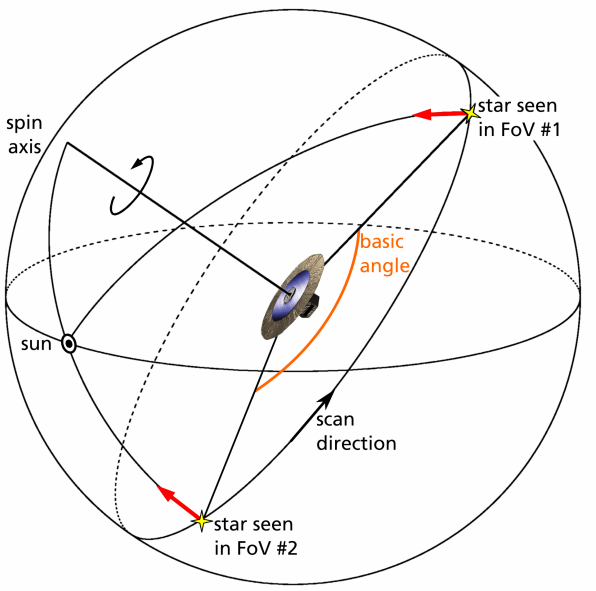

Figure 2: The parallax displacement (red arrows) is different in the two fields-of-view (FoV), allowing us to measure absolute parallaxes. (Figure: Lindegren & Michalik)

design and data analysis. Calibration of spacecraft attitude and the geometry of the optical instrument becomes immensely important. The mechanical and thermal design needs extra care to ensure that the mirrors are stable with accuracies better than nano-meters. Data processing requires highly accurate modelling of the instrument and of all perturbations, including relativistic effects in the light propagation from source to instrument, as well as of the barycentric motion of the satellite. Assuming all these can be overcome, one needs to start considering astrophysical limitations to the measurements, such as variations of the photocentre of a source caused by starspots (in case of stellar sources), or variations in the structure (in case of extra-galactic sources).

1.4 Absolute parallaxes through global astrometry

Astrometry can be done in a narrow field-of-view by measuring the instantaneous positions of stars relative to reference stars. This is routinely done from the ground and often in the near-infrared. Such measurements, for example, provided evidence for a super-massive black hole in the centre of the Milky Way (e.g., Gillessen et al. 2009). Parallaxes obtained from narrow-field measurements are relative, and unless the background objects have truly negligible parallax (e.g., quasars), the correction from relative to absolute will always introduce some additional uncertainty and possible bias. In the present context we ignore narrow-field astrometry.

By contrast, global astrometry attempts to measure long arcs by connecting widely different directions (e.g., Kovalevsky 1980). Traditionally, the connection was provided by

the smooth rotation of the Earth, for example using meridian circle instruments or long-baseline radio interferometry. Nowadays, global optical astrometry can be done by observing simultaneously two (or more) fields-of-view in different directions, which requires measurements to be done from space. The angle between the directions is called *basic angle* and needs to be large and very stable. Using a slowly spinning satellite one can connect measurements along a great circle. Repeating measurements along great circles of different orientations makes it eventually possible to reconstruct the entire celestial sphere. This ensures that the astrometric parameters of the sources are on the same coordinate system and allows us to obtain absolute parallax values: the parallax displacement in the two viewing directions is orientated differently in relation to the scan direction, and for some observations pairs one viewing direction will not be affected by a parallax displacement along the scan direction (see Fig. 2 and the scanning law description in Sect. 3.1).

2 Global astrometry from space

Absolute global astrometry is best done from space, to avoid the wavefront distortions caused by the Earth's atmosphere, to provide a stable and weightless environment for observations, and to allow continuous observations of the whole celestial sphere by a single instrument, without interruptions by daylight.

2.1 Hipparcos and Tycho

So far only two dedicated space missions for global astrometry have been launched, both by the European Space Agency ESA. The first was the *Hipparcos* satellite (1989–1993; Perryman 1989), about 25 years ago. It measured the positions, parallaxes, and proper motions of circa 118 000 stars to milli-arcsecond level (Perryman et al. 1997; van Leeuwen 2007). The Hipparcos catalogue is composed of a survey part, complete for magnitudes brighter than approximately 8, and a choice of fainter stars from an input catalogue (Turon et al. 1992); the faintest star is approximate magnitude 12.

Even at the (for modern standards) moderate accuracies of a milli-arcsecond (cf. Sect. 1.3), the Hipparcos mission made scientific history. It allowed important advances in understanding the dynamics of the Milky Way, in particular through direct distance determinations in the solar neighbourhood. It enabled the precise calibration of distance proxies reaching further out, and provided the basis for a wide variety of stellar and galactic research. A detailed discussion of the scientific outcome of the Hipparcos mission is provided by Perryman (2012). Hipparcos remains the state-of-the-art source for astrometry of the brightest stars and is the basis of most all-sky visualizations.

Table 1: Comparison of the key characteristics between Hipparcos, Tycho-2 (part of the Hipparcos mission), Gaia, and Nano-JASMINE. The performance values given for Gaia and Nano-JASMINE are end of mission predictions. Parts of the table originate from Lindegren & de Bruijne (2005).

	Hipparcos	Tycho-2	Nano-JASMINE	Gaia
Launch	1989	–	2016 (earliest)	2013
Telescope size	⌀0.29 m	–	⌀0.05 m	1.45 x 0.5 m^2
Basic angle	58 deg	–	99.5 deg	106.5 deg
Launch weight	1 140 kg	–	35 kg	2 030 kg
Magnitude limit, faintest	12 mag	13 mag	11 mag	20 mag
Magnitude limit, completeness	7–9 mag	11.5 mag	11 mag	20 mag
Number of stars	118 000	2.5 million	1 million	> 1 000 million
Number of quasars	1	1	0	0.5 million
Typical accuracy (at mag.)	1 mas (9)	7 mas (9)	3 mas (7.5)	0.024 mas (15)
Radial velocity determination	–	–	–	yes (< 16 mag)

The Hipparcos mission deployed an auxiliary starmapper instrument for determination of the spacecraft attitude, which was also used for complementary observations. This part of the mission resulted in the *Tycho* (Høg et al. 1997) and *Tycho-2* (Høg et al. 2000) catalogues. The Tycho reductions gave positions – but not parallaxes and proper motions – measured by the Hipparcos starmapper, at a few tens of milli-arcsecond accuracy level at the mean epoch of observation, 1991.25. Tycho-2 lists 2.5 million stars and supersedes the first Tycho reduction containing 1 million stars. Tycho-2 also includes proper motions derived from a comparison of the Tycho-2 measurements with century-old ground-based photographic plates. The Tycho-2 proper motions contain large systematic errors from the ground-based observations used to derive them. Therefore, these proper motions were not (and should not be) used as prior information for joint solutions with other missions. Throughout the thesis and the research articles we always mean the second reduction (Tycho-2) when we refer to the Tycho catalogue[2], unless specifically mentioned otherwise. The Tycho-2 catalogue is 90% complete down to approximate magnitude 11.5.

2.2 Gaia

The second dedicated astrometry mission, *Gaia* (de Bruijne 2012), is currently operational in space, following its launch on a Soyuz rocket in December 2013. Gaia, and specifically the processing of its data together with information from other sources, is the main focus of this thesis work. The mission's target is a minimum of five years of observations and the determination of astrometric parameters for over a billion of stars, at an accuracy of a few tens of micro-arcseconds at G magnitude 15. Gaia simultaneously determines photometric parameters and radial velocities from spectroscopy. Table 1 shows some of the key

[2]The Tycho-Gaia solution, for example, is based on Tycho-2, however, designating it the Tycho-2-Gaia solution would have made a particularly bad name.

characteristics of Gaia in direct comparison to other missions.

Gaia's astrometric accuracies are predicted to be approximately 100 times better than those of Hipparcos. Accurate parallax measurements, together with transverse velocities to within a few km s^{-1}, will be made for a very large volume and will reach far across the Galaxy. This will enable studies of the formation and evolution of the Milky Way and its accretion history. It will also give us a better understanding of the structure and distribution of the dark matter content of our Galaxy, as well as a much improved understanding of stellar evolution. The mission will detect tens of thousands of exo-planets, and catalogue hundreds of thousands of asteroids and comets in our Solar System. Among the more exotic objects, Gaia is expected to observe tens of thousands of brown dwarfs and a similar number of extragalactic supernovae. It will also provide new stringent tests of general relativity. Achieving all of this puts extreme requirements on the stability of the instrument and in particular on the basic angle $\Gamma = 106.5$ deg separating the two viewing directions (see Sect. 3.2, Sect. 4.5, and Paper VI).

The final data release for Gaia is foreseen for 2022, three years after the end of observations, and a series of intermediate releases is planned until then. According to the current release schedule[3] the first intermediate release of data anticipated in summer 2016 will contain only positions and single-epoch G magnitudes for the majority of stars. For the Hipparcos stars the release will also provide updated proper motions, based on the Hipparcos positions at 1991.25, the Gaia positions at approximately 2015, and the long temporal baseline in-between those two epochs. This part of the release is called the Hundred-Thousand-Proper-Motion project (HTPM; Mignard 2009). Sects. 4.2, 4.3, and 4.5, and Papers III, IV, and VI deal with the practical realisation of HTPM and its extensions.

2.3 Nano-JASMINE and future mission concepts

The Japanese astrometry community is planning three space astrometry missions (Gouda 2012). The objective of the JASMINE mission (launch planned for the first half of the 2020's) is near-infrared narrow-field observations, targeting the central regions of our Galaxy which are obscured by dust in visible light (i.e., not observable by Gaia). In preparation for this, two development missions are foreseen. Small-JASMINE (earliest launch date 2017, Yano et al. 2013) uses a similar observation principle and hardware as JASMINE but a much smaller aperture, whereas Nano-JASMINE (earliest launch date 2016; Yamada et al. 2013) relies on proven design and observation principles similar to a much simplified version of Gaia: the Nano-JASMINE spacecraft is a scanning mission where two fields-of-view separated by a basic angle of 99.5 deg are combined onto the same focal plane, allowing for global astrometry. It uses CCD detectors optimised for wavelengths towards the red end of the spectrum

[3] `http://www.cosmos.esa.int/web/gaia/release`

(z_w-band observations, 0.6–1.0 µm). Nano-JASMINE is a low-cost pathfinder mission for the Japanese community to gain experience with astrometric observations and their analysis, and aims at studying the design of key components and data processing strategies in preparation for (Small-)JASMINE. The satellite operates in a scanning mode similar to Gaia, albeit altered to suit its sun-synchronous polar geocentric orbit. Part of the work shown in Papers I and II (see also Sect. 4.1) concerns the development of a scanning law for the Nano-JASMINE mission and the study of its data processing. The satellite observes bright stars down to approximately z_w magnitude 10–11, at milli-arcsecond accuracy, similar to the Hipparcos/Tycho catalogues.

Many other concepts and missions have been suggested for the future, and the follow-up mission to Gaia is a topic that will become more and more important. However, no final conclusions have been reached so far. Assuming a future mission would be a scanning mission in the style of Gaia and Hipparcos, the concepts discussed in this thesis will remain valid and could then be applied to a combination of Hipparcos, Gaia, and the successor mission. This will greatly benefit the detection of long-period planetary companions (Høg 2014).

3 Gaia astrometry and prior information

3.1 The Gaia scanning law

Global astrometry satellites such as Gaia, Hipparcos, and Nano-JASMINE continuously scan the celestial sphere. They observe many different pairs of directions one after the other, and revisit them at a later point in time. This is realised through a scanning law, which aims at a homogeneous and repeating coverage of the entire sky, while keeping the spacecraft tilt angle towards the Sun constant for thermal stability reasons. The scanning laws are based on three motions: the spacecraft spin, the precession of the spin axis, and the orbit of the spacecraft around the Sun (Lindegren & Bastian 2011). In the following discussion we use the specific parameters of the Gaia scanning law.

The Gaia spacecraft slowly spins around its main symmetry axis with a period of 6 hours. The continuous spin links observations in different viewing directions along a great circle. The spin causes stellar images to transit the focal plane at a constant rate. Modern astrometry satellites such as Gaia operate CCD detectors in time-delay and integration (TDI) mode, which shifts the charges along the CCD pixels at the same rate as the spacecraft spin, allowing the integration of light along a CCD transit. Since the coordinate in scan direction (*along-scan*) establishes a link to the other viewing direction, it is more important than the perpendicular direction (*across-scan*). Gaia uses elongated apertures and pixels optimizing the along-scan accuracy. Somewhat simplified one could consider the observations one-

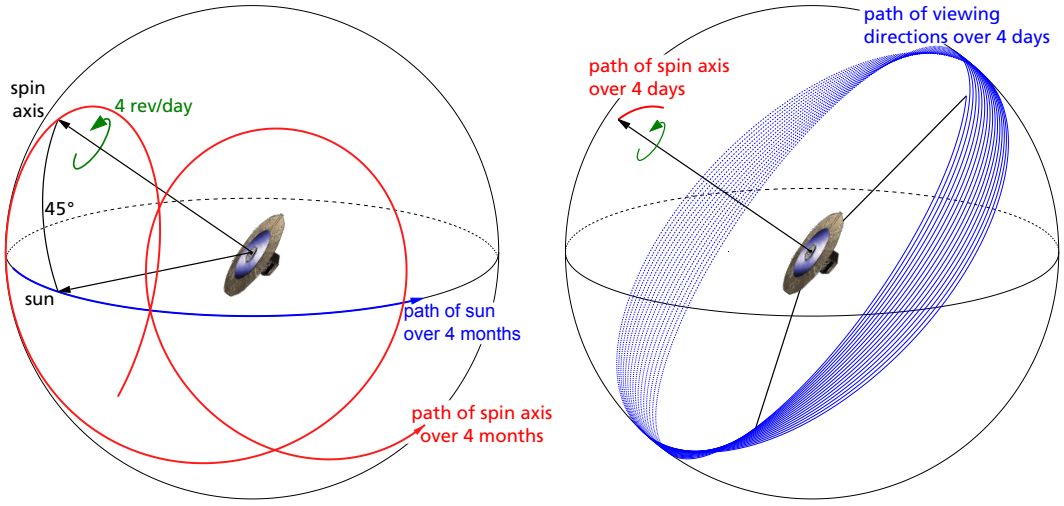

Figure 3: Illustration of the nominal scanning law of Gaia. (Figure: Lindegren & Michalik)

dimensional. It is important that different observations of the same source are carried out using different along-scan angles to allow a good sampling of the source. This is ensured by the nature of the scanning law.

The spin axis is tilted 45 deg away from the Sun and its direction precesses around the direction towards the Sun with a 63 days period, to ensure slowly overlapping great circles and a good sky coverage (see Fig. 3). Furthermore, the satellite orbits the Sun at the same angular rate as the Earth, scanning different portions of the sky. These three motions together result in Gaia covering the celestial sphere roughly once every six months. Over the full mission duration, each source transits the focal plane on average 80 times. The Gaia scanning law is further described in de Bruijne et al. (2010). Figure 4 shows two versions of the scanning used in our simulations. The left panel gives the coverage from the full mission duration in a nominal scenario. The right panel shows a more realistic version containing ecliptic pole scanning[4] and data gaps caused by, for example, satellite maintenance, orbit manoeuvres, and solar activity.

3.2 Basic angle stability requirements

In order to successfully reconstruct the sources on the celestial sphere from the observation pairs along a great circle, the stability of the basic angle between the two viewing directions is of utmost importance. This puts stringent requirements on the thermal and mechanical stability of the spacecraft. Temperature changes lead to material expansion and shrinkage, and thus to short-term variations in the basic angle, whereas ageing of components leads to long-term variations. Consider for example that the heat produced by electronic on-

[4]Ecliptic pole scanning is a special version of the scanning law which repeatedly observes the stars in the ecliptic pole regions. It served calibration purposes during the early operational phase of the mission.

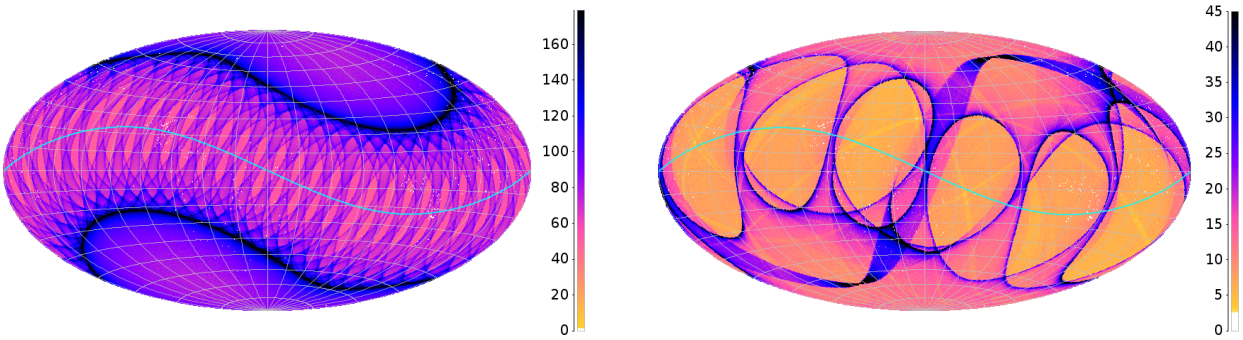

Figure 4: All-sky map showing the coverage of Gaia (number of focal plane transits as a function of sky position) as a result of the scanning law. *Left:* 5 years of nominal observations, no data gaps. *Right:* Mimicking the first year of real observations, i.e., 1 month of Ecliptic Pole Scanning, 11 months of regular observations, data gaps. (The colour scales are clipped to emphasize the overall structure. Figure: Michalik)

board components varies with processing load, which depends on the stellar density in the astrometric focal plane and is very different when scanning the Galactic plane compared to high latitudes. Symmetry in the spacecraft design and thermal decoupling between the service module and the payload are important factors to mitigate the effects, but they cannot entirely remove them. The heat produced from solar irradiation might vary depending on the spin phase. Other contributing factors might be discrete features such as material relaxation, orbit maintenance, or micro-meteoroid hits.

Basic angle variations lead to systematic errors in the resulting astrometric parameters unless accounted for in the data processing (Lindegren et al. 1992). As discussed in Paper VI, it is possible to fit some of the types of basic angle variations from the observations, but some other types might be highly correlated with the astrometric results themselves. In either case it is desirable to monitor the basic angle through on-board metrology.

Gaia contains an interferometric device, the Basic Angle Monitor (BAM). However, the question remains whether the BAM is inherently stable itself, or if some of the effects measured by it are artefacts not caused by actual basic angle variations. This requires cross-checking BAM information during data processing to ensure a consistent and correct handling of the basic angle variations. One important consistency check for BAM data is provided by quasars. Quasars are the bright point-like optical counterparts of active galactic nuclei. Because of their very large distances from us, their true parallaxes and proper motions can be assumed to be zero. They are one of the few kinds of objects where we have a general knowledge of the true parallax and proper motion values with high certainty. Hence, they are invaluable for BAM verifications. Sect. 4.5 and Paper VI discuss how quasars can be used to verify the parallax estimates in early Gaia solutions.

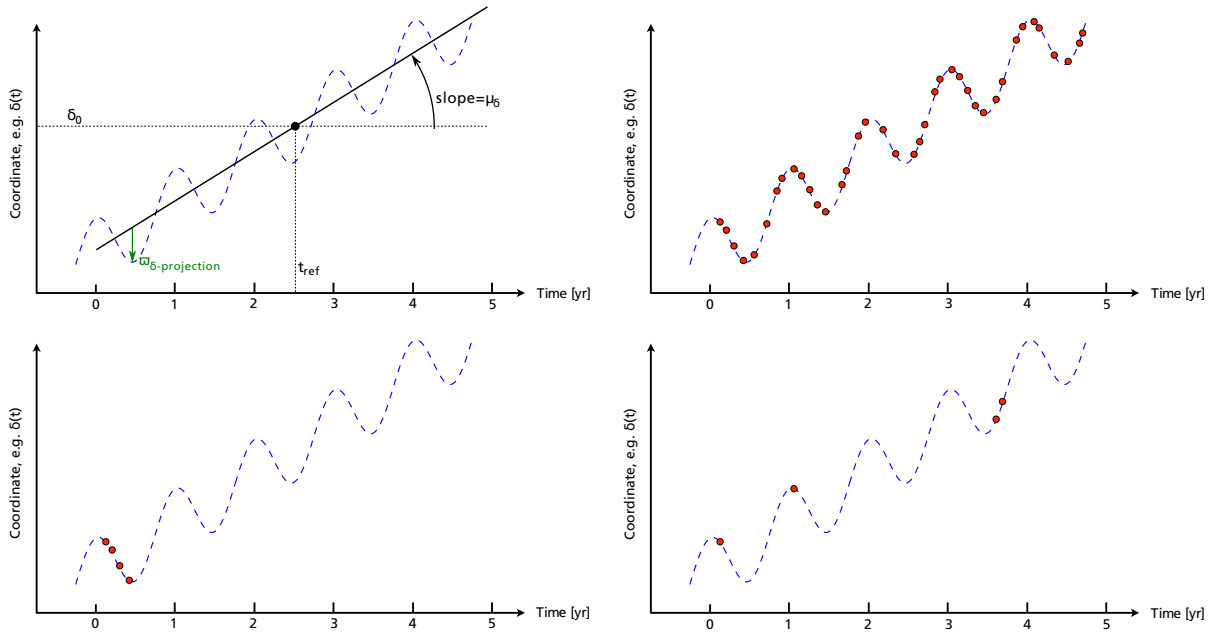

Figure 5: *Top left:* Change in observed coordinate of a source as a function of observation time, a superposition of periodic parallax displacement and linear proper motion. The position coordinate δ_0 is defined at a reference epoch $t_{\rm ref}$, typically the middle of the observation interval. *Top right:* Five years of observations (red dots) provide a good sampling to distinguish the different effects. *Bottom left:* Less than one year of observations (for example for the first release, or for transient objects anytime during the mission) may result in a degeneracy between parallax and proper motion. *Bottom right:* Objects with a magnitude close to the detection limit will be affected by a similar problem, although their observations may be spread out over the entire observation interval. (Figures: Michalik & Lindegren)

3.3 Disentangling the different astrometric parameters

Data processing takes the multiple observations per source and fits the astrometric parameters. This is typically done through a least-squares solution. The observations are cast in form of normal equations $\mathbf{N}\mathbf{x} = \mathbf{b}$, where $\mathbf{x}$ are (corrections to) the astrometric parameters of a source. However, the solution cannot be independently determined for each single source, since they are connected by a number of common 'nuisance' parameters, such as the attitude of the spacecraft itself and the geometric calibration parameters of the instrument. To achieve the required accuracy of Gaia, they must be estimated as additional unknowns in the data processing. This makes Gaia, in a sense, a self-calibrating instrument. The computational complexity of the normal equations for more than a billion sources requires the Gaia least-squares solution to be done in a complex iterative scheme. This is called the Astrometric Global Iterative Solution (AGIS; Lindegren et al. 2012).

Disentangling the five astrometric parameters requires that a source has been observed at least five times at different distinct moments, assuming one dimensional observations (see Sect. 2.1 of Paper IV). A certain level of redundancy is desirable for a more accurate determination of the attitude, calibration, and the detection of deviations from the expected uniform linear kinematic motion. The minimum number of five observations is obvious from a mathematical point of view since the system of equations would otherwise be under-

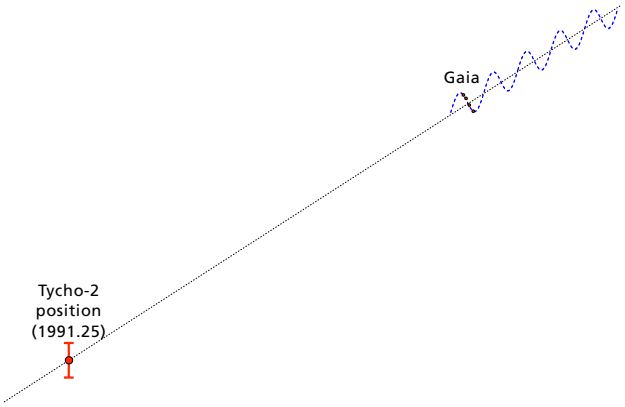

Figure 6: Adding additional observations as prior information (here from Tycho-2) can help overcoming the ambiguity between parallax and proper motion for short datasets. (Figure: Lindegren & Michalik)

determined. The requirements can also be considered from a geometrical point of view. A good solution requires a certain number of observations, but also that those observations are sufficiently distinct from one another in time or position angle. Preferably they should span a time interval larger than one year (see Fig. 5): parallax is a repeating elliptical displacement with a period of one year and proper motion a continuous uniformly linear trend. Trying to distinguish both in short datasets may be difficult and result in large correlations between the parameters, or it may be simply impossible for numerical reasons, if the observations become too scarce or span too short a time interval.

3.4 Prior information for insufficient datasets

Adding additional constraints allows us to overcome the parallax–proper motion degeneracy. Such prior information may consist of historic observations added on a long temporal baseline (see Fig. 6), which provide a good estimation of a source's proper motion and thus allow us to derive the parallax from the most recent measurements. This principle is used in Papers I–IV. If however no reliable observational prior exists for a given source, one can instead use constraints from general knowledge of astrometric properties, such as upper limits to parallax and proper motion for objects depending on their type, magnitude, or Galactic coordinates. The latter principle is used in Papers V and VI.

4 Main results of the research papers

The idea of combining Hipparcos and Gaia data is not new. Deriving updated proper motions with Gaia for the 100 000 Hipparcos stars (the HTPM project, see Sect. 2.2) was long foreseen to be part of the first Gaia data release and explored by Mignard (2009). HTPM is not only useful to get additional value out of the first Gaia data release. It also remains

an idea worth exploring with subsequent releases of Gaia, since HTPM derives long-baseline proper motions, which are important for the detection of hidden long-period companions of stars.

Mignard suggested a combination of the (first preliminary) Gaia catalogue and the Hipparcos catalogue in the form of an a posteriori combination, i.e., after the Gaia catalogue itself has been created. We propose a more generic way of combining catalogues, which is also applicable to the HTPM scenario. Instead of an a posteriori combination of astrometry data we suggest an immediate *joint solution* of data from the different missions as part of AGIS. For HTPM it means the integration of the Hipparcos catalogue as quasi additional observations into the Gaia data, before computing their astrometric solution. For that, we reconstruct the prior information $\mathbf{N}_p, \mathbf{b}_p$ corresponding to the Hipparcos data, add them to the Gaia normal equations, and then derive the joint estimates of the astrometric parameters. The normal matrix $\mathbf{N}_p$ is the inverse of the covariance matrix of the Hipparcos measurements and the right hand side $\mathbf{b}_p$ a measure of the distance of the current estimates from the Hipparcos parameters, as shown in Paper I (and with more detail in Paper III). Implementing the joint solution method in the Gaia data processing required modifications (detailed in Sects. 2.4, 2.6, and 2.7 of Paper III) of the AGIS algorithms. To test and evaluate the joint solution we carried out simulations of a realistic sky, its observations by Gaia, and the AGIS data processing, in different combination scenarios. For the simulations we used and expanded the software package AGISLab (Holl et al. 2012; Bombrun et al. 2012), a very flexible small-scale version of AGIS, meant to test and explore new developments for Gaia data processing. The set-up of our simulations is described in great detail in Sect. 3 of Paper III.

4.1 Demonstrating the concept of a joint solution (Papers I and II)

We initially explored the joint solution concept by investigating improvements made to the Nano-JASMINE data by combining it with Hipparcos (Paper I) and Gaia (Paper II). This is part of a European-Japanese collaboration with the aim of using a modified version of the Gaia astrometric data processing framework AGIS for the data reduction of Nano-JASMINE (Yamada et al. 2012).

Paper I

Concept study: Combination of Nano-JASMINE with Hipparcos through a joint solution

This paper comprises the first demonstration of the combination of data from two astrometry missions, through the reconstruction of information arrays and their incorporation in an iterative least-squares data processing. This paper applies the method to the historic data from the Hipparcos mission and simulated data from Nano-JASMINE, and shows the first performance prediction of jointly solved astrometric data.

Paper II

Concept study: Combination of Nano-JASMINE with Gaia and Hipparcos to improve bright star astrometry

Paper II takes the idea of a joint solution one step further, extending it to a scenario with three missions. The aim of this study is to explore the feasibility of obtaining updated astrometric measurements for the brightest stars through catalogue combination. The magnitude limit of Nano-JASMINE allows observing bright stars. These observations can be combined with the historic measurements from the Hipparcos mission, allowing us to derive long-baseline proper motions. Contemporary Gaia data provides an accurate reference frame. This study also presented updated performance predictions of Nano-JASMINE, following the development and implementation of a modified Nano-JASMINE scanning to adapt the satellite operations to a new potential orbit.

4.2 Applying the joint solution to the HTPM project (Paper III)

Given the success of a joint Nano-JASMINE and Hipparcos solution in our simulations, it was natural to apply it to a Gaia-Hipparcos combination.

Paper III

Hipparcos-Gaia proper motions

Paper III serves as a handbook for using the joint solution method as the baseline for the HTPM project. This gives the advantage of providing a simple and clean implementation scheme and allows us the additional estimation of parallaxes. It also ensures the immediate consistency of the Gaia solution with the Hipparcos reference frame. The paper provides a generalised formulation of the method, and looks into many of the smaller aspects of the project. Detailed performance predictions are made, and a simple recipe to calculate goodness-of-fit statistics is developed: the level of agreement of the joint solution with the individual estimates from the two separate missions enables the detection of binary candidates.

4.3 Eliminating the shortcomings of HTPM: the Tycho-Gaia project (Paper IV)

The joint solution method experiments for 100 000 stars unveiled one particular pitfall of the HTPM project: the number of stars included is too small to provide sufficient coverage for a stand-alone Gaia solution. Therefore, one needs to additionally include auxiliary stars for which only positions can be determined. This could bias the HTPM results, and could in particular lead to an underestimation of their parallax values (see Fig. 2 of Paper III).

Paper IV

The Tycho-Gaia Astrometric Solution

Paper IV introduces a major improvement of the HTPM project, replacing the random auxiliary stars by Tycho-2 stars. The positions at epoch 1991 of the Tycho-2 stars are known and can be used as prior information, enabling us to derive their full set of five astrometric parameters with less than one year of Gaia data. This avoids the biases introduced in HTPM by the auxiliary stars, and results in an additional 2.5 million parallaxes and updated proper motions. This paper also proposes how independent parallaxes can be derived for the Hipparcos stars when the Hipparcos parallax prior is removed from the joint solution.

4.4 Finding a prior for non-Tycho, non-Hipparcos sources (Paper V)

For insufficiently observed sources it was originally planned to set parallax and proper motion to strictly zero in the Gaia solution. This would not only potentially bias the position estimates, but also give underestimated formal errors of the results. As a remedy we explore

the use of general knowledge of the size of those astrometric parameters in the solution. We analyse stars from a realisation of a Galactic model, the Gaia Universe Model Snapshot (GUMS; Robin et al. 2012), which was created to aid simulations of Gaia data processing. We then experiment with the use of the typical sizes of parallaxes and proper motions as prior information in the data processing of sources with insufficient information, finding that we can get estimates with reliable statistical properties, if a large enough number of sources are part of the solution.

Paper V

Use of a general prior from GUMS

This paper provides the theoretical foundation of the joint solution method, and gives an extension of the catalogue-based prior to become completely generalised. We discuss the behaviour of astrometric solutions when priors are used, clarify that results obtained with priors are never independent, and suggest how to choose priors in a sensible way. Finally, we derive a sensible prior as a function of magnitude and Galactic direction from an analysis of the GUMS catalogue, and test it in simulations.

4.5 Verifying the TGAS results through quasars (Paper VI)

Following a first internal analysis of real data, it became clear that the quality of the TGAS results would be affected by basic angle variations on-board the Gaia spacecraft. These variations were found to be many times larger than originally anticipated. Although this can in principle be handled by using metrology data from BAM, it is desirable to independently verify the basic angle behaviour and the parallax results in a TGAS solution. For later releases of Gaia this is readily done through the use of quasars (see Sect. 3.2). However, in early solutions there are not enough data to obtain sensible quasar astrometry, hence some prior information needs to be added to overcome this limitation.

Paper VI

Quasars in TGAS

Paper VI applies the generalised framework of Paper V to quasars, as an extension to the Tycho-Gaia scenario discussed in Paper IV. It uses the assumption that quasar proper motions are (on average) zero as prior information, to allow us to derive their full set of astrometric parameters in a solution where nominally not enough data are available to do so. The paper shows, through simulations, that the quasar parallax results can be used to verify the zero-point of the TGAS parallaxes, even when the measurements are affected by a thermally induced periodic variation in the optomechanics of the Gaia satellite.

5 Conclusions

The research papers included in this thesis develop concepts with the aim of improving the understanding of early datasets of Gaia and the handling of stars with too few observations, by adding suitable prior information to the data processing. The feasibility of the proposals is demonstrated through detailed simulations of various scenarios focusing on different key aspects. The method is not only applicable to the first data release of Gaia, but also for sources with insufficient observation histories at the end of the mission, such as sources at the detection limit. The technique will also be useful for future astrometry mission, for example for combining Gaia data with a potential successor mission.

While writing this summary it has become clear that the Gaia Data Processing and Analysis Consortium (DPAC) is indeed trying the suggested concepts on real data for the first Gaia data release (DR-1). The method outlined in Paper III has now become the baseline for deriving the HTPM estimates, and Paper V was adopted for the derivation of the positions estimates and their uncertainties in DR-1. Even a real data TGAS (Paper IV) and the verification of BAM data using quasars (Paper VI) are being considered for DR-1. It however remains to be seen whether the quality of the resulting astrometric results will be sufficiently good to justify publication, given all the complications of real data.

So far the combination of Gaia data with Hipparcos and Tycho-2 has mostly been studied for the first intermediate release of preliminary Gaia data. In Paper III we briefly discussed a goodness-of-fit statistic which shows the deviation of the astrometric parameters between a joint solution and the estimates given in the individual catalogues. The level of agreement can be used to detect candidates for stars with unseen stellar or planetary companions. In principle, the goodness-of-fit will become more sensitive to deviations from uniform linear space motion with increasing amounts of Gaia data. In future work it should be explored

if potential scientific applications justify the repetition of HTPM and TGAS in later releases, and at the end of the Gaia mission. A contra-indication may be given by the loss of a fully independent solution when priors are added to an astrometric solution. Future work could instead consider computing the goodness-of-fit without changing the Gaia solution itself. This can for example be done through a secondary solution that does not modify the attitude and calibration parameters of the spacecraft.

6 References

Bombrun A., Lindegren L., Hobbs D., et al., Feb. 2012, A&A, 538, A77

de Bruijne J., Siddiqui H., Lammers U., et al., Jan. 2010, In: Klioner S.A., Seidelmann P.K., Soffel M.H. (eds.) IAU Symposium, vol. 261 of IAU Symposium, 331–333

de Bruijne J.H.J., Sep. 2012, Ap&SS, 341, 31

Gillessen S., Eisenhauer F., Trippe S., et al., Feb. 2009, ApJ, 692, 1075

Gouda N., Aug. 2012, In: Aoki W., Ishigaki M., Suda T., Tsujimoto T., Arimoto N. (eds.) Galactic Archaeology: Near-Field Cosmology and the Formation of the Milky Way, vol. 458 of Astronomical Society of the Pacific Conference Series, 417

Høg E., Aug. 2014, ArXiv e-print 1408.2190

Høg E., Bässgen G., Bastian U., et al., Jul. 1997, A&A, 323, L57

Høg E., Fabricius C., Makarov V.V., et al., Mar. 2000, A&A, 355, L27

Holl B., Lindegren L., Hobbs D., Jul. 2012, A&A, 543, A15

Kovalevsky J., Aug. 1980, Celestial Mechanics, 22, 153

Lindegren L., Bastian U., Feb. 2011, In: EAS Publications Series, vol. 45 of EAS Publications Series, 109–114

Lindegren L., de Bruijne J.H.J., Oct. 2005, In: Seidelmann P.K., Monet A.K.B. (eds.) Astrometry in the Age of the Next Generation of Large Telescopes, vol. 338 of Astronomical Society of the Pacific Conference Series, 25

Lindegren L., van Leeuwen F., Petersen C., Perryman M.A.C., Soderhjelm S., May 1992, A&A, 258, 134

Lindegren L., Lammers U., Hobbs D., et al., Feb. 2012, A&A, 538, A78

Mignard F., October 2009, The Hundred Thousand Proper Motions Project, URL `http://www.cosmos.esa.int/web/gaia/public-dpac-documents`, Gaia Data Processing and Analysis Consortium (DPAC) technical note GAIA-C3-TN-OCA-FM-040

Perryman M., Aug. 2012, Astronomical Applications of Astrometry

Perryman M.A.C., Jul. 1989, Nature, 340, 111

Perryman M.A.C., Lindegren L., Kovalevsky J., et al., Jul. 1997, A&A, 323, L49

Robin A.C., Luri X., Reylé C., et al., Jul. 2012, A&A, 543, A100

Turon C., Crézé M., Egret D., et al., Jul. 1992, Bulletin d'Information du Centre de Donnees Stellaires, 41, 9

van Altena W.F., 2013, Astrometry for Astrophysics

van Leeuwen F. (ed.), 2007, Hipparcos, the New Reduction of the Raw Data, vol. 350 of Astrophysics and Space Science Library

Yamada Y., Hara T., Yoshioka S., et al., Sep. 2012, In: Ballester P., Egret D., Lorente N.P.F. (eds.) Astronomical Data Analysis Software and Systems XXI, vol. 461 of Astronomical Society of the Pacific Conference Series, 585

Yamada Y., Fujita S., Gouda N., et al., Feb. 2013, In: de Grijs R. (ed.) IAU Symposium, vol. 289 of IAU Symposium, 429–432

Yano T., Gouda N., Kobayashi Y., et al., Feb. 2013, In: de Grijs R. (ed.) IAU Symposium, vol. 289 of IAU Symposium, 433–436

Scientific publications

Author contributions

Co-authors are abbreviated as follows:
Alexey G. Butkevich (AGB), David Hobbs (DH), Lennart Lindegren (LL), Uwe Lammers (UL), and Yoshiyuki Yamada (YY).

Paper I: Combining and Comparing Astrometric Data from Different Epochs: A Case Study with Hipparcos and Nano-JASMINE

Based on an initial idea by LL, I implemented the necessary algorithms for the joint solution, added software extensions to simulate Nano-JASMINE, and derived performance predictions. I analysed the results jointly with LL and DH and wrote the first draft of the manuscript. The Nano-JASMINE specifications for the simulations were provided by YY.

Paper II: Improving distance estimates to nearby bright stars: Combining astrometric data from Hipparcos, Nano-JASMINE and Gaia

Implementation of the updated Nano-JASMINE specifications, the simulations, and the data processing were done by me. Interpretation of the results and refinement of the simulations was done together with LL and DH. The triangular scanning law was theoretically developed by LL and implemented jointly by LL and me. The manuscript was drafted by me and improved in cooperation with the co-authors.

Paper III: Joint astrometric solution of Hipparcos and Gaia. A recipe for the Hundred Thousand Proper Motions project

The simulations and data processing were done by me. Set-up and interpretation of the results was done together with LL and DH. I produced the figures and wrote the first draft of the manuscript. LL developed and wrote the two appendices, and re-formulated large parts of the theoretical description (Sect 2).

Paper IV: The Tycho-Gaia astrometric solution. How to get 2.5 million parallaxes with less than one year of Gaia data

The simulations and data processing were done by me. The dead time implementation was added by DH. Set-up and interpretation of the results was done together with LL and DH. I drafted the manuscript and produced all plots except Fig. 1, which was created by LL.

Paper V: Gaia astrometry for stars with too few observations. A Bayesian approach

The implementation of the Bayesian prior and the simulations were done by me. The data analysis framework was implemented by LL and me, under his lead. The majority of the plots was produced by me. The manuscript was drafted jointly by LL and me, however most of the theory section was written by LL. AGB contributed parts of the theoretical formulation, the fit of the general prior (Sect. 3.4), and the Appendix.

Paper VI: Quasars can be used to verify the parallax zero-point of the Tycho-Gaia Astrometric Solution

The development, implementation, and simulations were done by me. LL provided advise and guidance along the way and helped with the interpretation of the results. The manuscript was written by me, and revised by LL and me.

Conference poster in Appendix A.1

Paper I

Astronomical Data Analysis Software and Systems XXI
ASP Conference Series, Vol. 461
Pascal Ballester, Daniel Egret, and Nuria P. F. Lorente, eds.

Combining and Comparing Astrometric Data from Different Epochs: A Case Study with Hipparcos and Nano-JASMINE

Daniel Michalik,[1] Lennart Lindegren,[1] David Hobbs,[1] Uwe Lammers,[2] and Yoshiyuki Yamada[3]

[1]*Lund Observatory, Lund University, Box 43, SE-22100 Lund, Sweden e-mail:* daniel.michalik, lennart, david@astro.lu.se

[2]*European Space Agency (ESA/ESAC), P.O. Box 78, ES-28691 Villanueva de la Cañada, Madrid, Spain, e-mail:* uwe.lammers@sciops.esa.int

[3]*Department of Physics, Kyoto University, Oiwake-cho Kita-Shirakaw Sakyo-ku, Kyoto, 606-8502, Japan, e-mail:* yamada@amesh.org

Abstract. The Hipparcos mission (1989-1993) resulted in the first space-based stellar catalogue including measurements of positions, parallaxes and annual proper motions accurate to about one milli-arcsecond. More space astrometry missions will follow in the near future. The ultra-small Japanese mission Nano-JASMINE (launch in late 2013) will determine positions and annual proper motions with some milli-arcsecond accuracy. In mid 2013 the next-generation ESA mission Gaia will deliver some tens of micro-arcsecond accurate astrometric parameters. Until the final Gaia catalogue is published in early 2020 the best way of improving proper motion values is the combination of positions from different missions separated by long time intervals. Rather than comparing positions from separately reduced catalogues, we propose an optimal method to combine the information from the different data sets by making a joint astrometric solution. This allows to obtain good results even when each data set alone is insufficient for an accurate reduction. We demonstrate our method by combining Hipparcos and simulated Nano-JASMINE data in a joint solution. We show a significant improvement over the conventional catalogue combination.

1. Introduction

Stellar proper motions have traditionally been computed by comparing positional catalogues based on observations made at different epochs (typically separated by several decades). Parallaxes were either ignored in this process, or determined by quite different instruments and methods. With the advent of Hipparcos and space astrometry, it has become necessary to treat the determination of positions, proper motions, and parallaxes in a unified manner, i.e., in a single least-squares solution. This was the principle used for the construction of the Hipparcos and Tycho catalogues (Perryman & ESA 1997), as well as for the new reduction of the Hipparcos data (van Leeuwen 2007), and it will be used for the Gaia mission and other planned space astrometry projects. In the future we will therefore have access to several independent astrometric catalogues, one for each space project. Improved proper motions can again be computed by comparing the positions in catalogues at different epochs. However rather then combining the

results of the catalogues in the conventional manner, we propose to make a *joint solution* of the data from the missions. In this paper we explore possible advantages of this approach, combining the Hipparcos Catalogue and simulated data from the Japanese Nano-JASMINE mission as a study case.

Nano-JASMINE (launch planned for late 2013) is an ultra-small Japanese satellite to measure the astrometric parameters of about one million celestial sources to 12th magnitude. The expected accuracy of the positions, parallaxes and annual proper motions of magnitude 7.5 objects is about 3 mas. Nano-JASMINE is a very small technological demonstrator for bigger follow-up missions. Its data will be reduced using the Astrometric Global Iterative Solution (AGIS) being developed for the Gaia mission at ESA/ESAC and Lund Observatory (Lindegren et al. 2011).

2. Theory

The estimation of stellar astrometric parameters from observational data can be cast as a linear least-squares problem. The optimum estimate of the unknowns $\boldsymbol{x}$ is obtained by solving the normal equations $\boldsymbol{Nx} = \boldsymbol{b}$ where the covariance of $\boldsymbol{x}$ is given by $\boldsymbol{N}^{-1}$ and where $\boldsymbol{b}$ are the residuals. In the conventional approach of combining two astrometric catalogues the least-squares solution of both data sets is done independently and the combination is done a posteriori. If σ_1 and σ_2 are the accuracies in the two catalogues, positions and parallaxes improve as $\sigma^{-2} = \sigma_1^{-2} + \sigma_2^{-2}$ by computing weighted means of the values of the two catalogues. Proper motions improve as $\sigma_{pm} = (\sigma^2_{pos1} + \sigma^2_{pos2})^{1/2}/\Delta T$ by taking the position difference divided by the epoch difference ΔT. Instead we propose to combine the normal equations of both missions *before* solving

$$(\boldsymbol{N_1} + \boldsymbol{N_2})\boldsymbol{x} = \boldsymbol{b_1} + \boldsymbol{b_2} \qquad \rightarrow \boldsymbol{Nx} = \boldsymbol{b}, \tag{1}$$

allowing us to retrieve directly $\hat{\boldsymbol{x}}_{joint}$ of the combined catalogues. This can also be understood in terms of Bayesian estimation (assuming multivariate Gaussian parameter errors), with $\boldsymbol{N}_1, \boldsymbol{b}_1$ presenting the prior information, $\boldsymbol{N}_2, \boldsymbol{b}_2$ the new data, and $\boldsymbol{N}, \boldsymbol{b}$ the posterior information. Even if each group is not solvable on its own, the combined data may be solvable.

3. Simulations

Simulations are carried out using AGISLab, a software package aiding the development of algorithms for the data reduction of Gaia, developed at Lund Observatory. For simulations the Hipparcos catalogue is used to generate observations. Three catalogues are created (see Figure 1):

The Hipparcos catalogue contains the source parameters read from the Hipparcos catalogue file including their covariance matrix. The Hipparcos data are available for the reference epoch J1991.25. To combine them with simulated Nano-JASMINE data the source parameters and covariance matrix have to be propagated to the mid mission reference epoch (which for Nano-JASMINE is expected to be J2015).

The noisy catalogue contains the starting values for the data processing. It is created by perturbing the original sources with random noise of a given amplitude.

The simulated "true" catalogue defines the sources used for creating the simulated true observations (which may be perturbed subsequently). For the real mission

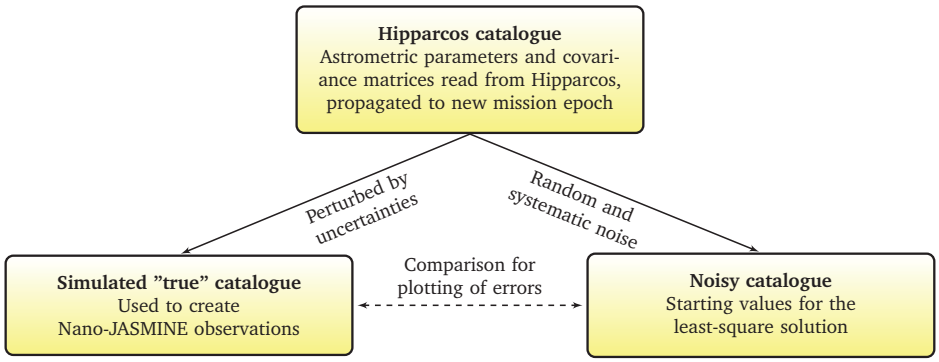

Figure 1. Relationships between catalogues

the true catalogue is not known. The Hipparcos sources give the observed astrometric parameters and their uncertainties. The true parameters of the sources are expected to be at an unknown position within the error space of the original sources. The five astrometric parameters of the simulated true catalogue require five independent Gaussian variates scaled by the square root of the covariance matrix $\boldsymbol{C}$. To find a unique square root we use the lower triangular matrix $\boldsymbol{L}$ resulting from the Cholesky decomposition $\boldsymbol{C} = \boldsymbol{L}\boldsymbol{L}^T$. Then $\boldsymbol{e} = \boldsymbol{L}\boldsymbol{g}$, where $\boldsymbol{g}$ is a vector of five independent unit Gaussian values and $\boldsymbol{e}$ is the resulting vector of errors to be applied to the astrometric parameters. Since $E(\boldsymbol{g}\boldsymbol{g}^T) = \boldsymbol{I}$, where $E(\ldots)$ denotes the expectation value and $\boldsymbol{I}$ is the identity matrix, it is readily verified that $\boldsymbol{e}$ has the desired covariance $E(\boldsymbol{e}\boldsymbol{e}^T) = \boldsymbol{C}$.

In order to make a joint solution the Hipparcos normal equations are reconstructed from the covariance inverse, $\boldsymbol{N}_{HIP} = \boldsymbol{C}_{HIP}^{-1}$. The right-hand side of the Hipparcos normal equations needs to be chosen such that solving for the Hipparcos information only, the update would bring the current parameter values back to the original Hipparcos values. This can be done by calculating a vector $\boldsymbol{d}$ defined as the difference between the original Hipparcos source parameters (subscript o) and the current values (subscript c) and choosing the right-hand side $\boldsymbol{b}_{\rm HIP}$ as

$$\boldsymbol{b}_{\rm HIP} = \boldsymbol{N}_{\rm HIP}\boldsymbol{d} = \boldsymbol{C}_{\rm HIP}^{-1}\begin{pmatrix} (\alpha_o - \alpha_c)\cos\delta_o \\ \delta_o - \delta_c \\ \pi_o - \pi_c \\ \mu_{\alpha\star o} - \mu_{\alpha\star c} \\ \mu_{\delta o} - \mu_{\delta c} \end{pmatrix}. \tag{2}$$

Solving $\boldsymbol{N}_{\rm HIP}\boldsymbol{x} = \boldsymbol{b}_{\rm HIP}$ gives $\boldsymbol{x} = \boldsymbol{d}$ and the application of this update to the current parameters obviously recovers the Hipparcos parameters.

4. Results

Table 1 shows results of simulation runs. As expected the combination of Hipparcos and Nano-JASMINE gives a great improvement in proper motions. Additionally we show that our proposed joint solution performs significantly better than the conventional catalogue combination method. This can be understood as follows. The astrometric parameters in the Hipparcos (or Nano-JASMINE) catalogue are correlated. The large improvement of the proper motions therefore brings some improvement also to the

other parameters, provided that the correlations are properly taken into account. This is the case for the joint solution, but not for the conventional combination.

	Position @J2015 [mas]		Parallax [mas]	Proper motions [mas/year]	
mag < 7.5, ~ 15 000 stars	α	δ	π	$\mu_{\alpha\star}$	μ_δ
Hipparcos only (Hip)	18.19	14.84	0.80	0.77	0.63
Nano-JASMINE only (NJ)	2.56	2.54	3.05	4.65	4.50
Conventional combination Hip + NJ	2.54	2.51	0.77	0.111	0.110
Joint solution Hip + NJ	**2.41**	**2.40**	**0.75**	**0.108**	**0.105**
Improvement of joint solution	5.2%	4.4%	3.5%	3.2%	4.4%
mag < 11.5, ~ 117 000 stars					
Hipparcos only (Hip)	27.06	22.35	1.18	1.14	0.94
Nano-JASMINE only (NJ)	4.57	4.53	5.43	8.38	8.02
Conventional combination Hip + NJ	4.51	4.44	1.15	0.197	0.194
Joint solution Hip + NJ	**4.43**	**4.26**	**1.11**	**0.188**	**0.185**
Improvement of joint solution	1.8%	3.9%	4.0%	4.5%	4.5%

Table 1. Conventional catalogue combination vs. a joint astrometric solution, for a subset of bright stars and for all Hipparcos stars. Simulations of Nano-JASMINE are based on a conservative observation performance model and an optimal scanning law. The positions from Hipparcos have been propagated to the Nano-JASMINE mid-mission epoch J2015.

4.1. Future work

We are planning to extend our studies of catalogue combination by simulating the improvements that can be gained by applying our method to catalogues from simulated Gaia and Nano-JASMINE data together with the Hipparcos and the Tycho-2 catalogues.

Furthermore, the goodness-of-fit of the combined solution is sensitive to small deviations of the stellar motions from the assumed (rectilinear) model. We are investigating how this can be used to identify binary candidates with orbital periods of decades to centuries. This will contribute to the census of the binary population within a few hundred parsecs from the sun by filling a difficult-to-observe gap between the shorter period spectroscopic binaries and the longer period visually resolved systems.

Acknowledgments. Our research is kindly supported by the Swedish National Space Board and the European Space Agency.

References

Lindegren, L., Lammers, U., Hobbs, D., O'Mullane, W., Bastian, U., & Hernandez, J. 2011, A&A, 538, A78

Perryman, M. A. C., & ESA 1997, The Hipparcos and Tycho Catalogues, vol. 1200 of ESA Special Publication

van Leeuwen, F. 2007, Hipparcos, the New Reduction of the Raw Data, vol. 350 of Astrophysics and Space Science Library (Springer)

Conference poster in Appendix A.2

Paper II

Advancing the Physics of Cosmic Distances
Proceedings IAU Symposium No. 289, 2012
Richard de Grijs, ed.

doi:10.1017/S1743921312021849

Improving distance estimates to nearby bright stars: Combining astrometric data from *Hipparcos*, *Nano-JASMINE* and *Gaia*

Daniel Michalik,[1] Lennart Lindegren,[1] David Hobbs,[1] Uwe Lammers,[2] and Yoshiyuki Yamada[3]

[1]Lund Observatory, Lund University, Box 43, SE-22100 Lund, Sweden
e-mail: [daniel.michalik, lennart, david]@astro.lu.se

[2]European Space Agency (ESA/ESAC), P. O. Box 78, ES-28691 Villanueva de la Cañada, Madrid, Spain
e-mail: uwe.lammers@sciops.esa.int

[3]Department of Physics, Kyoto University, Oiwake-cho Kita-Shirakaw Sakyo-ku, Kyoto, 606-8502 Japan
e-mail: yamada@amesh.org

Abstract. Starting in 2013, *Gaia* will deliver highly accurate astrometric data, which eventually will supersede most other stellar catalogues in accuracy and completeness. It is, however, limited to observations from magnitude 6 to 20 and will therefore not include the brightest stars. *Nano-JASMINE*, an ultrasmall Japanese astrometry satellite, will observe these bright stars, but with much lower accuracy. Hence, the *Hipparcos* catalogue from 1997 will likely remain the main source of accurate distances to bright nearby stars. We are investigating how this might be improved by optimally combining data from all three missions through a joint astrometric solution. This would take advantage of the unique features of each mission: the historic bright-star measurements of *Hipparcos*, the updated bright-star observations of *Nano-JASMINE*, and the very accurate reference frame of *Gaia*. The long temporal baseline between the missions provides additional benefits for the determination of proper motions and binary detection, which indirectly improve the parallax determination further. We present a quantitative analysis of the expected gains based on simulated data for all three missions.

Keywords. astrometry, catalogs, methods: data analysis, methods: statistical, reference systems

1. Introduction

The distance to a star can most directly be deduced from its trigonometric parallax. From the ground, this was only done for a few thousand very nearby stars, but with the advent of space astrometry this picture changed dramatically. *Hipparcos* (1989–1993) was the first satellite to determine astrometric parameters (stellar positions, parallaxes and proper motions) from space and yielded the distances to approximately 21,000 stars with an uncertainty of better than 10% (ESA 1997). Now, 25 years later, *Gaia* will further improve our knowledge of stellar astrometry significantly and provide millions of stellar parallaxes with unprecedented accuracy. *Gaia* is an ESA cornerstone mission which will be launched for its nominal five-year mission at the end of 2013. It will continuously scan the sky in a well-chosen pattern and observe up to a billion stars down to magnitude 20. However, because of CCD saturation it will not observe stars brighter than about magnitude 6. Hence the brightest ∼5000 stars are not observed by *Gaia*, and for these *Hipparcos* will continue to be a main source of distance information.

In addition to these two astrometry missions, the third upcoming mission is the ultra-small Japanese satellite *Nano-JASMINE*. Just like *Gaia*, this satellite is based on CCD

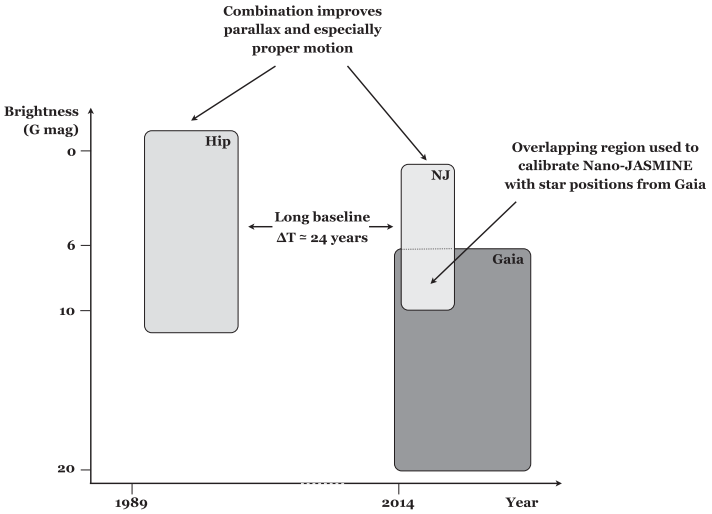

Figure 1. Magnitude range versus mission time for the three astrometry missions, *Hipparcos* ('Hip'), *Nano-JASMINE* ('NJ') and *Gaia*.

detections, and its scanning principle and observing strategy are derived from the *Gaia* pendants. This mission, however, is meant to be a technology demonstrator for larger follow-up missions and is therefore significantly smaller and less accurate. It is scheduled for launch by the end of 2013 and expected to provide astrometry for approximately one million stars in the visual magnitude range from ∼1 to 10 with an accuracy of ∼3 mas for objects of magnitude 7.5. *Gaia* data will be reduced using the Astrometric Global Iterative Solution (AGIS), developed by ESA and Lund Observatory (Lindegren *et al.* 2012). Thanks to a collaboration between the *Nano-JASMINE* Science Team and parts of the AGIS team, it is possible to use AGIS also for the core data reduction of *Nano-JASMINE*.

2. Catalogue combination by joint solution

While *Nano-JASMINE*'s uncertainties are not better than the uncertainties in the *Hipparcos* results, significant improvements for bright-star astrometry can be made by combining the results of *Hipparcos* and *Nano-JASMINE*, thanks to the long time baseline between the missions. The combination is done by incorporating the *Hipparcos* information directly in the astrometric solution for the *Nano-JASMINE* data. This is done using the *Hipparcos* data and the inverse of its covariances as starting values when accumulating the normal equations for the astrometric solution. In contrast to *a posteriori* catalogue combination, this 'joint solution' combines the data sets in a statistically optimal way (Michalik *et al.* 2012), taking into account the correlations between the different astrometric parameters.

In addition to the astrometric improvement facilitated by the combination described above, further improvement can be gained by incorporating (preliminary) results from *Gaia* during the *Nano-JASMINE* data processing: *Gaia* and *Nano-JASMINE* will both observe stars between magnitude 6 and 10. Since the astrometry of these stars is well-determined by *Gaia*, a joint solution can be used to determine the attitude and geometry deviations of *Nano-JASMINE* with better accuracy and therefore improve all *Nano-JASMINE* results. This includes calibrating the basic angle (the nominally fixed angle between the two fields of view of the satellite) which may be affected by thermal variations originating in the low-earth-orbit of the satellite. The basic angle stability is particularly critical to avoid zero-point errors thus allowing the determination of absolute parallaxes. Additionally, the *Nano-JASMINE* results are aligned with the *Gaia* reference frame.

Therefore, optimal results for bright stars are obtained by reducing the *Nano-JASMINE* data together with preliminary *Gaia* results and by combination of these with the historic *Hipparcos* measurements during data analysis (see Fig. 1). We quantify the expected improvements in parallax and proper-motion determination by simulating this scenario.

3. Simulations

Simulations are carried out using AGISLab, a software package developed at Lund Observatory to aid the development of algorithms for *Gaia* data processing (Holl *et al.* 2012). It is used to simulate *Nano-JASMINE* observations and process these data in the same manner as done for the real mission, i.e., by employing the AGIS algorithms. AGIS is an iterative scheme that implements a block-wise least-squares solution on very large data sets, i.e., as required to reduce data from large astrometry missions such as *Gaia*. *Nano-JASMINE* simulations are based on a realistic scanning law featuring a triangular spin-axis precession motion (see Fig. 2). The observation accuracy model assumes a (somewhat optimistic) centroiding uncertainty of $1/300^{\text{th}}$ of a pixel (∼7 mas) for stars brighter than magnitude 7, with additional photon noise for fainter stars (∼30 mas at magnitude 10).

The simulation data set consists of two parts. The first is composed of the 5026 brightest *Hipparcos* stars (mag < 6), with astrometric parameters and uncertainties taken from the *Hipparcos* Catalogue. They are used to evaluate the improvement in the uncertainties of the astrometric parameters of the bright stars. To these, we add 330,000 randomly distributed stars of magnitude 10 that represent stars observed in the overlapping magnitude range which were not included in the *Hipparcos* Catalogue. They represent the stars that will be seen by *Gaia* as well as by *Nano-JASMINE*, and for which the well-determined *Gaia* positions help to better constrain the solution.

First, we simulate the errors in the *Hipparcos* Catalogue, providing a reference case for the bright stars and initial values for the solutions (Cases B and C below), which incorporate the *Hipparcos* data. This is followed by three simulations.

Case A: We simulate *Nano-JASMINE* observations with the two data sets mentioned above and process the data without additional information, i.e. *Nano-JASMINE* only.

Case B: In a second run, we incorporate the information from *Hipparcos* into the data processing of *Nano-JASMINE* using the method described in Michalik *et al.* (2012).

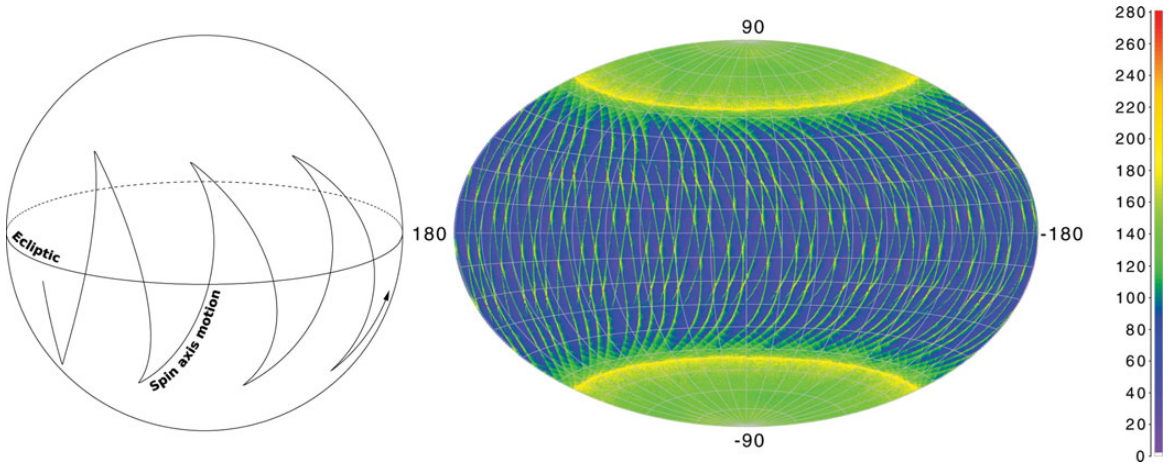

Figure 2. (left) 130 days of spin-axis motion. (right) Number of observations per star (ecliptical sky map), based on simulations of two years of the baseline *Nano-JASMINE* scanning law.

Table 1. Average uncertainties (RSE†) of 5026 *Hipparcos* stars between magnitude 1 and 6.

		Parallax (μas)	Proper motion (μas yr^{-1})
Reference	*Hipparcos only (Hip)*	740	673
Case A	*Nano-JASMINE only (NJ)*	1282	1844
Case B	*Hip + NJ*	595	50
Case C	**Hip + NJ + Gaia**	**588**	**43**

Case C: In a third run, we simulate the astrometric parameters with *Gaia* accuracy and fold expected Gaia covariances (de Bruijne 2012) into the *Nano-JASMINE* data processing. This is done by setting up the covariances of these sources with a σ according to the expected *Gaia* uncertainties and using it in a joint solution scheme. Under the optimistic assumption of uncorrelated parameters, the covariance is set up with zeros in all off-diagonal positions.

4. Results

We compare the three cases and our current knowledge of the bright-star astrometric uncertainties with the results in Table 1. Our current knowledge is represented by the *Hipparcos* Catalogue. The results of the *Nano-JASMINE* observations alone are less precise, but combined with *Hipparcos* they lead to a significant improvement with respect to our current knowledge. Including provisional *Gaia* results yields a further improvement thanks to the improved calibration of the geometry and attitude of *Nano-JASMINE*. This improvement is fairly small, but it needs to be emphasized that there is a second and very important advantage of the *Nano-JASMINE* joint solution with *Gaia* results, i.e. alignment of the *Nano-JASMINE* results with the *Gaia* reference frame.

5. Conclusions

Nano-JASMINE offers an opportunity to significantly improve the *Hipparcos* parallaxes and proper motions of the brightest ∼5000 stars which will not be observed by *Gaia*. In addition, a combined solution with *Gaia* data ensures that the results are in the same reference frame as the *Gaia* catalogue and that the parallaxes are absolute.

References

de Bruijne, J. H. J. 2012, *Ap&SS*, 341, 31

ESA 1997, *The Hipparcos and Tycho Catalogues*, ESA SP-1200

Holl, B., Lindegren, L., & Hobbs, D. 2012, *A&A*, 543, A15

Lindegren, L., Lammers, U., Hobbs, D., O'Mullane, W., Bastian, U., & Hernández, J. 2012, *A&A*, 538, A78

Michalik, D., Lindegren, L., Hobbs, D., Lammers, U., & Yamada, Y. 2012, *Astron. Soc. Pac. Conf. Ser.*, 461, 549

† "The Robust Scatter Estimate (RSE) is defined as 0.390152 times the difference between the 90^{th} and 10^{th} percentiles of the distribution of the variable. For a Gaussian distribution, it equals the standard deviation. The RSE is used as a standardized, robust measure of dispersion [within the *Gaia* core processing unit]." (Lindegren *et al.* 2012)

Paper III

A&A 571, A85 (2014)
DOI: 10.1051/0004-6361/201424606

Astronomy & Astrophysics

Joint astrometric solution of HIPPARCOS and *Gaia*

A recipe for the Hundred Thousand Proper Motions project⋆

Daniel Michalik[1], Lennart Lindegren[1], David Hobbs[1], and Uwe Lammers[2]

[1] Lund Observatory, Lund University, Box 43, 22100 Lund, Sweden
e-mail: [daniel.michalik;lennart;david]@astro.lu.se
[2] European Space Agency (ESA/ESAC), PO Box 78, 28691 Villanueva de la Cañada, Madrid, Spain
e-mail: uwe.lammers@sciops.esa.int

Received 15 July 2014 / Accepted 28 July 2014

ABSTRACT

Context. The first release of astrometric data from *Gaia* is expected in 2016. It will contain the mean stellar positions and magnitudes from the first year of observations. For more than 100 000 stars in common with the HIPPARCOS Catalogue it will be possible to compute very accurate proper motions due to the time difference of about 24 years between the two missions. This Hundred Thousand Proper Motions (HTPM) project is planned to be part of the first release.
Aims. Our aim is to investigate how early *Gaia* data can be optimally combined with information from the HIPPARCOS Catalogue in order to provide the most accurate and reliable results for HTPM.
Methods. The Astrometric Global Iterative Solution (AGIS) was developed to compute the astrometric core solution based on the *Gaia* observations and will be used for all releases of astrometric data from *Gaia*. We adapt AGIS to process HIPPARCOS data in addition to *Gaia* observations, and use simulations to verify and study the joint solution method.
Results. For the HTPM stars we predict proper motion accuracies between 14 and 134 μas yr^{-1}, depending on stellar magnitude and amount of *Gaia* data available. Perspective effects will be important for a significant number of HTPM stars, and in order to treat these effects accurately we introduce a formalism called scaled model of kinematics (SMOK). We define a goodness-of-fit statistic which is sensitive to deviations from uniform space motion, caused for example by binaries with periods of 10–50 years.
Conclusions. HTPM will significantly improve the proper motions of the HIPPARCOS Catalogue well before highly accurate *Gaia*-only results become available. Also, HTPM will allow us to detect long period binary and exoplanetary candidates which would be impossible to detect from *Gaia* data alone. The full sensitivity will not be reached with the first *Gaia* release but with subsequent data releases. Therefore HTPM should be repeated when more *Gaia* data become available.

Key words. astrometry – methods: data analysis – methods: numerical – space vehicles: instruments – proper motions – planets and satellites: detection

1. Introduction

Stellar proper motions have traditionally been determined by analysing the differences in position at different epochs, often separated by many decades and obtained using vastly different instruments and methods. In this process, parallaxes (and radial motions, albeit relevant to a much lesser extent) were mostly ignored.

With the advent of space astrometry, most notably the European satellite HIPPARCOS (1989–1993, see ESA 1997), it became necessary to treat data in a unified manner, i.e., by applying a single least-squares solution for the position, parallax, and annual proper motion. HIPPARCOS determined these parameters for nearly 120 000 stars[1] mostly brighter than magnitude 12, with a median uncertainty of about 1 milli-arcsecond (mas). The *Tycho-2* Catalogue (Høg et al. 2000) gave additional data for 2.5 million stars observed with the HIPPARCOS starmappers. The re-reduction of the HIPPARCOS raw data (van Leeuwen 2007a,b) significantly improved the main-mission results. Today, 25 years after the launch of the satellite, these catalogues remain the main source for the astrometric parameters of these stars.

The European space astrometry mission *Gaia* will soon change this picture. *Gaia*, launched at the end of 2013, will determine the astrometric parameters of up to a billion stars between magnitude 6 and 20 with unprecedented accuracies reaching a few tens of micro-arcseconds (μas) for *Gaia* magnitude $G \lesssim 15$. The vast amounts of data will be processed in a single coherent least-squares solution, which solves not only for the astrometric parameters but also for a large number of parameters describing the time-varying spacecraft attitude and the geometry of the optical instrument. Due to the very large number of parameters to be determined from the observational data the system cannot be solved directly (Bombrun et al. 2010) but has to be tackled in a block-iterative manner with the so called "Astrometric Global Iterative Solution" (AGIS). The AGIS software has been designed and implemented by groups at ESA/ESAC, Lund Observatory, and others, and is described in detail together with the fundamental algorithms and mathematical framework by Lindegren et al. (2012).

Astrometric measurements obtained in the past, even of moderate accuracy by modern standards, have lasting value as they represent a state of the Universe that is never repeated. A good example is the construction of proper motions in the

⋆ Appendices are available in electronic form at http://www.aanda.org

[1] We use "star" to denote a catalogue entry even when it refers to a non-single or extragalactic object. In the context of *Gaia* data processing the term "source" is commonly used for such objects.

Tycho-2 Catalogue using HIPPARCOS and century-old photographic positions. When the astrometric parameters are propagated over a long time interval, uncertainties in the tangential and radial motions accumulate to a significant positional uncertainty. Yet, long-term deviations from linear space motion (e.g., in long-period binaries) increase even more drastically with time. Such deviations might not be detectable within the time spans of the HIPPARCOS or *Gaia* missions individually, but could be detectable by combining the results of the two. Thus, although HIPPARCOS will soon be superseded by *Gaia* in terms of the expected accuracies at current epochs, its data form a unique comparison point in the past, very valuable in combination with later results. For this reason the first *Gaia* data release scheduled for 2016 will not only publish stellar positions and magnitudes based on the first *Gaia* observations, but also a combination of these observations with the HIPPARCOS Catalogue for all stars common between the two missions. This part of the release is called the Hundred Thousand Proper Motions project (HTPM), originally proposed by F. Mignard in a *Gaia*-internal technical document (Mignard 2009).

The present paper gives a recipe for the practical realisation of the HTPM project in the context of the already existing AGIS scheme for the astrometric solution of *Gaia* data. The proper motions in HTPM might be trivially computed from the positional differences between an early *Gaia* solution and the HIPPARCOS Catalogue – the "conventional catalogue combination" approach of Sect. 2.3. However, we argue that the more elaborate "joint solution" method described in Sect. 2.4 will have important advantages for the HTPM project, and in Sect. 3 we show how to implement it as part of AGIS. The validity and accuracy of the method is demonstrated by means of a joint solution of simulated *Gaia* observations of the HIPPARCOS stars (Sect. 4). In the final sections we discuss the limitations of the results and their validity in the light of *Gaia*'s full nominal mission performance, as well as possible applications of the joint solution method to other astrometric data.

The HTPM project should use the re-reduction of the raw HIPPARCOS data (van Leeuwen 2007b), as it represents a significant improvement over the original HIPPARCOS Catalogue (ESA 1997). Therefore it is also used in all our simulations. For the purpose of demonstrating the HTPM solution we regard all valid entries of the HIPPARCOS Catalogue as astrometrically well-behaved (effectively single) stars. Their space motions are therefore regarded as uniform (rectilinear, with constant speed) over the time interval covered by HIPPARCOS and *Gaia*. This is obviously a very simplified picture of the true content of the HIPPARCOS Catalogue. However, getting the solution right in this simple case is a first necessary step for any more sophisticated treatment of detected binaries and multiple stars in the HIPPARCOS Catalogue.

2. Theory

Combining astrometric catalogues requires that data are expressed in the same reference system and described in terms of a common kinematic model. In this section we describe the adopted model and how it is connected to the definition of the astrometric parameters. We outline the conventional approach to catalogue combination and develop the "joint solution" as an optimal generalisation of the method. We show how to detect deviations from the kinematic model or misfits between the datasets. We also outline how to reconstruct the required information from HIPPARCOS and how to integrate the proposed scheme in the astrometric solution algorithm of *Gaia*.

2.1. Kinematic model of stellar motion

The choice of astrometric parameters is a direct result of choosing a model of stellar motion. The most basic assumption is for stars to move uniformly, i.e., linearly and with constant speed, relative to the solar system barycentre (SSB). Note that this also means that the stars are assumed to be single. This is obviously not true for all of them, but a good basic assumption for most stars. During the data reduction stars that are not "well behaved" in an astrometric sense can be filtered out and treated further, e.g., by adding additional parameters for components of stellar systems or for acceleration through external influences.

A uniform space motion can be fully described by six parameters: three for the position in space at a chosen reference epoch, and three for the velocity. Traditionally, the three positional parameters are right ascension α, declination δ, and parallax ϖ relative to the SSB at the reference epoch of the catalogue. The motion is then described by three parameters, where $\mu_{\alpha*} = \dot{\alpha}\cos\delta$ and $\mu_\delta = \dot{\delta}$ are the proper motions in right ascension and declination, respectively, and the third parameter μ_r is the radial motion component. The radial component is more commonly given as the radial velocity v_r in km s^{-1}, but in an astrometric context it is conveniently expressed as the radial proper motion (equivalent to the relative change in distance over time, or $-\dot{\varpi}/\varpi$)

$$\mu_r = v_r\varpi/A, \tag{1}$$

where A is the astronomical unit expressed in km yr s^{-1}. Only the first five parameters are classically considered astrometric parameters. Based on only a few years of observations it is usually not possible to determine the radial component from astrometry with sufficient accuracy (Dravins et al. 1999). Hence the radial component is better determined by other techniques, i.e., from spectroscopy. For *Gaia* the radial component will be significant for many more stars, although the affected fraction remains very small (de Bruijne & Eilers 2012). Even though μ_r is not determined in the astrometric solution for the vast majority of sources, it is convenient and sometimes necessary to formulate astrometric problems with the full set of six astrometric parameters, as we do in this paper. We will also show how to treat the sixth component when the radial velocity is unknown or added from spectroscopy.

2.2. Dealing with non-linearities: SMOK

When comparing and subsequently combining astrometric catalogues one needs to deal with the fact that the mapping from rectilinear to spherical coordinates is strongly non-linear. This becomes significant at the μas level when the differences in α and δ exceed some $(1\ \mu\text{as})^{1/2} \simeq 0.5$ arcsec. For example, the barycentric direction traced out in $\alpha(t)$, $\delta(t)$ due to the proper motion will not be linear even though the star is assumed to move uniformly through space. The traditional way to deal with this is to introduce higher-order correction terms computed by Taylor expansion of the rigorous equations (e.g., Taff 1981). In this paper we take a different approach, based on the scaled modelling of kinematics (SMOK) concept described in Appendix A. For the present purpose it is sufficient to know that (α, δ) may be replaced by linear coordinates (a, d) relative to a designated, fixed comparison point, with time derivatives $\dot{a}$, $\dot{d}$ representing the components of proper motion in α and δ. The six parameters a, d, ϖ, $\dot{a}$, $\dot{d}$, $\dot{r}$ (where $\dot{r}$ is the SMOK equivalent of the radial proper motion) provide an alternative and equivalent parametrisation of the kinematics, more convenient for the catalogue combination than the usual set α, δ, ϖ, $\mu_{\alpha*}$, μ_δ, μ_r.

2.3. Conventional catalogue combination

In the conventional catalogue combination the astrometric parameters in each catalogue are independently estimated from separate sets of observations, and the combination is done a posteriori from the individual catalogues. Let (a_1, d_1, ϖ_1) at time t_1 be the position and parallax of a star in the first catalogue, and (a_2, d_2, ϖ_2) at time t_2 the corresponding information in the second catalogue. The proper motion parameters $\dot{a}$, $\dot{d}$ are then derived as the positional difference over time $\Delta t = t_2 - t_1$

$$\dot{a} = (a_2 - a_1)/\Delta t, \quad \dot{d} = (d_2 - d_1)/\Delta t, \tag{2}$$

which is possible thanks to the reformulation of the astrometric parameters in SMOK. The proper motion uncertainties are

$$\sigma_{\dot{a}} = \frac{\sqrt{\sigma_{a1}^2 + \sigma_{a2}^2}}{\Delta t}, \quad \sigma_{\dot{d}} = \frac{\sqrt{\sigma_{d1}^2 + \sigma_{d2}^2}}{\Delta t}, \tag{3}$$

where σ_{a1} is the uncertainty of a_1, etc. The third kinematic parameter $\dot{r}$ for the radial motion could in theory be derived from the (negative, relative) difference in parallax, but in practice it is derived from the spectroscopic radial velocity as discussed in Sect. 2.1.

While the proper motions are obtained by taking position differences over time, the combined parameters for position and parallax are formed as weighted means. For a this gives

$$\hat{a} = \frac{a_1\sigma_{a1}^{-2} + a_2\sigma_{a2}^{-2}}{\sigma_{a1}^{-2} + \sigma_{a2}^{-2}}, \tag{4}$$

referring to the mean epoch of the combination

$$\hat{t}_a = \frac{t_1\sigma_{a1}^{-2} + t_2\sigma_{a2}^{-2}}{\sigma_{a1}^{-2} + \sigma_{a2}^{-2}}. \tag{5}$$

The reference time $\hat{t}_a$ is the optimal time in-between the two catalogues at which the position and proper motion are uncorrelated and the uncertainty of $\hat{a}$ is minimal, given by $\sigma_{\hat{a}}^{-2} = \sigma_{a1}^{-2} + \sigma_{a2}^{-2}$. The expressions for $\hat{d}$ and $\hat{\varpi}$ are analogous.

This combination scheme has some limitations, in that it does not take correlations between the astrometric parameters into account, nor the individual proper motions that may exist in each catalogue. In the next section we describe a more general approach.

2.4. Joint solution

The reduction of astrometric data is typically done using least-squares solutions, resulting in a linear system of normal equations $\boldsymbol{N}\boldsymbol{x} = \boldsymbol{b}$. Here, $\boldsymbol{x}$ is the vector of resulting astrometric parameters, $\boldsymbol{N}$ the normal equations matrix, and $\boldsymbol{b}$ a vector constructed from the residuals of the problem[2]. The covariance $\boldsymbol{C}$ of the solution $\hat{\boldsymbol{x}} = \boldsymbol{N}^{-1}\boldsymbol{b}$ is formally given by $\boldsymbol{C} = \boldsymbol{N}^{-1}$.

In AGIS the observations of all well-behaved stars ("primary sources") must be considered together in a single, very large least-squares solution (Sect. 2.7). For n primary sources, $\boldsymbol{x}$ would then be the full vector of $6n$ astrometric parameters, with $\boldsymbol{N}$ and $\boldsymbol{b}$ of corresponding dimensions. However, for the present exposition it is sufficient to consider one star at a time, so that $\boldsymbol{x}$ and $\boldsymbol{b}$ are of length 6 and $\boldsymbol{N}$ has dimensions 6×6. In practice only five of the six parameters are estimated, and $\boldsymbol{N}^{-1}$ should hereafter be regarded as the inverse of the upper-left 5×5 submatrix[3].

On the assumption that the adopted kinematic model is valid for a particular star, the matrix $\boldsymbol{N}$ and vector $\boldsymbol{b}$ encapsulate the essential information on the astrometric parameters, as determined by the least-squares solution. Thus, in order to make optimal use of the HIPPARCOS data for a given star there is no need to consider the individual observations of that star: all we need is contained in the "information array" $[\boldsymbol{N}\ \boldsymbol{b}]$. In Sect. 2.6 we show how this array is reconstructed from the published HIPPARCOS Catalogue.

Let $[\boldsymbol{N}_1\ \boldsymbol{b}_1]$ and $[\boldsymbol{N}_2\ \boldsymbol{b}_2]$ be the information arrays for the same star as given by two independent astrometric catalogues. From the way the normal equations are calculated from observational data it is clear that the information arrays are additive, so that $[\boldsymbol{N}_1\ \boldsymbol{b}_1] + [\boldsymbol{N}_2\ \boldsymbol{b}_2]$ is the information array that would have resulted from processing the two datasets together. In Michalik et al. (2012) we have proposed that the optimum combination of the catalogues is done a priori, that is by adding the corresponding arrays *before* solving. The result,

$$\hat{\boldsymbol{x}} = (\boldsymbol{N}_1 + \boldsymbol{N}_2)^{-1}(\boldsymbol{b}_1 + \boldsymbol{b}_2), \tag{6}$$

is the *joint solution* of the astrometric parameters, with covariance $\hat{\boldsymbol{C}} = (\boldsymbol{N}_1 + \boldsymbol{N}_2)^{-1}$. The two catalogue entries for the star must use the same reference epoch and the same SMOK comparison point.

The joint solution has several advantages over the conventional combination method outlined in Sect. 2.3. Because it uses the full information in each catalogue it makes better use of the data and allows one to estimate the resulting uncertainties more accurately, taking the correlations into account. The individual proper motion information available in each catalogue is automatically incorporated in the joint proper motion. Moreover, a solution might be possible where the data in each set individually is insufficient to solve for all astrometric parameters, that is, $\boldsymbol{N}_1 + \boldsymbol{N}_2$ may be non-singular even if $\boldsymbol{N}_1$, $\boldsymbol{N}_2$, or both, are singular. In practice, if $\boldsymbol{N}_1$ comes from the HIPPARCOS data, it will always be non-singular (since there is a HIPPARCOS solution), and the sum is then also non-singular. Hence it will always be possible to make a joint solution for all five astrometric parameters of the HTPM stars. Finally, the joint solution scheme is a clean and rigorous approach and can be integrated into the existing implementation of the astrometric solution for *Gaia* with moderate effort.

The joint solution can be seen as a multidimensional generalisation of the conventional scheme in Sect. 2.3, with $\boldsymbol{N}$ representing the weights (σ^{-2}) and $\boldsymbol{b}$ the astrometric parameters multiplied by their weights (e.g., $a\sigma^{-2}$). Then Eq. (6) is the matrix-equivalent of Eq. (4). The joint solution can also be understood in terms of Bayesian estimation theory (assuming multivariate Gaussian parameter errors), with $\boldsymbol{N}_1, \boldsymbol{b}_1$ representing the prior information, $\boldsymbol{N}_2, \boldsymbol{b}_2$ the new data, and their sums the posterior information.

[2] The least squares problem can be solved using a number of alternative numerical algorithms, for example based on orthogonal transformations. However, as these algorithms are all *mathematically* equivalent to the use of normal equations, our results remain valid independent of the chosen solution algorithm.

[3] The full matrix is nevertheless needed for the covariance propagation in Sect. 2.6.

2.5. Goodness of fit of the joint solution

The goodness of fit of a least-squares solution can be described in terms of the sum of the squares of the normalized post-fit residuals,

$$Q = \sum_k \left(\frac{\eta_k^{(\mathrm{obs})} - \eta_k^{(\mathrm{calc})}}{\sigma_k} \right)^2 , \tag{7}$$

where $\eta_k^{(\mathrm{obs})}$ and $\eta_k^{(\mathrm{calc})}$ are the observed and calculated (fitted) angular focal-plane coordinates of the star in observation k, and σ_k is the standard error of the observation. Q is calculated for each star separately and is simply a function of $\boldsymbol{x} = (a, d, \varpi, \dot{a}, \dot{d}, \dot{r})'$. The least-squares solution $\hat{\boldsymbol{x}} = \boldsymbol{N}^{-1}\boldsymbol{b}$ minimizes Q and for any other parameter vector $\boldsymbol{x}$ we have

$$Q(\boldsymbol{x}) = Q(\hat{\boldsymbol{x}}) + (\boldsymbol{x} - \hat{\boldsymbol{x}})'\boldsymbol{N}(\boldsymbol{x} - \hat{\boldsymbol{x}}). \tag{8}$$

If the kinematic model is correct and the standard errors of the observations are correctly estimated one expects the minimum value $Q(\hat{\boldsymbol{x}})$ to follow the chi-square distribution with ν degrees of freedom, $Q(\hat{\boldsymbol{x}}) \sim \chi^2(\nu)$. Here $\nu = m - \mathrm{rank}(\boldsymbol{N})$ is equal to the number of observations m (that is the number of terms in Eq. (7)) diminished by the rank of $\boldsymbol{N}$. Note that this holds even if $\boldsymbol{N}$ is singular (i.e., $\mathrm{rank}(\boldsymbol{N}) < n$, where n is the number of fitted parameters). In the singular case $\hat{\boldsymbol{x}}$ is not unique, yet $Q(\hat{\boldsymbol{x}})$ has a well-defined value (which may be 0 or positive).

Analogous to Eq. (8), in the joint solution we minimize the total goodness of fit,

$$\begin{aligned} Q(\boldsymbol{x}) \;=\; & Q_1(\boldsymbol{x}) + Q_2(\boldsymbol{x}) = Q_1(\hat{\boldsymbol{x}}_1) + Q_2(\hat{\boldsymbol{x}}_2) \\ & + (\boldsymbol{x} - \hat{\boldsymbol{x}}_1)'\boldsymbol{N}_1(\boldsymbol{x} - \hat{\boldsymbol{x}}_1) + (\boldsymbol{x} - \hat{\boldsymbol{x}}_2)'\boldsymbol{N}_2(\boldsymbol{x} - \hat{\boldsymbol{x}}_2). \end{aligned} \tag{9}$$

Here $\hat{\boldsymbol{x}}_i = \boldsymbol{N}_i^{-1}\boldsymbol{b}_i$ is the solution obtained by using only catalogue $i = 1, 2$, i.e., minimizing $Q_i(\boldsymbol{x})$, which results in the minimum value $Q_i(\hat{\boldsymbol{x}}_i)$. It is readily seen that Eq. (9) is minimized precisely for the joint solution vector in Eq. (6).

Each of the four terms in Eq. (9) has a simple interpretation. The first term, $Q_1(\hat{\boldsymbol{x}}_1)$, is the chi-square obtained when fitting the astrometric parameters only to the first set of data (in our case the Hipparcos data); similarly, $Q_2(\hat{\boldsymbol{x}}_2)$ is the chi-square obtained when fitting only to the second set of data (from *Gaia*). The sum of the last two terms is minimized for $\boldsymbol{x} = \hat{\boldsymbol{x}}$, and shows how much the chi-square is increased by forcing the *same* parameters to fit *both* sets of data in the joint solution. This quantity is useful for assessing whether the two datasets are mutually consistent and we therefore introduce a separate notation for it,

$$\Delta Q = (\hat{\boldsymbol{x}} - \hat{\boldsymbol{x}}_1)'\boldsymbol{N}_1(\hat{\boldsymbol{x}} - \hat{\boldsymbol{x}}_1) + (\hat{\boldsymbol{x}} - \hat{\boldsymbol{x}}_2)'\boldsymbol{N}_2(\hat{\boldsymbol{x}} - \hat{\boldsymbol{x}}_2). \tag{10}$$

The two terms give the increase in chi-square due to the first and second dataset, respectively.

Long-period astrometric binaries may have significantly different proper motions at the Hipparcos and *Gaia* epochs, and these in turn may differ from the mean proper motion between the epochs. If the differences are significant, compared with the measurement precisions, they will result in an increased value of ΔQ. The null hypothesis, namely that the star is astrometrically well-behaved, should be rejected if ΔQ exceeds a certain critical value. In order to calculate the critical value it is necessary to know the expected distribution of ΔQ under the null hypothesis.

Let m_i and $\nu_i = m_i - \mathrm{rank}(\boldsymbol{N}_i)$ be the number of observations and degrees of freedom in catalogue i. The number of degrees of freedom in the joint solution is $\nu = (m_1 + m_2) - \mathrm{rank}(\boldsymbol{N}_1 + \boldsymbol{N}_2)$. Under the null-hypothesis we have $Q_i(\hat{\boldsymbol{x}}_i) \sim \chi^2(\nu_i)$ $(i = 1, 2)$, $Q(\hat{\boldsymbol{x}}) \sim \chi^2(\nu)$, and consequently

$$\Delta Q \sim \chi^2(k), \tag{11}$$

where

$$k = \nu - \nu_1 - \nu_2 = \mathrm{rank}(\boldsymbol{N}_1) + \mathrm{rank}(\boldsymbol{N}_2) - \mathrm{rank}(\boldsymbol{N}_1 + \boldsymbol{N}_2). \tag{12}$$

In the special case when $\boldsymbol{N}_1$, $\boldsymbol{N}_2$, and $\boldsymbol{N}_1 + \boldsymbol{N}_2$ all have full rank (equal to n, the number of astrometric parameters) we have $k = n$. At a significance level of 1% the critical values of ΔQ, above which the null hypothesis should be rejected, are 15.086, 13.277, 11.345, 9.210, and 6.635 for $k = 5$, 4, 3, 2, and 1, respectively (e.g., Abramowitz & Stegun 2012). With this criterion only 1% of the well-behaved stars should be accidentally misclassified as not well-behaved. The expected distribution of ΔQ can be verified in the simulations which, by design, only includes well-behaved stars.

2.6. Reconstruction of $\boldsymbol{N}_H$, $\boldsymbol{b}_H$ for the Hipparcos Catalogue

When using the joint solution for incorporating Hipparcos data in the solution of early *Gaia* data it is necessary to reconstruct the normal matrix $\boldsymbol{N}_\mathrm{H}$ and the right hand side $\boldsymbol{b}_\mathrm{H}$ from Hipparcos for each star. These are initially calculated for the reference epoch of the Hipparcos Catalogue (J1991.25) and later propagated to the adopted reference epoch of the joint solution (see Sect. 2.7).

Let a_H, d_H, ϖ_H, $\dot{a}_\mathrm{H}$, $\dot{d}_\mathrm{H}$ be the astrometric parameters from the Hipparcos Catalogue after transformation into the SMOK notation (see Appendix A). The upper-left 5×5 submatrix of the covariance matrix can be taken without changes from the Hipparcos Catalogue (see Appendix B for details) since $\sigma_{\alpha*} = \sigma_a$, $\sigma_\delta = \sigma_d$, ... with sufficient accuracy at the reference epoch of the catalogue and provided that the SMOK comparison point is close enough to the astrometric parameters of the star. The sixth parameter $\dot{r}_\mathrm{H}$ and its corresponding entries in the covariance matrix need to be added from external sources or set to sensible values if not available (see below). Then the normal matrix is simply the inverse of the covariance matrix $\boldsymbol{N}_\mathrm{H} = \boldsymbol{C}_\mathrm{H}^{-1}$ and

$$\boldsymbol{b}_\mathrm{H} = \boldsymbol{N}_\mathrm{H}\left(a_\mathrm{H}, d_\mathrm{H}, \varpi_\mathrm{H}, \dot{a}_\mathrm{H}, \dot{d}_\mathrm{H}, \dot{r}_\mathrm{H}\right)' . \tag{13}$$

ESA (1997), Vol. 1, Eq. (1.5.69) shows how to reconstruct the elements $[\boldsymbol{C}_0]_{i6} = [\boldsymbol{C}_0]_{6i}$ $(i = 1 \ldots 6)$, that is the sixth column and row of the covariance matrix corresponding to the radial motion μ_r. Let $\bar{v}_r$, $\bar{\varpi}$, $\bar{\mu}_r$ be the true values and δv_r, $\delta\varpi$, $\delta\mu_r$ the errors. The expression in Eq. (1.5.69) for the diagonal element $[\boldsymbol{C}_0]_{66}$ is only valid if the relative uncertainties in the radial velocity and parallax are small, i.e., $|\delta v_r/\bar{v}_r|, |\delta\varpi/\bar{\varpi}| \ll 1$. If this is not the case we need to consider the complete expression for the calculated radial motion,

$$\mu_r = \bar{\mu}_r + \delta\mu_r = (\bar{v}_r + \delta v_r)(\bar{\varpi} + \delta\varpi)/A, \tag{14}$$

where $\bar{\mu}_r = \bar{v}_r\bar{\varpi}/A$, leading to

$$\delta\mu_r = (\bar{v}_r\delta\varpi + \bar{\varpi}\delta v_r + \delta v_r\delta\varpi)/A. \tag{15}$$

Squaring and taking the expectation while assuming that the errors in parallax and radial velocity are uncorrelated gives

$$E(\delta\mu_r^2) = \left(E(v_r^2\delta\varpi^2) + E(\varpi^2\delta v_r^2) + E(\delta v_r^2\delta\varpi^2)\right)/A^2, \tag{16}$$

where we replaced the true quantities by the observed ones. The third term is the required generalisation if v_r or ϖ is zero, or if

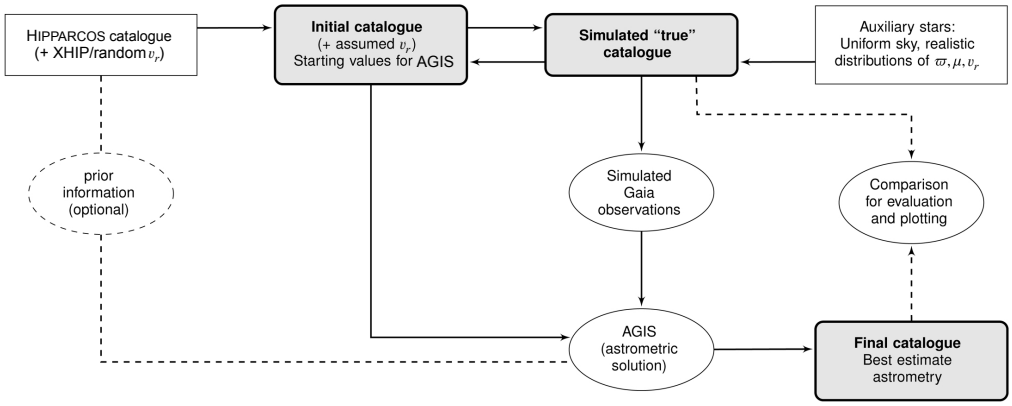

Fig. 1. Relationships between catalogues during simulation runs.

the relative errors are large. For example, if parallax and radial motion are unknown they could be assumed to be zero with a large uncertainty. The generalized version of Eq. (1.5.69) in ESA (1997) reads

$$[\boldsymbol{C}_0]_{66} = (v_{r0}/A)^2\,[\boldsymbol{C}_0]_{33} + (\varpi_0/A)^2\,\sigma^2_{vr0} + (\sigma_{vr0}/A)^2\,[\boldsymbol{C}_0]_{33},$$
$$[\boldsymbol{C}_0]_{i6} = [\boldsymbol{C}_0]_{6i} = (v_{r0}/A)\,[\boldsymbol{C}_0]_{i3}, \quad i = 1\ldots5. \tag{17}$$

The HIPPARCOS Catalogue contains numerous entries for non-single stars, for which additional parameters are given, describing deviations from uniform space motion. These additional parameters are ignored in our simulations, which regard every star as single. In the actual HTPM solution many of these stars may require more specialised off-line treatment. This is not further discussed in this paper.

2.7. Joint solution in AGIS

In reality the astrometric solution cannot be done separately for each star as described in Sect. 2.4 but must consider all the stars together with the spacecraft attitude and instrument calibration. Without prior information on the astrometric parameters this leaves the solution undetermined with respect to the reference frame. This is not the case for the joint solution, however, as the HIPPARCOS prior information contains positions and proper motions that are expressed in a specific reference frame, namely the HIPPARCOS realisation of the International Celestial Reference System (ICRS; Feissel & Mignard 1998). The incorporation of the HIPPARCOS prior in the joint solution automatically ensures that the resulting data are on the HIPPARCOS reference frame. If required, the data can later be transformed into a more accurate representation of the ICRS (see Sect. 5.3).

Due to the size of the data reduction problem, AGIS does not directly solve $\boldsymbol{N}\boldsymbol{x} = \boldsymbol{b}$ but iteratively improves the astrometric parameters by computing the updates $\Delta\boldsymbol{x}$, i.e., the difference to the current best estimate values. When incorporating HIPPARCOS data this requires us to also express the HIPPARCOS data (subscript H) as a difference to the current best estimate (subscript c). Therefore we construct

$$\Delta\boldsymbol{b}_{\rm H} = \boldsymbol{N}_{\rm H}\Delta\boldsymbol{x} = \boldsymbol{N}_{\rm H}\begin{pmatrix} a_{\rm H} - a_{\rm c} \\ d_{\rm H} - d_{\rm c} \\ \varpi_{\rm H} - \varpi_{\rm c} \\ \dot{a}_{\rm H} - \dot{a}_{\rm c} \\ \dot{d}_{\rm H} - \dot{d}_{\rm c} \\ \dot{r}_{\rm H} - \dot{r}_{\rm c} \end{pmatrix}. \tag{18}$$

Before solving we add the corresponding matrices for the *Gaia* data. If no additional *Gaia* data would be added the solution would immediately recover the HIPPARCOS Catalogue parameters.

The reference epoch of the joint solution can be arbitrarily chosen. In practice the *Gaia* data are much better than the HIPPARCOS data, therefore the optimal reference epoch would always be very close to the epoch of the *Gaia* data alone. Assuming one releases *Gaia*-only data and HTPM results at the same time it might be convenient to publish both for the same reference epoch, i.e., the *Gaia*-only reference epoch of the data release.

3. Simulations

3.1. Logic of simulations

Simulations are based on AGISLab (Holl et al. 2012), a small-scale version of the AGIS data reduction created and maintained at Lund Observatory. It is used to aid the development of algorithms for the astrometric data reduction of *Gaia*. Simulation runs are carried out in the following steps (cf. Fig. 1):

1. Creating catalogues of all the stars used in the simulation, namely the HIPPARCOS stars and the auxiliary stars (see below). Two catalogues are needed: a simulated "true" catalogue to generate *Gaia* observations and to evaluate the uncertainties of the astrometric performance, and an initial catalogue of starting values for the data reduction.
2. Simulating observations of the stars using the Nominal Scanning Law (de Bruijne et al. 2010), including perturbations according to the expected precision of *Gaia* measurements.
3. Improving the astrometry of the initial catalogue through the astrometric solution (AGIS), resulting in the final catalogue. This can be done with or without incorporation of prior information from HIPPARCOS.
4. Evaluating the error of the resulting solution by comparing the final catalogue with the true catalogue.

Details of the first two steps are given below, while remaining steps are covered in Sect. 4.

3.2. Simulating the stellar catalogues

All catalogues consist of two parts, the HIPPARCOS stars and the additional auxiliary stars. The HIPPARCOS stars are necessary for the realisation of the HTPM scheme, and 113 396 stars

are within the nominal magnitude range of *Gaia* ($G \simeq 6$–20). In order to obtain a reliable astrometric solution with a realistic modelling of the attitude constraints we find that a minimum of one million stars is needed, uniformly distributed on the sky. 886 604 auxiliary stars are therefore added to the HIPPARCOS stars in the solution. The astrometric results for the auxiliary stars are not included in the statistics for the HTPM performance, which is based only on the results for the HIPPARCOS stars. However, they contribute indirectly to the HTPM solution via the attitude.

3.2.1. Simulated "true" catalogue

The true catalogue defines the stars used for creating the simulated *Gaia* observations. For the real mission the true catalogue is of course not known.

To derive the HIPPARCOS portion of the true catalogue we assume that the true parameters deviate from the HIPPARCOS values by random amounts consistent with the HIPPARCOS covariances. The HIPPARCOS Catalogue is taken from CDS and contains the astrometric parameters for the reference epoch J1991.25, including their covariance matrices (Appendix B). For each star let $\boldsymbol{C}$ be its covariance matrix, $\boldsymbol{L}$ the lower triangular matrix resulting from the Cholesky decomposition $\boldsymbol{C} = \boldsymbol{L}\boldsymbol{L}'$, and $\boldsymbol{g}$ a vector of six independent standard Gaussian random variables (zero mean, unit standard deviation). Then the true parameters (subscript T) are obtained by applying the error vector $\boldsymbol{e} = \boldsymbol{L}\boldsymbol{g}$ to the astrometric parameters from the HIPPARCOS Catalogue (subscript H):

$$\boldsymbol{x}_{\mathrm{T}} = \boldsymbol{x}_{\mathrm{H}} + \boldsymbol{e}. \tag{19}$$

Since $E(\boldsymbol{g}) = \boldsymbol{0}$, where $E(\ldots)$ denotes the expectation value, it follows that $E(\boldsymbol{e}) = \boldsymbol{0}$. Moreover, since $E(\boldsymbol{g}\boldsymbol{g}') = \boldsymbol{I}$ (the identity matrix), it is readily verified that $\boldsymbol{e}$ has the desired covariance $E(\boldsymbol{e}\boldsymbol{e}') = \boldsymbol{C}$. For a joint solution with simulated *Gaia* data the HIPPARCOS Catalogue needs to be propagated to the reference epoch used in the solution.

Rigorous propagation of the astrometric parameters must take into account the radial motions of the stars, for which radial velocities are needed. We use data from XHIP (Anderson & Francis 2012), a compilation of radial velocities and other data for the HIPPARCOS stars from 47 different sources. We only use radial velocities with quality flag "A" or "B" in XHIP. This makes for a total of 40 171 radial velocities which are used as true values in our simulations. For the remaining HIPPARCOS stars we assign random radial velocities from a Gaussian distribution with $v_r = 0$, $\sigma_{vr} = 30$ km s^{-1} using Eq. (19), based on the assumption that radial velocities are typically smaller than that. The radial velocity uncertainty (taken from XHIP or using 30 km s^{-1}) is also used to expand the 5×5 covariance matrix by a sixth column and row for the uncertainty and correlation of the radial motion, using Eq. (17).

For the auxiliary stars, the positions are chosen to give a random uniform distribution across the sky with a mean density of about 21 stars deg^{-2}, corresponding to one million stars needed for the solution. We assume magnitude $G = 13$ for all auxiliary stars. Since the number density of actual stars with $G \leq 13$ is about 60 deg^{-2} at the Galactic poles, the assumed distribution is a rather conservative estimate of the density of bright stars available for the astrometric solution. The parallaxes of the auxiliary stars are assumed to have a log-normal distribution with median parallax 2.5 mas and a standard deviation of 0.6 dex[4]. The true proper motions and radial velocities are calculated by assuming an isotropic velocity distribution relative to the Sun with a standard deviation of 30 km s^{-1}.

3.2.2. Initial catalogue and astrometric solution

The initial catalogue contains the starting values for the data processing. The HIPPARCOS portion of it is identical to the astrometric parameters read from the HIPPARCOS Catalogue. For the auxiliary stars the initial positions are obtained by perturbing the true positions with Gaussian noise of standard deviation 100 mas in each coordinate, while the initial parallax and proper motion are set to zero. This is similar to a real life scenario where one would assume initial stellar positions from ground based observations or the first published *Gaia* positions without additional knowledge on the parallax or proper motion. The astrometric values in the initial catalogue are subsequently updated by the AGIS processing, resulting in the final catalogue once the solution is found. We do not solve for the radial motion but set the radial velocity to either zero (assuming no knowledge about it) or the true value (assuming it is perfectly known). In the first case perspective acceleration may show up for some stars as discrepancies in the solution, which disappear when the true radial velocities are used instead (see Sect. 4.3).

3.2.3. Final catalogue

The final catalogue contains the astrometric parameters after data processing. The difference to the simulated true catalogue gives the final errors of the reduced data and is used to evaluate the quality of the astrometric results. In this evaluation we focus on the improvement in the astrometric parameters of the HIPPARCOS stars.

3.3. Simulating Gaia observations

The observations of the one million stars described above are simulated using the Nominal Scanning Law of *Gaia*. We neglect so called "dead time" (when no data can be accumulated for example due to orbit maintenance manoeuvres and micrometeoroid hits), which may amount to up to 15% of the mission time. We do, however, account for the dead time originating from stellar transits coinciding with gaps between the CCDs in the focal plane, i.e., our simulations remove such observations before further processing of the data.

To account for observation noise, i.e., the expected centroiding performance of *Gaia*, we use a simplified noise model that ignores the gating scheme that *Gaia* exploits for bright star detection. This noise model assumes a constant centroiding performance for all HIPPARCOS stars, identical to the centroiding performance for the brightest ungated stars at magnitude 13. The typical along-scan standard error due to photon statistics is 94 μas. A second noise component is added to account for various effects, such as attitude modelling errors (Risquez et al. 2013) and uncertainties originating from geometrical calibration parameters of the spacecraft. Although this additional noise component may be correlated between individual CCD observations, we model it by quadratically adding a conservative RMS value of 300 μas to the photon statistical standard error per CCD.

[4] Neglecting extinction, this corresponds to a Gaussian distribution of absolute magnitudes M_{G} with mean value +5 and standard deviation 3 mag. This is not unreasonable for a local magnitude-limited stellar sample; cf. the HR diagram for nearby HIPPARCOS stars, such as Fig. 1 in Dehnen & Binney (1998). The assumed distribution of true parallaxes and proper motions has some impact on our case B simulation results as discussed in Sect. 5.2.

Table 1. Number of astrometric parameters per star estimated in the four astrometric solution scenarios.

	Case A (optimistic)		Case B (conservative)	
	Gaia 12	HTPM	*Gaia* 12	HTPM
HIPPARCOS stars	5	5	2	5
Auxiliary stars	5	5	2	2

Based on the current *Gaia* data release scenario[5] we assume that the HTPM project will initially be based on one year of *Gaia* data. The simulation results presented in Sect. 4 use one year of *Gaia* observations centred around the adopted reference epoch J2015.0.

4. Results

4.1. Astrometric solution scenarios

Table 1 gives an overview of the four different solution scenarios investigated in this paper. The two cases called *Gaia* 12 do not use any prior data from the HIPPARCOS Catalogue, but only the 12 months of *Gaia* observations. The other two, called HTPM, use the HIPPARCOS covariances and astrometric parameters as priors in the processing of the same *Gaia* observations as in *Gaia* 12. A comparison between the HTPM and *Gaia* 12 scenarios thus allows one to assess the improvement brought by the HIPPARCOS prior information.

The scenarios are subdivided into cases A and B. In case A we assume that there is sufficient *Gaia* data to perform a full five-parameter astrometric solution for all stars even without the HIPPARCOS prior. This is an optimistic assumption, since in reality one year of data is only barely sufficient for a five-parameter solution under ideal conditions, i.e., without data gaps. Dead time as outlined before and the actual temporal distribution of observations over the year could mean that the solution must be constrained to estimate only the two positional parameters for most of the stars. We simulate this in case B by conservatively assuming that all stars for which we do not include a prior will have a two-parameter solution. In such a solution the parallaxes and proper motions are effectively assumed to be zero, which gives a large additional error component in the estimated positions[6]. While the *Gaia* 12-B solution is then restricted to two parameters for all stars, HTPM-B can still solve all five parameters of the HIPPARCOS stars. Case B might be closer to the foreseen first release of *Gaia* data and the first release of HTPM. Case A on the other hand demonstrates the capabilities of *Gaia* and HTPM once sufficient data for a full astrometric solution are available in subsequent releases of *Gaia* data.

4.2. Predicted astrometric accuracies of HTPM

Table 2 summarizes the results for the entire set of HIPPARCOS stars, and subdivided by magnitude. No results are given for the auxiliary stars, but they are similar to the results for the HIPPARCOS stars in the *Gaia* 12 scenarios. For comparison we also give the formal uncertainties from the HIPPARCOS Catalogue. For the positions they are given both at the original epoch J1991.25 and at the epoch J2015 of the *Gaia* data. It should be noted that the simulations include stars which in the HIPPARCOS Catalogue are described with more than five parameters, but are here treated as single stars. Excluding them from the statistics would systematically reduce the HIPPARCOS uncertainties in Table 2. The real HTPM solution will also include all HIPPARCOS stars independent of the type of solution in the HIPPARCOS Catalogue. A poor fit between the *Gaia* and HIPPARCOS data will then be used to filter out binary candidates for further treatment.

All *Gaia* 12 and HTPM uncertainties in Table 2 are derived from the distribution of the actual errors (calculated values minus true values) obtained in the solutions, using the robust scatter estimate (RSE)[7]. Rather than stating the uncertainty of α and δ separately we give the mean of the RSE in the two coordinates as the position uncertainty. Similarly the proper motion uncertainty is the mean RSE of the errors in $\mu_{\alpha*}$ and μ_δ.

Proper motion. The joint solution shows a big improvement in the proper motion uncertainties compared with the HIPPARCOS data. The improvement factor of HTPM compared with HIPPARCOS alone is 32 in case A and 25 in case B. The factors are similar because the HIPPARCOS position uncertainty dominates over the *Gaia* uncertainty in both cases. In the optimistic case A, the proper motions from the *Gaia*-only data are already better than HIPPARCOS alone, but not as good as the joint HTPM solution.

Using Eq. (3) to estimate the expected precision of the conventional combination we find in case A proper motions of 16 and 137 μas yr^{-1} for the brightest and faintest magnitude bins, compared with 14 and 94 μas yr^{-1} in the HTPM-A results. In case B we find 143 and 602 μas yr^{-1}, respectively, compared with 27 and 134 μas yr^{-1} in HTPM-B. The joint solution thus gives consistently better results, as discussed in Sect. 2.4.

Parallax. The improved proper motions allow better to disentangle the five parameters in the joint astrometric solution (cf. Fig. 3), resulting in improved parallax uncertainties. In case A we find that the parallax uncertainties in the joint solution improve by a factor 23 compared with HIPPARCOS, and a factor 2 compared with *Gaia* 12. However, in the more realistic case B the improvement is much smaller (a factor 3 compared with HIPPARCOS) and the parallaxes are strongly biased as shown in Fig. 2. This bias originates from the assumption of zero parallax and proper motion in the two-parameter solution of the auxiliary stars. The true positive parallaxes result in a biased attitude, which propagates into the five-parameter solution of the HIPPARCOS stars making their parallaxes systematically too small. (As discussed in Sect. 5.2, this bias can be entirely avoided in later releases of *Gaia* data through a proper selection of primary sources.)

[5] See http://www.cosmos.esa.int/web/gaia/release (2014 July 23). The first release of *Gaia* data is foreseen for summer 2016. Discounting in-orbit commissioning, ecliptic pole scanning, and time for data processing leaves us with about one year of *Gaia* data.

[6] Forcing a two-parameter solution in case B for the stars without a prior creates residuals that are much larger than the formal uncertainties of the *Gaia* observations. The astrometric solution copes with this situation by means of the excess noise estimation described in Sect. 3.6 of Lindegren et al. (2012). Effectively this reduces the weight of the *Gaia* observations but does not affect the HIPPARCOS prior. Without excess noise estimation the errors of the HTPM proper motions in case B would be several times larger.

[7] The RSE is defined as 0.390152 times the difference between the 90th and 10th percentiles of the distribution of the variable. For a Gaussian distribution it equals the standard deviation. Within the *Gaia* core processing community the RSE is used as a standardized, robust measure of dispersion (Lindegren et al. 2012).

Table 2. Predicted uncertainties of the astrometric parameters of the HIPPARCOS stars.

Mag.	Number	Position [μas]						Parallax [μas]					Proper motion [μas yr^{-1}]				
		Hip	Hip_{2015}	*Gaia* 12		HTPM		*Hip*	*Gaia* 12		HTPM		*Hip*	*Gaia* 12		HTPM	
				A	B	A	B		A	B	A	B		A	B	A	B
6–7	9381	367	10 892	41	3388	36	312	501	82	–	43	250[a]	458	207	–	14	27
7–8	23 679	497	14 434	41	2692	35	318	684	81	–	43	261[a]	608	204	–	19	30
8–9	40 729	682	19 947	41	2369	35	330	939	77	–	43	271[a]	840	197	–	26	35
9–10	27 913	936	27 629	40	2663	35	333	1284	77	–	43	274[a]	1165	194	–	35	43
10–11	8563	1403	41 352	42	5240	36	343	1921	83	–	46	283[a]	1744	205	–	50	60
11–12	2501	2125	61 896	41	13 687	35	357	2882	78	–	47	291[a]	2607	195	–	70	85
≥12	630	3248	109 030	42	13 926	38	378	4291	80	–	51	295[a]	4578	209	–	94	134
all	113 396	753	22 148	41	2856	35	328	1033	79	–	44	271[a]	932	199	–	29	38

Notes. We compare the HIPPARCOS data alone (Hip) with a solution using only 12 months of *Gaia* data (*Gaia* 12), and a joint solution of HIPPARCOS and *Gaia* data (HTPM). Case A and B refer to the optimistic and conservative scenarios, respectively, described in the text. The two rightmost columns give the predicted HTPM proper motion uncertainties in the two cases. [(a)] Case B parallaxes are biased as shown in Fig. 2. This bias is not included in the RSE values given here.

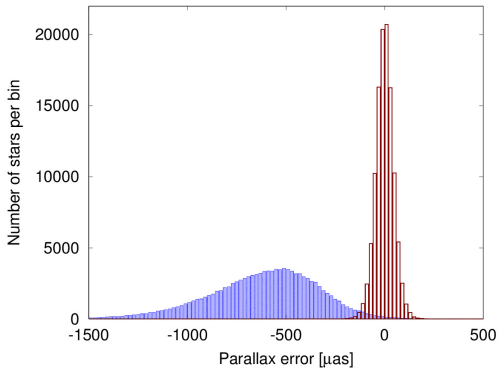

Fig. 2. Parallax errors in the HTPM solution for two cases. Bin width is 20 μas. In case A (full five-parameter astrometric solution for all stars, red/right histogram) the parallax errors are unbiased. In case B (two-parameter solution of the auxiliary stars, blue/left histogram) the median parallax error is −591 μas.

Position. The extremely good *Gaia* observations lead to an improvement by up to a factor ∼600 compared with HIPPARCOS positions propagated to J2015. In case A the slight improvement in the HTPM positions compared with *Gaia* 12 comes from the better determination of proper motion and parallax. In case B the *Gaia*-only positions show a high uncertainty due to the two-parameter solution which neglects the true parallaxes and proper motions of the stars. The increase in position uncertainties is especially pronounced for the fainter stars due to preferential selection of nearby high-proper motion stars in the non-survey part of the HIPPARCOS Catalogue, which means that their (neglected) parallaxes and proper motions are statistically much larger than for the brighter (survey) stars. In the HTPM solution for case B all five parameters are solved for the HIPPARCOS stars, so the sizes of their parallaxes and proper motions have no direct impact on the accuracy of the solution. However, the positional uncertainties are still much increased compared with case A, because the two-parameter solutions for the auxiliary stars degrade the attitude estimate.

4.3. Goodness of fit statistics

As discussed in Sect. 2.5 the goodness of fit value ΔQ from Eq. (10) describes how well the joint astrometric solution fits the individual observations of both missions together. If all the observations are consistent with the kinematic model, then ΔQ is expected to follow a χ^2 distribution with five degrees of freedom. Larger values indicate deviations from the model, for example non-uniform motion caused by invisible companions or astrometric binaries. In the present simulations we do not include any such objects, so we expect ΔQ to follow the theoretical distribution.

The top two diagrams in the left column in Fig. 4 shows that this is indeed true in case A, if the radial velocities assumed in the solution are the true ones. The result would have been the same if the assumed radial velocities had only been wrong by a few km s^{-1}. If instead we assume zero radial velocities for all stars, as was done in the bottom two diagrams (while the observations were still generated with non-zero radial velocities), we find a small number of outliers. It turns out that all of them are nearby, high-velocity stars (Table 3) expected to show significant perspective acceleration, that is the change in proper motion due to the changing stellar distance and the changing angle between the line of sight and motion of the star (Schlesinger 1917; van de Kamp 1977; Murray 1983). This perspective acceleration is not taken into account in the solution when the radial velocities are assumed to be zero, giving a mismatch between the HIPPARCOS data and the observed *Gaia* position. The positional offset due to the perspective acceleration after Δt years amounts to

$$\Delta\theta_{\text{persp}} = \mu\mu_r\Delta t^2, \tag{20}$$

where $\mu = (\mu_{\alpha*}^2 + \mu_\delta^2)^{1/2}$ is the total proper motion. As shown in Table 3, the stars with a large ΔQ also have a large offset $\Delta\theta_{\text{persp}}$ at the *Gaia* epoch, compared with the positional uncertainty of the solution at that epoch.

This demonstrates that knowledge of radial velocities is required for a number of stars to avoid false positives in the detection of non-uniform space motion (de Bruijne & Eilers 2012). It also shows that ΔQ is a useful statistic for detecting non-uniform space motion in general.

The right column in Fig. 4 shows the corresponding results in case B. Here ΔQ follows a scaled version of the expected distribution with a somewhat extended tail. The two bottom panels show that ΔQ is still a useful measure of deviations from the adopted kinematic model although it is much less sensitive than in case A. As a result only two outliers due to the perspective acceleration are found if the assumed radial velocities are set to zero. This demonstrates the strong dependency of ΔQ on the quality of the *Gaia* solution.

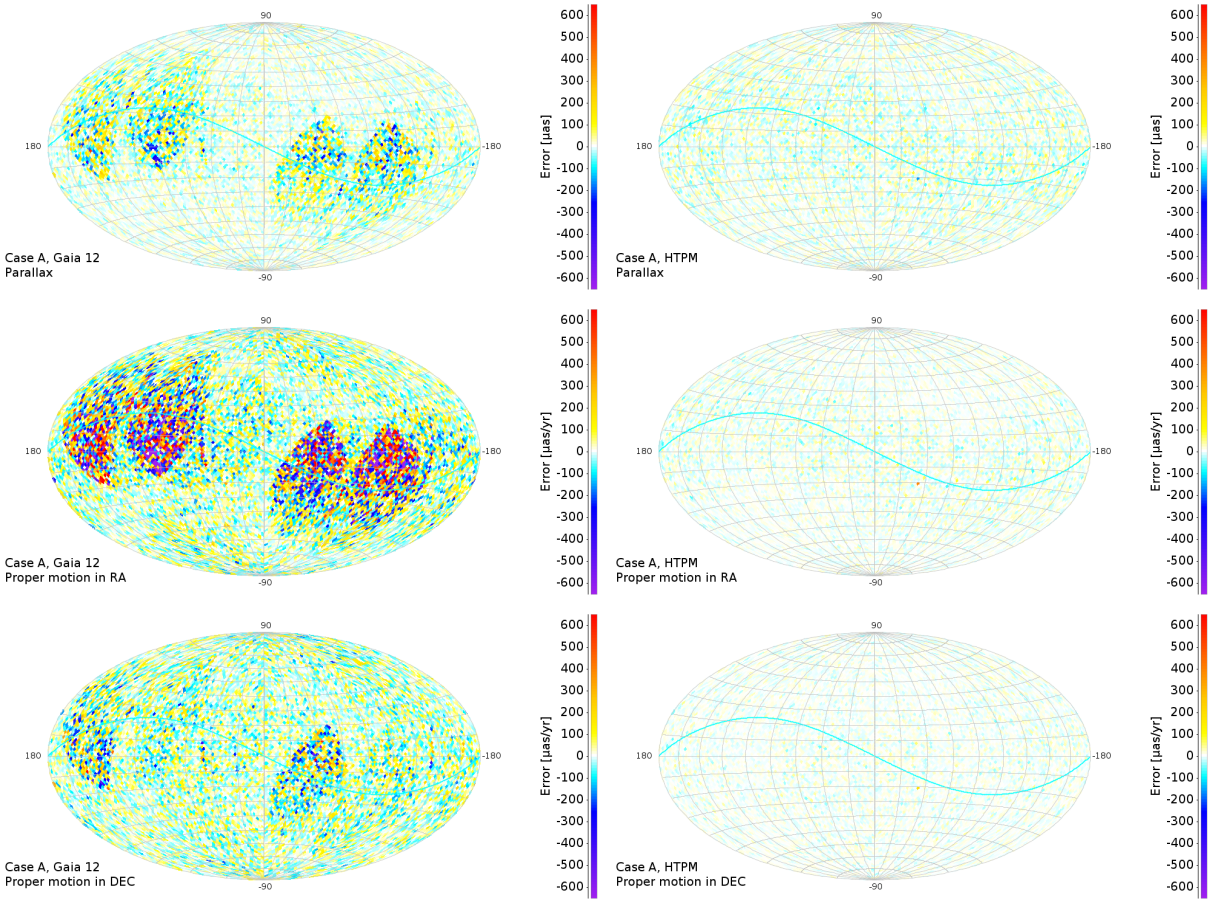

Fig. 3. Distribution of the parallax and proper motion errors on a Hammer-Aitoff equatorial projection of the sky. All maps are for case A (full five-parameter solutions for all stars). *Left figures*: results from the 12 months' *Gaia*-only simulation. Some regions of the sky are poorly observed resulting in zonal errors. *Right figures*: HTPM results for the same stars. The prior helps to disentangle proper motion and parallax, therefore we find a more homogeneous distribution of errors at an overall lower level. The cyan line follows the ecliptic for reference.

5. Discussion

5.1. Longevity of the HTPM solution: detection of binary and exoplanetary candidates

As *Gaia* collects further data the accuracy of the proper motions determined from *Gaia* data alone will eventually supersede that of HTPM. Assuming nominal mission performance and that the proper motion uncertainty scales with mission length as $L^{-1.5}$, this will happen already after 2–3 years of *Gaia* data have been accumulated. Still, HTPM will remain a valuable source of information as it is based on a much longer time baseline. This is relevant for long period companions which create astrometric signatures that cannot be seen in *Gaia* data alone. We therefore suggest that HTPM should be repeated with future *Gaia* releases. The goodness-of-fit of the combined solution is sensitive to small deviations of the stellar motions from the assumed (rectilinear) model. This sensitivity will dramatically increase with more *Gaia* data, namely when the *Gaia*-only proper motions become as good as the combined HTPM proper motions.

The potential for detecting faint (stellar or planetary) companions to nearby stars can be illustrated by a numerical example. Consider a 1 $M_\odot$ star at 10 pc distance (ϖ = 100 mas) from the Sun, with an invisible companion of mass m orbiting at a period of $P \simeq 25$ years (semi-major axis $a \simeq 8.5$ au). The astrometric signature of the companion (i.e., the angular size of the star's orbit around their common centre of mass; Perryman 2014) is $a_* \simeq a\varpi(m/M_\odot) \simeq 850(m/M_\odot)$ mas if the orbit is seen face-on, and the instantaneous proper motion of the star relative to the centre of mass is $2\pi a_*/P \simeq 200(m/M_\odot)$ mas yr^{-1}. If HIPPARCOS effectively measures this instantaneous proper motion which is extrapolated over $\Delta t = 25$ years, the extrapolated position from HIPPARCOS (with its uncertainty of about 22 mas, see Table 2) and the position observed by *Gaia* (with an uncertainty much lower than from HIPPARCOS) could differ by up to $\simeq$5000$(m/M_\odot)$ mas. Assuming that detection is possible if the position difference is at least twice as large as the positional uncertainty[8], we find that the initial HTPM results could be sensitive to companion masses down to $\simeq 10^{-2}$ $M_\odot$, that is brown dwarf or super-Jupiter companions.

If we instead let *Gaia* measure the instantaneous proper motion of the system and propagate backwards to the HIPPARCOS epoch, we can take advantage of the much better uncertainties

[8] Table 3 shows that ΔQ in case A may be sensitive to positional deviations at the *Gaia* epoch as small as 21 mas.

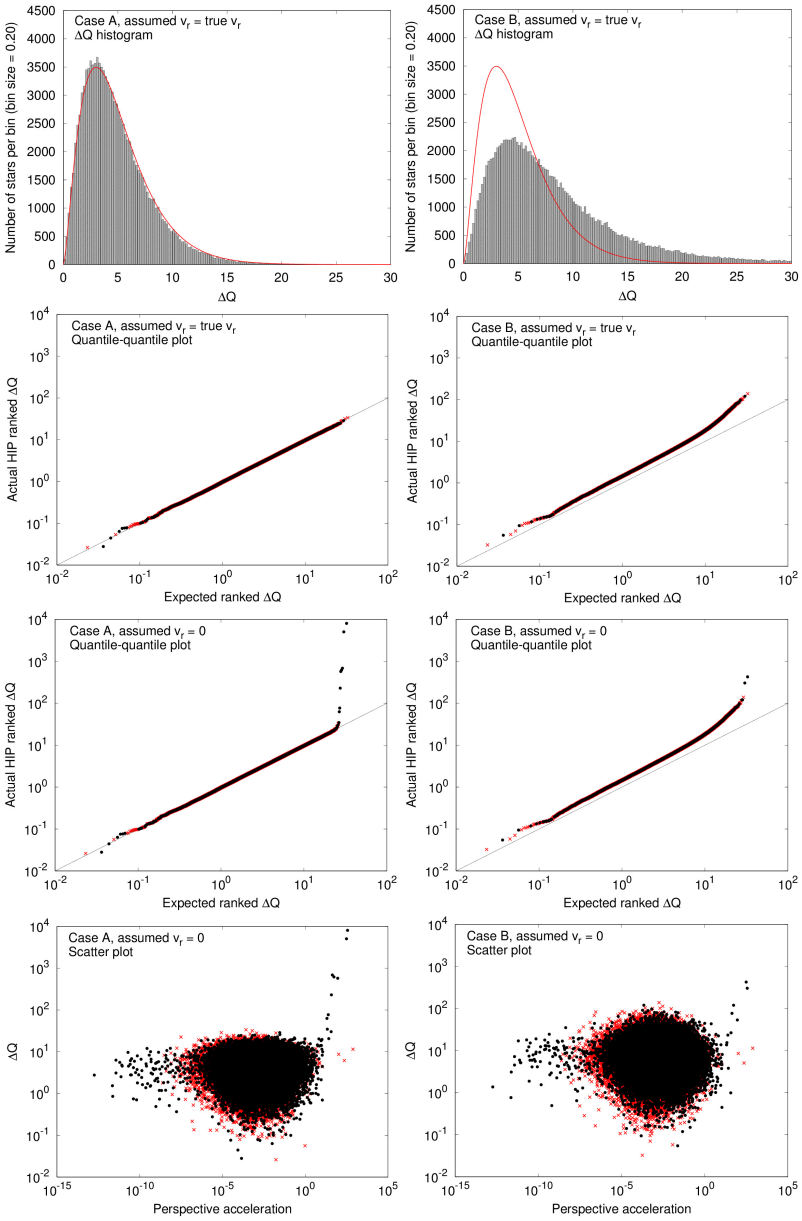

Fig. 4. *Left column*: Goodness of fit values ΔQ for case A simulations. *From top to bottom*, the ΔQ values (grey bars) follow a χ^2 distribution (red line) with five degrees of freedom. If the assumed radial velocities in the solution equal the true values, the actual and expected distributions agree perfectly. If the assumed radial velocity is unknown (set to zero) deviations from the expected distributions are seen. These outliers are caused by perspective acceleration. The markers in the quantile-quantile and scatter plots correspond to stars with radial velocities from XHIP (black dots) and to stars with random radial velocities (red crosses). The three rightmost red crosses in the scatter plots correspond to HIP 80190, HIP 80194, and HIP 67694 which have very large uncertainties in the HIPPARCOS Catalogue. Therefore they do not show a large ΔQ value even though they have large perspective acceleration. *Right column*: same plots for case B simulations (see Sect. 2.5).

of the *Gaia* astrometry. Two to three years of *Gaia* data already give proper motion uncertainties better than 30 μas yr^{-1} for the bright stars, and hence extrapolated position uncertainties better than HIPPARCOS at its own epoch, or ≃0.75 mas (Table 2). Therefore the HTPM sensitivity increases roughly by a factor 30, allowing the detection of companion masses down to about 3×10^{-4} $M_\odot$, or Saturn-type objects at a Saturn-like distance to the host star.

This demonstrates that the results of HTPM can be used to find candidates for long period exoplanets around nearby stars, with a highly interesting companion mass range opening up with subsequent releases of *Gaia* data when combined with HIPPARCOS. These companions cannot be detected from *Gaia* data alone even at the full mission length, and are hard to detect through classical methods due to their long periods, low transit probability and small radial velocity signatures. Since ΔQ

Table 3. List of stars with $\Delta Q > 30$ in HTPM case A, with assumed radial velocities set to zero.

HIP	ΔQ	Hp	ϖ [mas]	$\sqrt{\mu_{\alpha*}^2+\mu_\delta^2}$ [mas yr^{-1}]	v_r [km s^{-1}]	μ_r [mas yr^{-1}]	$\Delta\theta_{\rm persp}$ [mas]	Remark
87937	8 044.46	9.490	548.31	10 358.94	−110.51	−12 782.22	361.87	Barnard's star
24186	5 053.12	8.932	255.66	8 669.40	245.19	13 223.43	312.01	Kapteyn's star
57939	686.11	6.564	109.99	7 059.03	−98.35	−2 281.95	43.72	Groombridge 1830
104217	618.09	6.147	285.88	5 172.58	−64.07	−3 863.82	54.70	61 Cyg B[a]
54035	572.73	7.506	392.64	4 801.04	−84.69	−7 014.64	92.31	
70890	229.59	10.761	771.64	3 852.57	−22.40	−3 646.21	38.32	Proxima Centauri
74235	76.86	9.200	34.65	3 681.26	310.12	2 266.79	24.80	
439	62.69	8.618	230.42	6 100.36	25.38	1 233.65	20.64	
74234	34.62	9.568	35.14	3 680.96	310.77	2 303.67	21.63	
54211	30.13	8.803	206.27	4 510.10	68.89	2 997.58	36.97	

Notes. The threshold 30 was set for a probability of false alarm $\sim 10^{-5}$, assuming that ΔQ follows the χ^2 distribution with 5 degrees of freedom. The columns contain the HIPPARCOS identifier, HIPPARCOS magnitude, parallax, and total proper motion (all from the HIPPARCOS Catalogue), the radial velocity from XHIP, and the calculated radial motion and positional offset over $\Delta t = 23.75$ yr due to perspective acceleration. [(a)] 61 Cyg A (HIP 104214) was not included in the simulations since it is brighter than the nominal *Gaia* bright star limit.

is sensitive to deviations from uniform space motion, whether they are seen in the HIPPARCOS or in the *Gaia* data, or both, this statistic can be used to find candidate systems in all these cases. The further exploration of the candidate systems will, however, require specialised analysis tools.

In a future publication we will explore in more detail how ΔQ can be used to identify binary and exoplanetary candidates with orbital periods of decades to centuries. Apart from the possibility to detect substellar companions for the nearest stars, this will contribute to the census of the binary population within a few hundred parsecs from the sun by filling a difficult-to-observe gap between the shorter period spectroscopic and astrometric binaries and the visually resolved long-period systems.

5.2. Two versus five parameters

When evaluating the results of our simulations, case B deserves additional attention since it is the more realistic case for the first *Gaia* data release, and the first simulation of this case published so far. The two-parameter solution (*Gaia* 12-B in Table 2) leads to a large position error of several mas. This is caused by assuming the parallax, proper and radial motion to be zero in the solution, whereas in reality they are not. The actual positional uncertainties in this case depend on the true distribution of parallaxes and proper motions for all the stars, including the auxiliary stars, which are not very well known. The numerical values given here are based on the very schematic distribution model for the auxiliary stars described in Sect. 3.2.1, and should therefore be interpreted with caution.

This position error is also relevant for the case B HTPM scenario, where the solution of the auxiliary stars is two parameters only, but where one solves all five parameters for the HIPPARCOS stars while incorporating prior information from the HIPPARCOS Catalogue. The position error of the auxiliary stars causes a poor attitude determination. This in turn leads to increased errors in the case B HTPM results (compare HTPM B and A in Table 2), with a bias in the parallax errors (see Sect. 4 and Fig. 2). For a parallax-unbiased solution it is necessary to estimate all five parameters for all stars included in the solution. Any mixture in the estimation of five and two parameters in the same solution will lead to a bias in the resulting parallaxes. This is not only true for the HTPM scenario described in this paper but also in all *Gaia*-only data releases. Referring to the terminology used in Sect. 6.2 of Lindegren et al. (2012), any star for which not all five astrometric parameters can be solved must be treated as a "secondary source", meaning that it does not contribute to the attitude determination and instrument calibration. This is necessary in order to avoid biases for the stars where all five parameters are estimated.

5.3. Frame rotation of the combined solution

For the final AGIS solution of *Gaia* the reference frame will be established by means of quasars, both by linking to the optical counterparts of radio (VLBI) sources defining the orientation of the International Celestial Reference Frame, and by using the zero proper motion of quasars to determine a non-rotating frame[9]. This can also be done for earlier *Gaia* data releases, at least for the orientation part, while the shorter time span will limit the determination of the spin. It is desirable to rotate the HTPM results into the same reference frame as used for the first *Gaia* data release. This must be done in two steps. First, a provisional HTPM must be computed in the HIPPARCOS frame (as it will be when the HIPPARCOS data are used as prior, see Sect. 2.7), without imposing any other constraints on the frame. This solution will contain (many) non-HIPPARCOS stars with only *Gaia* observations which include a multitude of quasars. Their positions and proper motions are used in a second step to correct the provisional HTPM (and other data in the same solution) for the estimated orientation and spin. Since the HTPM solution is integrated in AGIS, the estimation and correction of the frame can be accomplished using the procedures and tools developed for AGIS (Lindegren et al. 2012, Sect. 6.1).

5.4. Other applications of the joint solution method

The joint solution is applicable also to other combinations of astrometric data. Here we give two examples.

Nano-JASMINE (Hatsutori et al. 2009; Yamada et al. 2013) is an ultra-small Japanese satellite, a technology demonstrator for the JASMINE series of near-infrared astrometry missions, scheduled for launch in 2015. It targets bright stars between magnitude 1 and 10, although the exact limits are not yet determined. Based on current performance estimates the uncertainties

[9] The apparent proper motion of quasars due to the Galactocentric acceleration is expected to have an amplitude of ~ 4 μas yr^{-1} and is taken into account when determining the spin of the reference frame.

in stellar parameters will be similar to or slightly worse than the uncertainties of the HIPPARCOS data. However, the data will still be very valuable since astrometric catalogues are best at their respective epochs and Nano-JASMINE may be the only astrometric mission at its epoch observing the brightest stars in the sky. The Nano-JASMINE data can be analysed together with HIPPARCOS data analogously to the HTPM project to improve the proper motions of bright stars that may not be observed by *Gaia* (Michalik et al. 2013).

The *Tycho-2* Catalogue (Høg et al. 2000) gives positions for 2.5 million stars, derived from starmapper observations of HIPPARCOS. The positions at the reference epoch J1991.25 have a median internal standard error of 7 mas for stars brighter than $V_T = 9$ mag and 60 mas for the whole catalogue. Combining the *Tycho-2* positions with *Gaia* data using the joint solution scheme would allow us to derive proper motions for these stars with median uncertainties of 0.3 and 2.5 mas yr^{-1}, respectively. This is true even in the conservative scenario (*Gaia* 12-B), since the major uncertainty comes from the *Tycho-2* positions. In this combination the proper motions given in *Tycho-2* should not be used, as they may contain systematic errors of a similar magnitude due to the incorporated old photographic material. However, the derived proper motions from a *Tycho-Gaia* Astrometric Solution (TGAS) could be used to correct the photographic positions in order to take advantage of a much longer temporal baseline.

6. Conclusions

We have developed the joint solution method for incorporating priors in the core astrometric solution of *Gaia*. The method can be used in the processing of early *Gaia* data to improve the proper motions of the HIPPARCOS stars, the so-called Hundred Thousand Proper Motions project.

Combining astrometric data from very different epochs requires careful treatment of the non-linear effects of the mapping from spherical to rectilinear coordinates and for high velocity stars due to perspective acceleration. Therefore we have introduced a scaled model of kinematics (SMOK), which allows one to handle these effects in a simple and rigorous manner.

Using simulations we have verified that HTPM, using the joint solution method, gives the expected large improvements in proper motion uncertainties for over 100 000 stars in the HIPPARCOS Catalogue. The predicted proper motion uncertainties range from 14 to 134 μas yr^{-1} depending on the amount of *Gaia* data used and the stellar magnitude, about a factor 30 improvement compared with the HIPPARCOS uncertainties.

We have shown that HTPM also delivers improved parallaxes, which, however, may be strongly biased unless a full five-parameter solution can be obtained from *Gaia*-only data also for all non-HIPPARCOS stars. Whether these parallaxes should be published as part of an HTPM release should be decided based on the amount and quality of *Gaia* data available at the time.

The joint solution is applicable also to a combination of *Tycho-2* positions with early *Gaia* data to derive parallaxes and improved proper motions for the 2.5 million stars. We suggest that this possibility of a *Tycho-Gaia* Astrometric Solution (TGAS) should be considered in the *Gaia* data release plan.

The proposed method to calculate HTPM provides a goodness-of-fit measurement ΔQ which is sensitive to deviations from the uniform linear space motion. However, accurate radial velocities are required for nearby fast moving stars in order to avoid mistaking outliers in ΔQ for companion signatures. We recommend to publish ΔQ as well as the radial velocities used for the HTPM data reduction. This will allow further investigations of outliers which might indicate binary or exoplanetary candidates, and will permit a correction of the HTPM results if better radial velocities become available.

The full power of HTPM will not be reached with the first *Gaia* data, but only in subsequent releases benefiting from the increased sensitivity of ΔQ with improved *Gaia* results. Because of the long temporal baseline and the combination of current with historic astrometry, HTPM will remain relevant throughout the final *Gaia* release for the detection and measurement of binary and exoplanetary candidates.

Acknowledgements. We thank F. van Leeuwen for clarification on certain data items in the HIPPARCOS Catalogue and for providing valuable feedback as the referee. We also thank C. Fabricius for many useful comments. This work was partly carried out under ESA Contract No. 4000105564/12/NL/GE. Support from the Swedish National Space Board and the Royal Physiographic Society in Lund is gratefully acknowledged.

References

Abramowitz, M., & Stegun, I. 2012, Handbook of Mathematical Functions (New York: Dover Publications)
Anderson, E., & Francis, C. 2012, Astron. Lett., 38, 331
Bombrun, A., Lindegren, L., Holl, B., & Jordan, S. 2010, A&A, 516, A77
Brinker, R. C., & Minnick, R. 1995, The Surveying Handbook, 2d. edn. (Dordrecht: Kluwer)
de Bruijne, J., Siddiqui, H., Lammers, U., et al. 2010, in Relativity in Fundamental Astronomy: Dynamics, Reference Frames, and Data Analysis, eds. S. A. Klioner, P. K. Seidelmann, & M. H. Soffel, IAU Symp., 261, 331
de Bruijne, J. H. J., & Eilers, A.-C. 2012, A&A, 546, A61
Dehnen, W., & Binney, J. J. 1998, MNRAS, 298, 387
Dravins, D., Lindegren, L., & Madsen, S. 1999, A&A, 348, 1040
Eichhorn, H., & Rust, A. 1970, Astron. Nachr., 292, 37
ESA 1997, The HIPPARCOS and Tycho Catalogues (Noordwijk: ESA), ESA SP, 1200
Feissel, M., & Mignard, F. 1998, A&A, 331, L33
Hatsutori, Y., Suganuma, M., Kobayashi, Y., et al. 2009, Transactions of Space Technology Japan, 7, 19
Høg, E., Fabricius, C., Makarov, V. V., et al. 2000, A&A, 355, L27
Holl, B., Lindegren, L., & Hobbs, D. 2012, A&A, 543, A15
Lindegren, L., Lammers, U., Hobbs, D., et al. 2012, A&A, 538, A78
Michalik, D., Lindegren, L., Hobbs, D., Lammers, U., & Yamada, Y. 2012, in Astronomical Data Analysis Software and Systems XXI, ed. P. Ballester, D. Egret, & N. P. F. Lorente, ASP Conf. Ser., 461, 549
Michalik, D., Lindegren, L., Hobbs, D., Lammers, U., & Yamada, Y. 2013, in Advancing the Physics of Cosmic Distances, ed. R. de Grijs, IAU Symp., 289, 414
Mignard, F. 2009, The Hundred Thousand Proper Motions Project, Gaia Data Processing and Analysis Consortium (DPAC) technical note GAIA-C3-TN-OCA-FM-040
Murray, C. A. 1983, Vectorial astrometry (Bristol: Adam Hilger)
Perryman, M. 2014, The Exoplanet Handbook (Cambridge, UK: Cambridge University Press)
Risquez, D., van Leeuwen, F., & Brown, A. G. A. 2013, A&A, 551, A19
Schlesinger, F. 1917, AJ, 30, 137
Taff, L. G. 1981, Computational spherical astronomy (New York: Wiley-Interscience)
van Altena, W. F. 2013, Astrometry for Astrophysics (Cambridge, UK: Cambridge University Press)
van de Kamp, P. 1977, Vistas in Astronomy, 21, 289
van Leeuwen, F. 2007a, HIPPARCOS, the New Reduction of the Raw Data (Springer), Astrophys. Space Sci. Libr., 350
van Leeuwen, F. 2007b, A&A, 474, 653
Wilson, E. B., & Hilferty, M. M. 1931, Proc. of the National Academy of Science, 17, 684
Yamada, Y., Fujita, S., Gouda, N., et al. 2013, in Advancing the Physics of Cosmic Distances, ed. R. de Grijs, IAU Symp., 289, 429

Pages 13 to 15 are available in the electronic edition of the journal at http://www.aanda.org

Appendix A: Scaled modelling of kinematics (SMOK)

A formalism called SMOK is introduced in this paper to facilitate a rigorous manipulation of small (differential) quantities in the celestial coordinates. It is reminiscent of the "standard" or "tangential" coordinates in classical small-field astrometry (e.g., Murray 1983; van Altena 2013), using a gnomonic projection onto a tangent plane of the (unit) celestial sphere, but extends to three dimensions by adding the radial coordinate perpendicular to the tangent plane. This simplifies the modelling of perspective effects.

Figure A.1 illustrates the concept. In the vicinity of the star let $\boldsymbol{c}$ be a comparison point fixed with respect to the solar system barycentre (SSB). As shown in the diagrams:

1. The barycentric motion of the star is scaled by the inverse distance to $\boldsymbol{c}$, effectively placing the star on or very close to the unit sphere.
2. Rectangular coordinates are expressed in the barycentric $[\boldsymbol{p}_\mathrm{c}\ \boldsymbol{q}_\mathrm{c}\ \boldsymbol{r}_\mathrm{c}]$ system with $\boldsymbol{r}_\mathrm{c}$ pointing towards $\boldsymbol{c}$, and $\boldsymbol{p}_\mathrm{c}$, $\boldsymbol{q}_\mathrm{c}$ in the directions of increasing right ascension and declination.

The first point eliminates the main uncertainty in the kinematic modelling of the star due to its poorly known distance. The second point allows us to express the scaled kinematic model in SMOK coordinates a, d, r that are locally aligned with α, δ, and the barycentric vector.

Up to the scale factor $|\boldsymbol{c}|^{-1}$ discussed below, the SMOK coordinate system is completely defined by the adopted comparison point $(\alpha_\mathrm{c},\ \delta_\mathrm{c})$ using the orthogonal unit vectors

$$\boldsymbol{p}_\mathrm{c} = \begin{bmatrix} -\sin\alpha_\mathrm{c} \\ \cos\alpha_\mathrm{c} \\ 0 \end{bmatrix}, \quad \boldsymbol{q}_\mathrm{c} = \begin{bmatrix} -\sin\delta_\mathrm{c}\cos\alpha_\mathrm{c} \\ -\sin\delta_\mathrm{c}\sin\alpha_\mathrm{c} \\ \cos\delta_\mathrm{c} \end{bmatrix}, \quad \boldsymbol{r}_\mathrm{c} = \begin{bmatrix} \cos\delta_\mathrm{c}\cos\alpha_\mathrm{c} \\ \cos\delta_\mathrm{c}\sin\alpha_\mathrm{c} \\ \sin\delta_\mathrm{c} \end{bmatrix}. \tag{A.1}$$

$[\boldsymbol{p}_\mathrm{c}\ \boldsymbol{q}_\mathrm{c}\ \boldsymbol{r}_\mathrm{c}]$ is the "normal triad" at the comparison point with respect to the celestial coordinate system (Murray 1983)[10]. We are free to choose $(\alpha_\mathrm{c},\ \delta_\mathrm{c})$ as it will best serve our purpose, but once chosen (for a particular application) it is fixed: it has no proper motion, no parallax, and no associated uncertainty. Typically $(\alpha_\mathrm{c},\ \delta_\mathrm{c})$ is chosen very close to the mean position of the star.

The motion of the star in the Barycentric Celestial Reference System (BCRS) is represented by the function $\boldsymbol{b}(t)$, where $\boldsymbol{b}$ is the vector from SSB to the star as it would be observed from the SSB at time t. The scaled kinematic model $\boldsymbol{s}(t) = \boldsymbol{b}(t)|\boldsymbol{c}|^{-1}$ is given in SMOK coordinates as

$$a(t) = \boldsymbol{p}_\mathrm{c}'\boldsymbol{s}(t), \quad d(t) = \boldsymbol{q}_\mathrm{c}'\boldsymbol{s}(t), \quad r(t) = \boldsymbol{r}_\mathrm{c}'\boldsymbol{s}(t), \tag{A.2}$$

and can in turn be reconstructed from the SMOK coordinates as

$$\boldsymbol{s}(t) = \boldsymbol{p}_\mathrm{c}a(t) + \boldsymbol{q}_\mathrm{c}d(t) + \boldsymbol{r}_\mathrm{c}r(t). \tag{A.3}$$

a, d, r are dimensionless and the first two are typically small quantities ($\lesssim 10^{-4}$), while r is very close to unity.

The whole point of the scaled kinematic modelling is that $\boldsymbol{s}(t)$ can be described very accurately by astrometric observations, even though $\boldsymbol{b}(t)$ may be poorly known due to a high uncertainty in distance. This is possible simply by choosing the scaling such that $|\boldsymbol{s}(t)| = 1$ at some suitable time. This works even if the distance is completely unknown, or if it is effectively infinite (as for a quasar).

The scale factor is $|\boldsymbol{c}|^{-1} = \varpi_\mathrm{c}/A$, where ϖ_c is the parallax of $\boldsymbol{c}$ and A the astronomical unit. The measured parallax can be regarded as an estimate of ϖ_c.

In the following we describe some typical applications of SMOK coordinates.

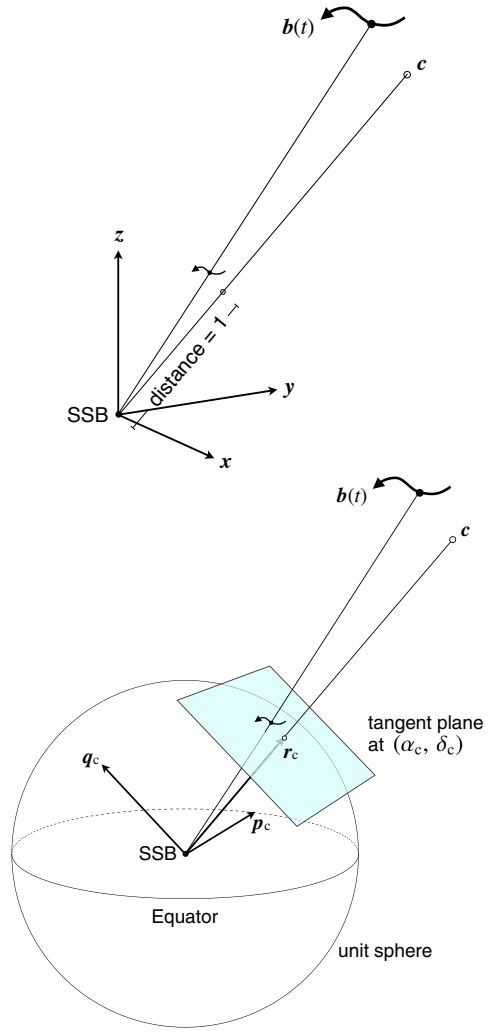

Fig. A.1. Two steps in the definition of SMOK coordinates. In the *top* diagram the motion of an object in the vicinity of the fixed point $\boldsymbol{c}$ is modelled by the function $\boldsymbol{b}(t)$ expressed in the barycentric $[\boldsymbol{x}\ \boldsymbol{y}\ \boldsymbol{z}]$ system. A scaled version of the model is constructed such that the scaled $\boldsymbol{c}$ is at unit distance from the solar system barycentre (SSB). In the *bottom* diagram new coordinate axes $[\boldsymbol{p}_\mathrm{c}\ \boldsymbol{q}_\mathrm{c}\ \boldsymbol{r}_\mathrm{c}]$ are chosen in the directions of increasing right ascension, declination, and distance, respectively, at the comparison point $(\alpha_\mathrm{c},\ \delta_\mathrm{c})$ being the projection of $\boldsymbol{c}$ on the unit sphere.

A.1. Uniform space motion

The simplest kinematic model is to assume that the star moves uniformly with respect to the SSB, that is

$$\boldsymbol{b}(t) = \boldsymbol{b}_\mathrm{ep} + (t - t_\mathrm{ep})\boldsymbol{v}, \tag{A.4}$$

[10] $\boldsymbol{p}_\mathrm{c}$ and $\boldsymbol{q}_\mathrm{c}$ point to the local "East" and "North", respectively, provided that $|\delta_\mathrm{c}| < 90°$. However, the coordinate triad in Eq. (A.1) is well-defined even *exactly* at the poles, where α_c remains significant for defining $\boldsymbol{p}_\mathrm{c}$ and $\boldsymbol{q}_\mathrm{c}$.

where $\boldsymbol{b}_{\rm ep}$ is the barycentric position at the reference epoch $t_{\rm ep}$, and $\boldsymbol{v}$ is the (constant) space velocity. The scaled kinematic model expressed in the BCRS is

$$\boldsymbol{s}(t) = \boldsymbol{s}_{\rm ep} + (t - t_{\rm ep})\dot{\boldsymbol{s}}, \tag{A.5}$$

where

$$\boldsymbol{s}_{\rm ep} = \boldsymbol{p}_{\rm c} a(t_{\rm ep}) + \boldsymbol{q}_{\rm c} d(t_{\rm ep}) + \boldsymbol{r}_{\rm c} r(t_{\rm ep}) \tag{A.6}$$

and

$$\dot{\boldsymbol{s}} = \boldsymbol{p}_{\rm c}\dot{a} + \boldsymbol{q}_{\rm c}\dot{d} + \boldsymbol{r}_{\rm c}\dot{r} \tag{A.7}$$

are constant vectors. The uniform motion can also be written in SMOK coordinates as

$$\left.\begin{aligned} a(t) &= a(t_{\rm ep}) + (t - t_{\rm ep})\dot{a},\\ d(t) &= d(t_{\rm ep}) + (t - t_{\rm ep})\dot{d},\\ r(t) &= r(t_{\rm ep}) + (t - t_{\rm ep})\dot{r}. \end{aligned}\right\} \tag{A.8}$$

The six constants $a(t_{\rm ep})$, $d(t_{\rm ep})$, $r(t_{\rm ep})$, $\dot{a}$, $\dot{d}$, $\dot{r}$ are the kinematic parameters of the scaled model; however, to get the actual kinematics of the star we also need to know $\varpi_{\rm c}$.

A.2. Relation to the usual astrometric parameters

Choosing $(\alpha_{\rm c}, \delta_{\rm c})$ to be the barycentric celestial coordinates of the star at $t_{\rm ep}$, and $\varpi_{\rm c}$ equal to the parallax at the same epoch, we find

$$\left.\begin{aligned} a(t_{\rm ep}) = 0, \quad d(t_{\rm ep}) = 0, \quad r(t_{\rm ep}) = 1,\\ \dot{a} = \mu_{\alpha*}, \quad \dot{d} = \mu_{\delta}, \quad \dot{r} = \mu_r, \end{aligned}\right\} \tag{A.9}$$

where $\mu_{\alpha*}$, μ_δ are the tangential components of the barycentric proper motion at the reference epoch $t_{\rm ep}$, and μ_r is the "radial proper motion" allowing one to take the perspective effects into account. μ_r is usually calculated from the measured radial velocity and parallax according to Eq. (1).

A.3. Differential operations

Uniform space motion does not map into barycentric coordinates $\alpha(t)$, $\delta(t)$ that are linear functions of time. The non-linearity derives both from the curvilinear nature of spherical coordinates and from perspective foreshortening depending on the changing distance to the object. Both effects are well known and have been dealt with rigorously by several authors (e.g., Eichhorn & Rust 1970; Taff 1981). The resulting expressions are non-trivial and complicate the comparison of astrometric catalogues of different epochs. For example, approximations such as

$$\mu_{\alpha*} = \frac{\alpha(t_2) - \alpha(t_1)}{t_2 - t_1}\cos\delta, \quad \mu_\delta = \frac{\delta(t_2) - \delta(t_1)}{t_2 - t_1} \tag{A.10}$$

cannot be used when the highest accuracy is required. By contrast, the linearity of Eq. (A.8) makes it possible to write

$$\dot{a} = \frac{a(t_2) - a(t_1)}{t_2 - t_1}, \quad \dot{d} = \frac{d(t_2) - d(t_1)}{t_2 - t_1} \tag{A.11}$$

to full accuracy, provided that the same comparison point is used for both epochs. (Strictly speaking, the same scale factor must also be used, so that in general $r(t_2) - r(t_1) = (t_2 - t_1)\dot{r} \neq 0$.) If the position at the reference epoch coincides with the comparison point used, the resulting $\dot{a}$, $\dot{d}$ are the looked-for proper motion components according to Eq. (A.9); otherwise a change of comparison point is needed (see below).

A.4. Changing the comparison point

Let (α_1, δ_1) and (α_2, δ_2) be different comparison points with associated triads $[\boldsymbol{p}_1\ \boldsymbol{q}_1\ \boldsymbol{r}_1]$ and $[\boldsymbol{p}_2\ \boldsymbol{q}_2\ \boldsymbol{r}_2]$. If $a_1(t)$, $d_1(t)$, $r_1(t)$ and $a_2(t)$, $d_2(t)$, $r_2(t)$ describe the same scaled kinematics we have by Eq. (A.3)

$$\boldsymbol{s}(t) = \boldsymbol{p}_1 a_1(t) + \boldsymbol{q}_1 d_1(t) + \boldsymbol{r}_1 r_1(t) = \boldsymbol{p}_2 a_2(t) + \boldsymbol{q}_2 d_2(t) + \boldsymbol{r}_2 r_2(t). \tag{A.12}$$

Thus, given $a_1(t)$, $d_1(t)$, $r_1(t)$ one can compute $\boldsymbol{s}(t)$ from the first equality in Eq. (A.12), whereupon the modified functions are recovered as

$$a_2(t) = \boldsymbol{p}_2'\boldsymbol{s}(t), \quad d_2(t) = \boldsymbol{q}_2'\boldsymbol{s}(t), \quad r_2(t) = \boldsymbol{r}_2'\boldsymbol{s}(t). \tag{A.13}$$

This procedure can be applied to $\boldsymbol{s}(t)$ for any particular t as well as to linear operations on $\boldsymbol{s}$ such as differences and time derivatives.

A.5. Epoch propagation

An important application of the above formulae is for propagating the six astrometric parameters $(\alpha_1, \delta_1, \varpi_1, \mu_{\alpha*1}, \mu_{\delta1}, \mu_{r1})$, referring to epoch t_1, to a different epoch t_2. This can be done in the following steps:

1. Use (α_1, δ_1) as the comparison point and compute $[\boldsymbol{p}_1\ \boldsymbol{q}_1\ \boldsymbol{r}_1]$ by Eq. (A.1). At time t_1 the SMOK parameters relative to the first comparison point are $a_1(t_1) = d_1(t_1) = 0$, $r_1(t_1) = 1$, $\dot{a}_1 = \mu_{\alpha*1}$, $\dot{d}_1 = \mu_{\delta1}$, $\dot{r}_1 = \mu_{r1}$.
2. Calculate $\boldsymbol{s}(t_1)$ and $\dot{\boldsymbol{s}}$ using Eqs. (A.6)–(A.7).
3. Calculate $\boldsymbol{s}(t_2)$ by means of Eq. (A.5). Let $s_2 = |\boldsymbol{s}(t_2)|$ be its length (close to unity).
4. Calculate $\boldsymbol{r}_2 = \boldsymbol{s}(t_2)/s_2$ and hence the second comparison point (α_2, δ_2) and triad $[\boldsymbol{p}_2\ \boldsymbol{q}_2\ \boldsymbol{r}_2]$.
5. Use Eq. (A.13) to calculate the SMOK parameters at t_2 referring to the second comparison point. For the position one trivially gets $a_2(t_2) = d_2(t_2) = 0$ and $r_2(t_2) = s_2$. For the proper motion parameters one finds $\dot{a}_2 = \boldsymbol{p}_2'\dot{\boldsymbol{s}}$, $\dot{d}_2 = \boldsymbol{q}_2'\dot{\boldsymbol{s}}$, and $\dot{r}_2 = \boldsymbol{r}_2'\dot{\boldsymbol{s}}$.
6. The astrometric parameters at epoch t_2 are α_2, δ_2, $\varpi_2 = \varpi_1/s_2$, $\mu_{\alpha*2} = \dot{a}_2/s_2$, $\mu_{\delta2} = \dot{d}_2/s_2$, $\mu_{r2} = \dot{r}_2/s_2$.

This procedure is equivalent to the one described in Sect. 1.5.5, Vol. 1 of *The* HIPPARCOS *and Tycho Catalogues* (ESA 1997).

Appendix B: The HIPPARCOS Catalogue

This Appendix describes the calculation of relevant quantities from the new reduction of the HIPPARCOS Catalogue by van Leeuwen (2007b). Data files were retrieved from the Strasbourg astronomical Data Center (CDS) in November 2013 (catalogue I/311). These files differ slightly from the ones given on the DVD published along with the book (van Leeuwen 2007a), both in content and format, as some errors have been corrected. The data needed for every accepted catalogue entry are:

- the five astrometric parameters $(\alpha,\ \delta,\ \varpi,\ \mu_{\alpha*},\ \mu_\delta)$;
- the 5×5 normal matrix $\boldsymbol{N}$ from the least-squares solution of the astrometric parameters (for a 5-parameter solution this equals the inverse of the covariance matrix $\boldsymbol{C}$);
- the chi-square goodness-of-fit quantity Q for the 5-parameter solution of the HIPPARCOS data;
- the degrees of freedom ν associated with Q.

The astrometric parameters at the HIPPARCOS reference epoch J1991.25 are directly taken from the fields labelled `RArad`, `DErad`, `Plx`, `pmRA`, and `pmDE` in the main catalogue file `hip2.dat`. Units are [rad] for α and δ, [mas] for ϖ, and [mas yr^{-1}] for $\mu_{\alpha*}$ and μ_δ. It is convenient to express also positional differences (such as SMOK coordinates a and d) and positional uncertainties in [mas]. The elements of $\boldsymbol{N}$ thus have units [mas^{-2} yr^p], where $p = 0$, 1, or 2, depending on the position of the element in the matrix.

The calculation of $\boldsymbol{N}$, Q, and ν is described hereafter in some detail as the specification of $\boldsymbol{C}$ deviates in some details from the published documentation. Clarification on certain issues was kindly provided by van Leeuwen (priv. comm.).

The number of degrees of freedom is

$$\nu = N_{\rm tr} - n, \tag{B.1}$$

where $N_{\rm tr}$ is the number of field transits used (label `Ntr` in `hip2.dat`) and n is the number of parameters in the solution (see below; most stars have $n = 5$). The goodness-of-fit given in field `F2` is the "gaussianized" chi-square (Wilson & Hilferty 1931)

$$F_2 = \left(\frac{9\nu}{2}\right)^{1/2}\left[\left(\frac{Q}{\nu}\right)^{1/3} + \frac{2}{9\nu} - 1\right] \tag{B.2}$$

computed from Q, the sum of the squared normalized residuals, and ν. For "good" solutions Q is expected to follow the chi-square distribution with ν degrees of freedom ($Q \sim \chi^2(\nu)$), in which case F_2 approximately follows the standard normal distribution, $F_2 \sim N(0, 1)$. Thus, $F_2 > 3$ means that Q is "too large" for the given ν at the same level of significance as the $+3\sigma$ criterion for a Gaussian variable (probability $\lesssim$0.0044)[11]. Given F_2 from field `F2`, and ν from Eq. (B.1), it is therefore possible to reconstruct the chi-square statistic of the n-parameter solution as

$$Q = \nu\left[\left(\frac{2}{9\nu}\right)^{1/2} F_2 + 1 - \frac{2}{9\nu}\right]^3. \tag{B.3}$$

We also introduce the square-root of the reduced chi-square,

$$u = \sqrt{Q/\nu}, \tag{B.4}$$

which is expected to be around 1.0 for a "good" solution (see further discussion below). u is sometimes referred to as the standard error of unit weight (Brinker & Minnick 1995).

The catalogue gives the covariance matrix in the form of an upper-diagonal "weight matrix" $\boldsymbol{U}$ such that, formally, $\boldsymbol{C} = (\boldsymbol{U}'\boldsymbol{U})^{-1}$. This inverse exists for all stars where a solution is given. (For the joint solution we actually need the normal matrix $\boldsymbol{N} = \boldsymbol{U}'\boldsymbol{U}$, see below.) For solutions with $n = 5$ astrometric parameters there are $n(n + 1)/2 = 15$ non-zero elements in $\boldsymbol{U}$. For some stars the solution has more than five parameters, and the main catalogue then only gives the first 15 non-zero elements, while remaining elements are given in separate tables.

Let $U_1, U_2, \ldots, U_{15}$ be the 15 values taken from the fields labelled `UW` in `hip2.dat`. The matrix $\boldsymbol{U}$ is computed as

$$\boldsymbol{U} = \begin{bmatrix} f_1U_1 & U_2 & U_4 & U_7 & U_{11} \\ 0 & f_2U_3 & U_5 & U_8 & U_{12} \\ 0 & 0 & f_3U_6 & U_9 & U_{13} \\ 0 & 0 & 0 & f_4U_{10} & U_{14} \\ 0 & 0 & 0 & 0 & f_5U_{15} \end{bmatrix}. \tag{B.5}$$

Here f_i, $i = 1 \ldots n$, are scaling factors which for the CDS data must be calculated as

$$f_1 = u/\sigma_{\alpha*}, \qquad f_2 = u/\sigma_\delta, \qquad f_3 = u/\sigma_\varpi,$$
$$f_4 = u/\sigma_{\mu\alpha*}, \qquad f_5 = u/\sigma_{\mu\delta}, \tag{B.6}$$

where u is given by Eq. (B.4) and $\sigma_\cdot$ are the standard errors given in fields `e_RArad` through `e_pmDE` of `hip2.dat`. Equation (B.6) applies to data taken from the CDS version of the catalogue (I/311). For catalogue data on the DVD accompanying the book (van Leeuwen 2007a), scaling factors $f_i = 1$ apply, although those data are superseded by the CDS version.

The 5×5 matrix $\boldsymbol{N} = \boldsymbol{U}'\boldsymbol{U}$ computed using the first five rows and columns in $\boldsymbol{U}$, as given in Eq. (B.5), contains the relevant elements of the normal matrix for any solution with $n \geq 5$. Thus, for solutions with $n > 5$ there is no need, for the catalogue combination, to retrieve the additional elements of $\boldsymbol{U}$ from `hip7p.dat`, etc. The situation is different when the covariance matrix is needed: it is then necessary to compute the full $n \times n$ normal matrix $\boldsymbol{N}$ before $\boldsymbol{C} = \boldsymbol{N}^{-1}$ can be computed.

The normal matrix $\boldsymbol{N}$ computed as described above incorporates the formal uncertainties of the observations; as described in van Leeuwen (2007a) these are ultimately derived from the photon statistics of the raw data after careful analysis of the residuals as function of magnitude, etc. If the adopted models are correct we expect the F_2 statistic to be normally distributed with zero mean and unit standard deviation, and the standard error of unit weight, u, to be on the average equal to 1. In reality we find (for solutions with $n = 5$) that their distributions are skewed towards higher values, especially for the bright stars where photon noise is small and remaining calibration errors are therefore relatively more important. To account for such additional errors the published standard errors $\sigma_{\alpha*}$, etc., in `hip2.dat` include, on a star-by-star basis, a correction factor equal to the unit weight error u obtained in its solution. This is equivalent to scaling the formal standard errors of the data used in the solution by the same factor. In order to make the computed normal matrix, covariance matrix, and goodness-of-fit statistics consistent with the published standard errors it is then necessary to apply the corresponding corrections, viz.:

$$\boldsymbol{N}_{\rm corr} = \boldsymbol{N}u^{-2}, \quad \boldsymbol{C}_{\rm corr} = \boldsymbol{C}u^2, \quad Q_{\rm corr} = \nu, \quad u_{\rm corr} = 1. \tag{B.7}$$

For the catalogue combination we use $\boldsymbol{N}_{\rm corr}$ and $Q_{\rm corr}$ whenever $u > 1$, but $\boldsymbol{N}$ and Q if $u \leq 1$.

[11] This transformation was also used to generate the F2 statistic given in field H30 of the HIPPARCOS and *Tycho* Catalogues (ESA 1997).

Paper IV

A&A 574, A115 (2015)
DOI: 10.1051/0004-6361/201425310

Astronomy & Astrophysics

The *Tycho-Gaia* astrometric solution

How to get 2.5 million parallaxes with less than one year of *Gaia* data

Daniel Michalik, Lennart Lindegren, and David Hobbs

Lund Observatory, Department of Astronomy and Theoretical Physics, Lund University, Box 43, 22100 Lund, Sweden
e-mail: [daniel.michalik;lennart;david]@astro.lu.se

Received 10 November 2014 / Accepted 24 December 2014

ABSTRACT

Context. The first release of astrometric data from *Gaia* will contain the mean stellar positions and magnitudes from the first year of observations, and proper motions from the combination of *Gaia* data with HIPPARCOS prior information (HTPM).
Aims. We study the potential of using the positions from the *Tycho*-2 Catalogue as additional information for a joint solution with early *Gaia* data. We call this the *Tycho-Gaia* astrometric solution (TGAS).
Methods. We adapt *Gaia*'s Astrometric Global Iterative Solution (AGIS) to incorporate *Tycho* information, and use simulated *Gaia* observations to demonstrate the feasibility of TGAS and to estimate its performance.
Results. Using six to twelve months of *Gaia* data, TGAS could deliver positions, parallaxes, and annual proper motions for the 2.5 million *Tycho*-2 stars, with sub-milliarcsecond accuracy. TGAS overcomes some of the limitations of the HTPM project and allows its execution half a year earlier. Furthermore, if the parallaxes from HIPPARCOS are not incorporated in the solution, they can be used as a consistency check of the TGAS/HTPM results.

Key words. astrometry – methods: data analysis – methods: numerical – space vehicles: instruments – parallaxes – proper motions

1. Introduction

The ESA astrometry satellite *Gaia* was launched in December 2013 with the aim of mapping more than a billion stars ($V \lesssim 20$) in our Galaxy (Perryman et al. 2001; de Bruijne 2012). For stars brighter than $V = 15$ mag, it is expected to yield positions, parallaxes and annual proper motions at an accuracy level of 5–25 μas. This accuracy can only be achieved after a global reduction of observations collected over an extended period of time (nominally five years), during which each star is seen crossing the focal plane of *Gaia* on average about 70 times. The multiple observations of a given star over several years are crucial for a successful disentanglement of the effects of stellar parallax and proper motion. A certain redundancy of observations is also required to estimate the additional parameters for the spacecraft attitude and calibration.

While the final *Gaia* results are thus expected post-2020, intermediate (provisional and less accurate) releases of astrometric data will be made; the first one is expected in mid-2016. Being based on a much shorter stretch of observations, it is envisaged that this first release will only give the mean positions of the stars, as the remaining parameters may not be reliably resolved. In previous work (Michalik et al. 2014, hereafter the HTPM paper) we have shown that the inclusion of HIPPARCOS data permits us to compute an astrometric solution for all five astrometric parameters of the HIPPARCOS stars, based on only one year of *Gaia* observations. This Hundred Thousand Proper Motions (HTPM, Mignard 2009) project benefits from the ∼24 yr time difference between HIPPARCOS and *Gaia* to improve the proper motions and, for example, detect long-period astrometric binaries. However, a serious limitation of HTPM is that the HIPPARCOS stars are not numerous enough to perform an adequate calibration and attitude determination of *Gaia*. As described in the HTPM paper, additional "auxiliary stars" must therefore be employed. Potentially this could bias the HTPM solution if the *Gaia* data alone do not allow all five astrometric parameters to be determined for the auxiliary stars.

In the present paper we show that some problems with the HTPM solution can be overcome if the auxiliary stars are replaced by stars from the *Tycho*-2 Catalogue (Høg et al. 2000b), using their positions at the HIPPARCOS epoch to constrain the proper motions[1]. This allows us to solve the full set of astrometric parameters for the *Tycho* stars as well as for the HIPPARCOS stars, thus avoiding the potential bias from auxiliary stars. Moreover, we find that such a solution is possible with even less *Gaia* data than required for HTPM. The resulting *Tycho-Gaia* astrometric solution (TGAS) could become the first full-sky astrometric solution using *Gaia* data, providing an important early validation of the instrument, calibration, and data processing, at the sub-mas level. Clearly the resulting parallaxes and proper motions of a few million *Tycho* stars are extremely interesting also from a scientific viewpoint, e.g. for local Galactic dynamics and cluster studies.

Tycho refers to the star catalogues derived from the star mapper instrument of the HIPPARCOS satellite. The original *Tycho*-1 Catalogue (Perryman & ESA 1997) gave positions and magnitudes for about 1 million stars. The later reduction, *Tycho*-2 (Høg et al. 2000b), extended this to about 2.5 million stars, almost complete to $V \lesssim 11.5$, and with uncertainties of 5–70 mas at the mean epoch of observation (∼1991.25). *Tycho*-2 also gives proper motions, derived from a comparison with old photographic catalogues. These proper motions have uncertainties of a few mas yr^{-1}, but as they may contain systematic errors from the old data, they are not used in the TGAS solution.

[1] In the following, "*Tycho*" always refers to the *Tycho*-2 Catalogue.

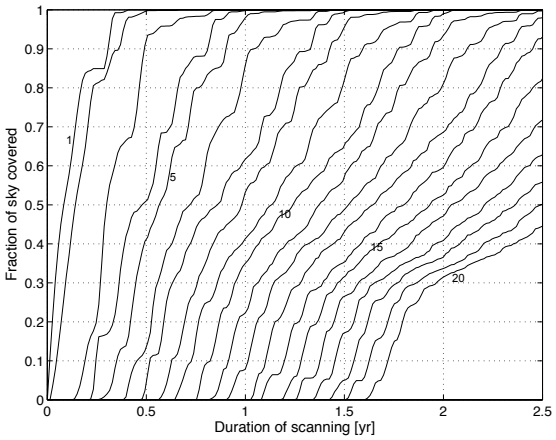

Fig. 1. Fractions of the celestial sphere covered by 1, 2, ..., 20 distinct observations according to the nominal scanning law of *Gaia*, as functions of duration. No dead time is assumed.

2. Prerequisites for a *Tycho-Gaia* solution

2.1. How much Gaia data are needed?

A good astrometric solution for (apparently) single stars requires that five astrometric parameters $(\alpha, \delta, \varpi, \mu_{\alpha*}, \mu_\delta)$ are determined for each star (e.g., Lindegren et al. 2012). A sixth parameter (μ_r) representing the radial motion (along the line of sight) is formally required for a complete representation of the space motion. In the present context it can be ignored, except for a limited number of nearby, fast-moving stars with significant perspective acceleration, for which it is assumed to be known. Thus, at least five distinct measurements are needed for every star, where "distinct" means that the measurements differ significantly either in time or direction. The scanning law of *Gaia* causes the direction of its spin axis to change by 4° day^{-1} (de Bruijne 2012), so that any two scans of the same star separated by at least 5 days may count as distinct. Figure 1 shows that after 0.5 yr, more than 90% of the sky is covered by at least three distinct scans, which together with the two measurements (in α and δ) from *Tycho* should in principle suffice to determine the five astrometric parameters. The scans are not purely one-dimensional, but contain some across-scan information (Sect. 3), which is crucial for the determination of the satellite's attitude and calibration parameters.

The real data are affected by significant dead time, increasing the time needed for sufficient sky coverage (Sect. 4.2). Considering that another half year of scanning in principle adds full redundancy to the whole sky, we estimate that the actual amount of *Gaia* data required for TGAS corresponds to between 0.5 and 1.0 yr including dead time.

2.2. Incorporating the Tycho and Hipparcos information

TGAS uses the "joint solution" method described in the HTPM paper (Michalik et al. 2014). That is, the prior information taken from the Hipparcos or *Tycho* Catalogue is cast in the form of normal equations $\boldsymbol{N}_{\rm pri}\boldsymbol{x} = \boldsymbol{b}_{\rm pri}$ for the astrometric parameters represented by the vector $\boldsymbol{x}$. These equations are then added to the normal equations $\boldsymbol{N}_{\rm obs}\boldsymbol{x} = \boldsymbol{b}_{\rm obs}$ derived from the *Gaia* observations before calculating the solution $\hat{\boldsymbol{x}} = (\boldsymbol{N}_{\rm pri} + \boldsymbol{N}_{\rm obs})^{-1}(\boldsymbol{b}_{\rm pri} + \boldsymbol{b}_{\rm obs})$. The main difference compared with HTPM concerns the setting up of the prior information for the non-Hipparcos stars in the *Tycho* Catalogue, which is described below. For the subset of Hipparcos stars, the prior information is taken from van Leeuwen (2007) and set up exactly as for the HTPM solution (see Sect. 2.6 in the HTPM paper). In addition to this nominal scenario, we show in Sect. 4.3 that a solution can be made without the Hipparcos parallaxes.

For a *Tycho*-only star the prior information in the *Tycho* Catalogue consists of the position α, δ at the epoch J1991.25 together with its uncertainties $\sigma_{\alpha*}$, σ_δ and correlation coefficient ρ. Remaining parameters should be treated as essentially unknown, which means that they can be set to some arbitrary values with very large uncertainties. For the simulated solutions in Sect. 3 they are set to zero with uncertainties $\sigma_\varpi = 1000$ mas, $\sigma_{\mu\alpha*} = \sigma_{\mu\delta} = 1000$ mas yr^{-1}, and $\sigma_{\mu r} = \sigma_{\rm vr}\sigma_\varpi/A$, where $\sigma_{\rm vr} = 100$ km s^{-1} is the prior radial velocity uncertainty and A the astronomical unit (HTPM paper, Eq. (17)). The prior astrometric parameters at J1991.25 are thus taken to be $(\alpha, \delta, 0, 0, 0, 0)$ with covariance

$$\boldsymbol{C}_{\rm pri} = \begin{bmatrix} \sigma^2_{\alpha*} & \rho\sigma_{\alpha*}\sigma_\delta & 0 & 0 & 0 & 0 \\ \rho\sigma_{\alpha*}\sigma_\delta & \sigma^2_\delta & 0 & 0 & 0 & 0 \\ 0 & 0 & \sigma^2_\varpi & 0 & 0 & 0 \\ 0 & 0 & 0 & \sigma^2_{\mu\alpha*} & 0 & 0 \\ 0 & 0 & 0 & 0 & \sigma^2_{\mu\delta} & 0 \\ 0 & 0 & 0 & 0 & 0 & \sigma^2_{\mu r} \end{bmatrix}. \quad (1)$$

The prior information including the covariance is subsequently propagated to the *Gaia* reference epoch (~2015) and $\boldsymbol{N}_{\rm pri}$ is calculated as the inverse of the propagated covariance matrix. $\boldsymbol{b}_{\rm pri}$ is calculated from the difference between the prior astrometric parameters and the current best estimate in the solution, as described in the HTPM paper, Eq. (18).

3. Simulations

In order to study the feasibility of TGAS and its potential performance we have made numerical simulations of joint *Tycho-Gaia* solutions using the AGISLab (Holl et al. 2012) software package. AGISLab was created at Lund Observatory to develop and test *Gaia* astrometric data processing strategies. While employing the same solution algorithms as the AGIS software used to process the real *Gaia* data (Lindegren et al. 2012), it runs in a much simplified framework which also allows us to generate simulated input data (CCD transits). The present experiments are made in a similar manner as described in the HTPM paper, to which we refer for details. A main difference is that the auxiliary stars in HTPM are replaced by *Tycho* stars, for which prior positions are used as described in the previous section.

Another difference is that we make the more conservative assumption that calibration errors contribute a constant RMS noise of 300 μas and 1000 μas per individual CCD observation, in the along-scan and across-scan direction, respectively. Finally, we use a (more realistic) dynamical attitude model (DAM; Risquez et al. 2013). DAM includes a detailed modelling of the attitude perturbations caused by a number of effects such as micro-propulsion thruster noise and micro-meteoroid hits. The observations are simulated using the so-called "astrometric attitude" (Risquez et al. 2013), which is the physical attitude averaged over the time required for a source to cross a CCD. Most of the stars are bright which implies that observations are gated (Kohley et al. 2012) and use a shorter integration time, resulting in a less smoothed attitude. However, we use the attitude computed for the full CCD integration time of 4.4 s, since the additional noise contribution of shorter integration times is less

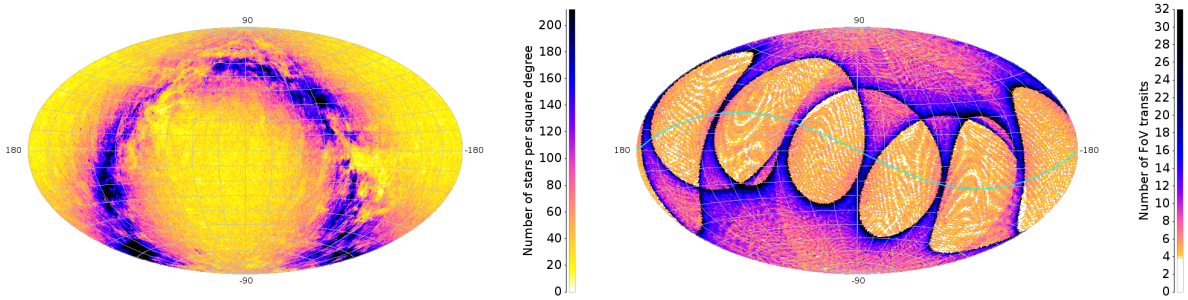

Fig. 2. All-sky maps in equatorial Hammer-Aitoff projection (pixel size 0.85 deg^2). *Left*: stellar distribution on the sky. *Right*: number of field of view transits per star. The cyan line denotes the ecliptic.

than 12.7 μas, see Table 1 in Risquez et al. (2013), and therefore negligible in the present context.

The real TGAS must cope with a number of complications which are ignored in the present experiments aiming to demonstrate the basic feasibility of the concept. The simplifying assumptions include (i) that there are no data gaps in the observations; (ii) that all stars are assumed to be single, and their motions thus consistent with the astrometric model represented by the five (or six) astrometric parameters; and (iii) that it is possible to adequately calibrate the gates used to observe the bright stars. In Sect. 5.1 we briefly discuss the consequences of these simplifications.

The main steps of the simulations are as follows:

1. Astrometric parameters and uncertainties are read from the *Tycho* and Hipparcos Catalogues and used to set up the prior information as described in Sect. 2.2 and in the HTPM paper, Sects. 2.6 and 2.7. These parameters are also used as initial values from which the iterative astrometric solution is started.
2. An artificial sky (Fig. 2, left) is created, representing the simulated "true" catalogue (see below). This is required in order to generate *Gaia* observations of the stars, and as a comparison point to evaluate the quality of the astrometric solution.
3. The *Gaia* observations (Fig. 2, right) of the Hipparcos and *Tycho* stars are generated according to the nominal scanning law, including the perturbations from DAM, and observation noise. For the latter we conservatively assume that all Hipparcos and *Tycho* stars are measured with the same accuracies, per CCD observation, as a star of magnitude $G = 13$, independent of the actual magnitude ($\sigma_{\rm AL} = 94$ μas, $\sigma_{\rm AC} = 489$ μas in the astrometric field).
4. The prior data and simulated observations are processed through the astrometric solution which effectively computes a least-squares estimate of all astrometric parameters together with the parameters describing the instrument attitude as a function of time. The components of the attitude quaternion are represented by cubic splines with a knot interval of 30 s. No special provision is made to handle the rate and angle discontinuities introduced by the use of DAM. The astrometric solution is made for the observation interval 2014.5–2015.0 (0.5 yr), with the reference epoch centred on the observations, i.e., at J2014.75. The reference frame is effectively determined by the positions and proper motions in the Hipparcos subset.
5. The resulting astrometric catalogue is compared with the "true" catalogue and the statistics of the differences are used to characterize the uncertainties of the solution.

The generation of the simulated "true" catalogue is done slightly differently for the Hipparcos stars and the *Tycho*-only stars (those that are not in the Hipparcos Catalogue). For the Hipparcos subset, "true" astrometric parameters are simulated by perturbing the prior data (i.e., the Hipparcos Catalogue) by amounts that are consistent with the prior covariances. This subset is further described in Sect. 3.2.1 of the HTPM paper. For the *Tycho*-only stars, the "true" positions are similarly obtained by perturbing the prior values according to their assigned uncertainties and correlations. For the proper motions we regard the values given in *Tycho*-2 as "true" for the present purpose; this is acceptable as they are not used anywhere in the solution, not even as priors. As the *Tycho*-2 Catalogue does not contain parallaxes, we simulate their true values based on the apparent magnitudes, neglecting extinction and assuming that the absolute magnitudes have a normal distribution with mean value +5 mag and standard deviation 3 mag (see HTPM paper, footnote 4). Although it would have been possible to make the parallax distribution dependent on the proper motion of the individual star, we do not consider the added complication worthwhile, as the results are rather insensitive to the assumed distribution. Radial velocities are simulated assuming a centred normal distribution with a conservatively chosen $\sigma_{\rm vr} = 100$ km s^{-1}.

4. Results

4.1. Nominal scenario

Table 1 summarizes the results obtained in the nominal scenario, i.e., using the full prior information from Hipparcos and assuming no dead time. The upper part of the table gives statistics for the *Tycho*-only stars, the lower part for the Hipparcos stars. As the priors are very different for the two subsets, they are separately discussed in the following.

4.1.1. *Tycho*-only stars

Any attempt to solve five parameters with 0.5 yr of *Gaia* data without a prior utterly fails. Remarkably, however, the inclusion of the *Tycho* positions allows us to solve not only the proper motions, but also the parallaxes for the 2.5 million *Tycho* stars with sub-mas precision. Here the proper motions rely entirely on the *Tycho* positions, as shown by the strong variation of the uncertainty with magnitude, mainly reflecting the variation of positional uncertainty in the *Tycho* Catalogue. In spite of the fact that the prior parallaxes are set to zero, the posterior estimates have very little bias (the median parallax error is -0.7 μas).

Table 1. Uncertainties of the astrometric parameters when processing 0.5 yr of simulated *Gaia* data jointly with *Tycho* and HIPPARCOS priors, nominal scenario.

Mag.	Number[a]	Position [μas]	Parallax [μas]	Prop. motion [μas yr^{-1}]
Subset *Tycho* without HIPPARCOS				
6–7	411	244	399	198
7–8	8072	198	348	264
8–9	63 630	191	327	403
9–10	257 243	230	407	680
10–11	686 866	329	601	1145
11–12	993 139	379	722	1522
≥12	302 511	349	702	1615
all (≥6)	2 311 872	332	631	1259
Subset HIPPARCOS				
6–7	9381	116	180	17
7–8	23 679	120	192	21
8–9	40 729	125	198	29
9–10	27 912	133	217	39
10–11	8563	154	253	58
11–12	2501	128	211	87
≥12	630	151	248	135
all (≥6)	113 395	127	203	32

Notes. Nominal scenario refers to the results obtained from a simulation without data gaps (see Sect. 4.2) and using the full HIPPARCOS prior (see Sect. 4.3). Uncertainties are calculated as the Robust Scatter Estimate (RSE; see footnote 18 in Lindegren et al. 2012) of the differences between estimated parameters and "true" values. [(a)] A small fraction of stars present in the HIPPARCOS and *Tycho* Catalogues is not observed in this simulated 0.5 yr interval of *Gaia* observations.

4.1.2. HIPPARCOS stars

It is interesting to compare the HIPPARCOS subset of this solution with the (conservative) HTPM case B, where only the positions were solved for the auxiliary non-HIPPARCOS stars (see Sect. 4.1 in the HTPM paper). The TGAS simulation is based on half as much *Gaia* data as HTPM-B, uses more conservative assumptions for attitude and calibration noise, but still provides improvements in all respects: the positions are at least a factor two better and the proper motions improved by about 16%. More importantly, the resulting parallax errors are 26% smaller and centred on zero (median error -0.03 μas), while HTPM-B gave systematically underestimated parallaxes for the HIPPARCOS stars (median error -591 μas). This clearly demonstrates that the additional prior provided by the *Tycho* positions also benefits the HIPPARCOS subset.

4.1.3. Spatial characteristics of the solution

The quality of the TGAS results for a particular star depends on the number and temporal distribution of its *Gaia* observations, which in turn depends on the position in the sky. Figure 2 (right) shows the number of field-of-view transits per star as set by the scanning law, yielding relatively few transits in areas within 45° of the ecliptic. Figure 3 shows the error characteristics for the *Tycho*-only subset. Panel a displays the median of the actual parallax errors (TGAS solution minus the simulated true values). In the well observed areas these are centred on zero, showing that the parallaxes are unbiased. The statistical scatter is larger in areas with few observations and unfavourable temporal distributions. There the errors could also be correlated over several degrees. The overall median of the actual parallax errors is -0.6 μas. The error maps for the other astrometric parameters have similar characteristics. The size of the actual errors is shown in panel b, displaying the RSE per pixel.

In an astrometric solution of real data the errors cannot be assessed by comparing the solution with the true values. Error estimates must instead come from the formal standard errors (uncertainties), computed as the square-roots of the diagonal elements of the covariance matrix (possibly adjusted depending on the size of the residuals in the solution). It is important that the formal standard errors (panel c) correctly characterize the actual errors. In the ideal case, the normalized error, i.e., the ratio of the actual error to the formal standard error, should follow a normal distribution with zero mean and unit standard deviation all over the sky. It was already shown (by the maps of the actual errors) that the mean values are close to zero. Panel d then shows the RSE values of the normalized parallax errors. These are around 1.0 everywhere[2], with a relatively small scatter in the Galactic plane, where there are more stars per pixel. A larger scatter is seen in the more sparsely populated areas of the sky, where the statistical uncertainty of the calculated RSE values is higher. The global RSE value is 1.03, the global RMS value 1.09. This shows that TGAS, under the given assumptions, provides formal standard errors that essentially correctly characterize the actual errors.

4.2. Simulation including data gaps

The results presented so far and in Table 1 are based on a simulation which includes all observations according to the nominal scanning law over the assumed period of 0.5 yr. The real mission has numerous data gaps of varying lengths, caused for example by orbit maintenance manoeuvres, eclipses by the moon, and solar activity. With no observations acquired at these times, the attitude modelling cannot take advantage of the physical continuity of the attitude across the gaps. The result is a globally weakened astrometric solution, which potentially could make the TGAS solution infeasible for a dataset as short as 0.5 yr. We investigate this in a separate simulation including data gaps.

The acquisition dead time for *Gaia* (the fraction of time during which no observations are acquired) is estimated to be ≃6%. Additionally, individual observations may be lost due to cosmic rays, CCD defects, charge injection, telemetry losses, etc. Such losses are less damaging to the astrometric solution as they do not create gaps in the attitude determination and sky coverage, although they do affect the results in a statistical way. For bright stars the additional observation dead time is estimated to be about 5%, resulting in a total dead time of 11%.

To explore the robustness of the TGAS solution to acquisition dead time we apply the actual time sequence of data gaps obtained during six months of the early *Gaia* operations[3] to the nominal simulation described in Sect. 3. While most of the applied gaps are shorter than 10 min, the two longest ones are 5.0 and 2.6 days. The total length of the gaps is 15.6 days, corresponding to 8.5% of acquisition dead time. Compared to the nominal value (6%) this simulation is therefore conservative, although we ignore the additional observation dead time.

[2] The scale of this panel was chosen to emphasize that most pixel values are close to 1.0. This resulted in 13 of the 12 288 pixels being saturated; the three largest values are 11.2, 3.9, and 3.4.

[3] April to September 2014, including part of the commissioning phase which ended on July 18th.

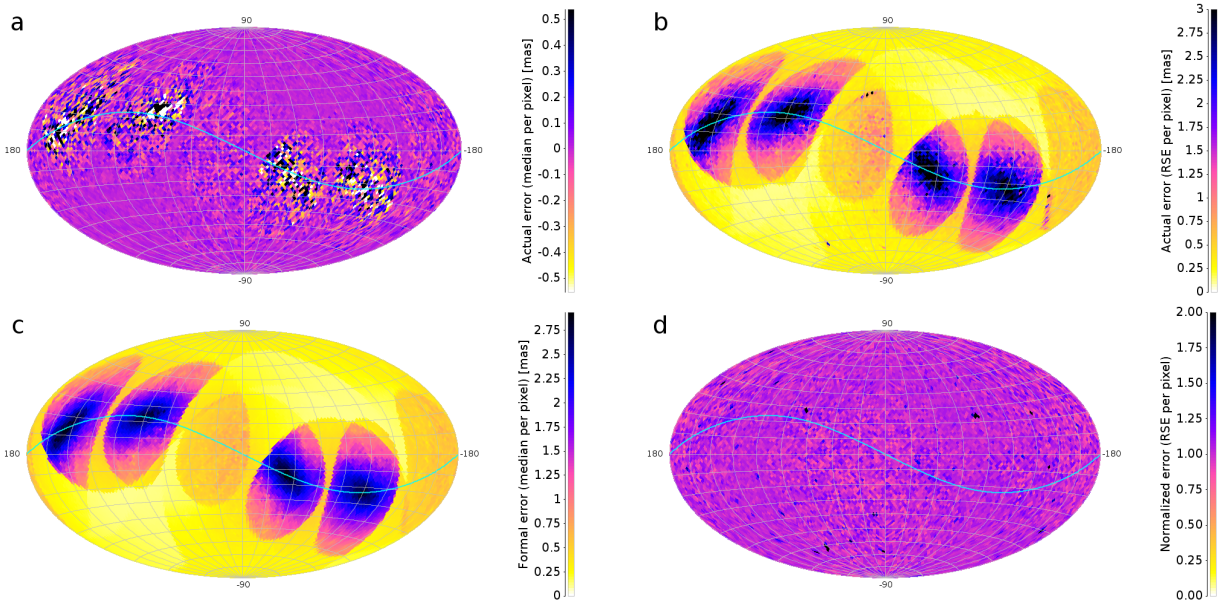

Fig. 3. All-sky maps characterizing the astrometric performance of the nominal TGAS solution (pixel size 3.4 deg^2). The cyan line denotes the ecliptic. **a)** Actual errors in parallax (TGAS solution minus simulated true values), median per pixel to show that the solution is unbiased. **b)** Same as before, but RSE per pixel to characterize the size of the actual errors. **c)** Formal standard errors in parallax as computed in the astrometric solution. **d)** RSE values of the normalized errors in parallax.

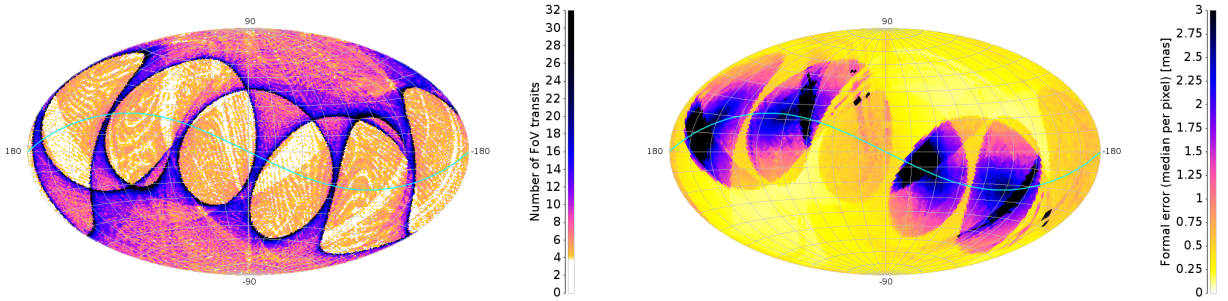

Fig. 4. All-sky maps for a TGAS simulation with simulated data gaps (see Sect. 4.2). *Left*: number of field of view transits per star. *Right*: formal standard errors (uncertainties) in parallax as computed in the astrometric solution.

Removing all observations corresponding to these gaps we find that a stable solution is still possible. Compared with the solution without gaps some stars are observed less, resulting in larger formal errors. About 1000 stars are not observed at all, and were removed from the solution and subsequent statistics. As shown in Fig. 4, the gaps cause considerable inhomogeneity in the sky coverage and formal errors. The white lines and wedges in the left panel show the areas most affected by the data gaps. As expected, stars in those areas also have large formal errors, as seen in the right panel. The formal errors are plotted on the same scale as Fig. 3, panel c, to show that only the areas affected by dead time suffer from larger errors. 441 pixels are saturated, all of these corresponding to areas affected by dead time. For 3.5% of the sky the formal errors are larger than 3 mas. Globally, the parallax and position errors are about 16% higher than in the solution without data gaps. The proper motion errors, which are dominated by the errors in the *Tycho* positions, are less affected.

4.3. Solution without HIPPARCOS parallax prior

For validation purposes it is desirable to compare the parallax values of the TGAS solution with HIPPARCOS. This is problematic when using the nominal TGAS since it already incorporates the HIPPARCOS parallaxes as a prior. As shown in Fig. 5 (left panel) this leads to a statistical correlation between the two datasets (correlation coefficient +0.23). As a result the differences between the parallaxes have a smaller spread than expected from their combined standard errors (right panel of Fig. 5).

To derive independent parallaxes, we propose a TGAS solution incorporating only the position and proper motion information from the HIPPARCOS Catalogue. This is achieved by setting the prior parallax value and the corresponding row and column in the HIPPARCOS prior normal matrix to zero before adding the information arrays. As shown in Fig. 6 this removes the

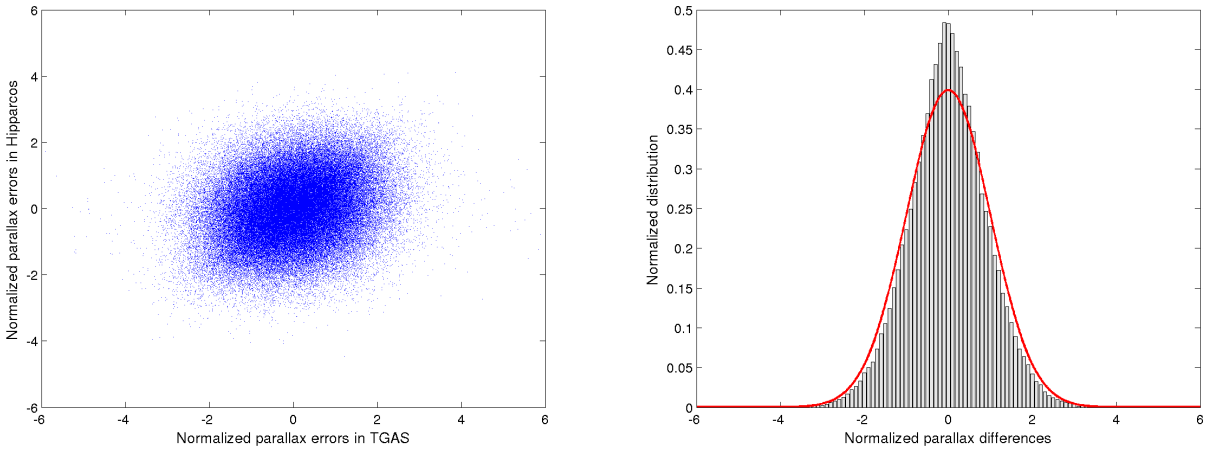

Fig. 5. Comparison of the parallaxes in TGAS and the HIPPARCOS Catalogue (nominal TGAS run, i.e., using the HIPPARCOS parallaxes as prior). *Left*: the normalized parallax errors (calculated minus the simulated true values, divided by their formal standard errors) are correlated. *Right*: the differences of the actual parallax values (normalized by their combined standard errors) follow a Gaussian distribution with standard deviation 0.91, less than 1.0 because of the correlation. The solid red line is a Gaussian distribution with unit width.

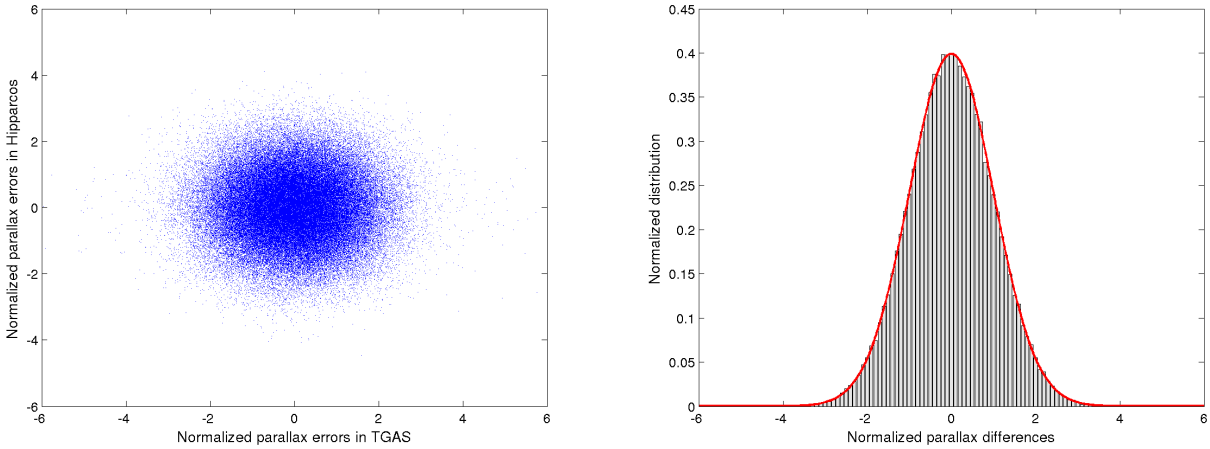

Fig. 6. Same as Fig. 5, but for the TGAS run without parallax prior (Sect. 4.3). *Left*: the normalized parallax errors are uncorrelated. *Right*: the normalized differences of the actual parallax values have unit standard deviation.

Table 2. Same as Table 1 (bottom), but without incorporation of the parallax prior from HIPPARCOS.

Mag.	Number	Position [μas]	Parallax [μas]	Prop. motion [μas yr^{-1}]
Subset HIPPARCOS				
6–7	9381	158	270	18
7–8	23 679	147	241	23
8–9	40 729	142	232	30
9–10	27 912	147	244	40
10–11	8563	164	276	60
11–12	2501	129	212	90
≥12	630	156	251	138
all (≥6)	113 395	147	244	34

correlation entirely (correlation coefficient −0.0043) at the expense of a moderate increase in astrometric uncertainties of the HIPPARCOS subset (Table 2). The results for the *Tycho* subset are not shown since the values found are virtually identical to the nominal scenario in Table 1.

5. Discussion

5.1. Consequences of the simplifying assumptions

Data gaps: our simulations show that TGAS is robust to data gaps according to a realistic distribution of acquisition dead time. The data gaps result in an inhomogeneous sky distribution of actual and formal errors, but do not significantly degrade the performance in well-observed regions. Affected areas can be recovered through additional observations after the first half year. The actual length of *Gaia* observations necessary for a good solution over the whole sky is difficult to estimate without detailed knowledge about the actual distribution of gaps. However, since the whole sky is nominally covered by multiple scans every half year (cf. Fig. 1), it is reasonable to conclude that the required time is less than 1 yr.

Non-single stars: a large fraction of the TGAS stars are in reality binaries or multiple stars, but not recognised as such in the *Tycho* Catalogue and thus treated as single in TGAS. Some of

them will be resolved by *Gaia* thanks to its higher resolution, which makes it possible to discard these objects or treat them appropriately.

For systems which are unresolved also by *Gaia* the space motions of their photocentres will deviate from the linear uniform model represented by the astrometric parameters. In the later astrometric solutions of *Gaia* data, objects that do not fit the single-star astrometric model will be detected and filtered out for special treatment, but this mechanism is not effective in TGAS due to the small redundancy of observations. TGAS will contain some fraction of such systems with significant deviations from the adopted five-parameter model, which will remain unrecognised in the solution. Their actual astrometric errors will be underestimated by the formal uncertainties. This may be a common characteristic of the early data releases, typically based on datasets with low redundancy and imperfect calibrations.

The impact of astrometric binaries on the derived proper motions should nevertheless be small thanks to the 24 yr baseline of TGAS. The same is true for the TGAS parallaxes as they are dominated by the *Gaia* observations and at most only a fraction of the error in the annual proper motion contributes to the parallax error. Comparing the proper motions from TGAS and those in *Tycho*-2 (which incorporate century-old ground-based observations) could reveal not only systematic errors in the *Tycho*-2 proper motions but also some long-period astrometric binaries.

Bright-star performance and calibration issues: like any other AGIS solution, TGAS will use the generic calibration model described in Lindegren et al. (2012), Sects. 3.4 and 3.5, which takes into account the actual geometry of the optics and detectors as well as calibrations linked to chromatic image displacements, basic-angle variations, and radiation-induced image displacements. However, a specific complication of TGAS is that it almost exclusively uses stars brighter than magnitude ∼12, for which *Gaia* employs CCD gates (Kohley et al. 2012) to avoid saturation. The gated observations need a separate calibration for each gate, but with the limited amount of *Gaia* data in a TGAS solution there may not be sufficient observations of bright stars to do so. Gate 4 is used for the brightest stars with magnitudes $G \lesssim 8.84$. If it turns out that this gate cannot be reliably calibrated with half a year of *Gaia* data, we would in the worst case lose all stars brighter than $G \simeq 8.84$ in the TGAS solution, or about 2.3% of the *Tycho* stars. The reduced number of stars degrades the solution somewhat (for example because the attitude is less accurately determined), but we have verified that TGAS works with as few as one million *Tycho* stars. The bright-star performance is a more serious issue for the HTPM solution, as more than half of the HIPPARCOS stars are brighter than 8.84 mag.

5.2. Systematics in the Tycho-2 data

The present TGAS experiments assume that the *Tycho* positions give the barycentric directions to the stars at the standard HIPPARCOS epoch J1991.25. In reality the *Tycho*-2 positions refer to slightly different epochs, which could even be different in α and δ. The actual TGAS solution should use the mean effective epoch $(t_\alpha + t_\delta)/2$ of each star rather than J1991.25.

A potentially more serious complication is that the *Tycho* positions do not strictly represent the barycentric directions at the given epochs of observation. The positions were derived from the stacked star mapper photon count records accumulated over the whole HIPPARCOS mission (Høg et al. 2000a). Parallaxes were typically not taken into account in this process, and the resulting positions are therefore offset by a fraction of the parallax. Both the fraction and direction of the offset depend in a complex way on the distribution, geometry, and weights of the photon count records. There is no simple way to correct for this effect in TGAS, nor was it included in our simulations. However, we argue that its impact on the TGAS results should be very small. The *Tycho* positions are mainly used to derive the proper motions on a baseline of 24 years. Since the parallax of a given star is typically of similar size as its annual proper motion, and the position offset is just a fraction of the parallax, it follows that the resulting annual proper motion is typically only offset by a few per cent of the parallax. This, in turn, should have an almost negligible impact on the parallax, which is mainly derived from the *Gaia* observations relative to the extrapolated linear motion.

5.3. Reference frame of TGAS

The *Tycho* positions around 1991 and the *Gaia* observations around 2015 are by themselves not sufficient to determine the spin of the reference frame for TGAS, only its orientation at the *Tycho* epoch. By incorporating positions and proper motions from HIPPARCOS in TGAS, in the same way as described in the HTPM paper, the TGAS results are effectively on the HIPPARCOS reference frame.

6. Conclusions

The currently foreseen contents of the first *Gaia* data release include positions from a two-parameter solution of the early ($\lesssim$1 yr) data, because a full five-parameter solution will not be feasible, or reliable enough, based on these data alone. Incorporating prior information into the solution makes it possible to solve all five astrometric parameters (i.e., including parallax and proper motion) with significantly less *Gaia* data. The HTPM project incorporates the HIPPARCOS Catalogue, resulting in greatly improved astrometry for the $\sim 10^5$ HIPPARCOS stars. However, as shown in Michalik et al. (2014), such a solution should be based on at least one year of continuous *Gaia* data, as otherwise the results will be biased by the use of auxiliary stars for which the full set of parameters cannot be resolved.

TGAS extends the original HTPM proposal and takes the idea of a joint solution one step further by combining, in a single global astrometric solution, measurements from the early *Gaia* mission with data from the *Tycho* and HIPPARCOS Catalogues. In this paper we have shown that the approximate positions at the earlier epoch provided by *Tycho* are sufficient to disentangle the ambiguity between parallax and proper motion in a short stretch of *Gaia* observations. Therefore TGAS allows us to derive positions, parallaxes, and proper motions for up to 2.5 million stars half a year earlier than the proposed first *Gaia* data release containing only two parameters, and one year earlier than the proposed second *Gaia* data release containing the first five parameter solution. Using the five parameter solutions of the *Tycho* stars for HTPM avoids the risk of biasing the HTPM parallaxes and improves the resulting astrometry for the HIPPARCOS stars. This is true even when the prior parallaxes from HIPPARCOS are not used at all in the TGAS/HTPM solution, which provides a stringent test of its consistency with the HIPPARCOS parallaxes (see Sect. 4.3). The moderate increase in astrometric uncertainties of such a solution compared to the nominal scenario seems to be a price worth paying for the benefit of a catalogue of independent parallaxes. We therefore propose that the solution not using the HIPPARCOS parallaxes should be the baseline for TGAS/HTPM.

Our simulations of TGAS suggest that the accuracy of the resulting astrometry for the *Tycho* stars will be similar to the HIPPARCOS Catalogue, and possibly significantly better depending on the exact scenario of the number of *Gaia* observations available, dead time intervals, calibration, etc. Moreover, the dataset would be almost complete to $V \simeq 11.5$, or 3–4 mag fainter than the survey part of the HIPPARCOS Catalogue. Although the scientific lifetime of the data would be limited, in view of the expected later releases from *Gaia*, the potential applications cover many areas of stellar and galactic astronomy. Perhaps even more importantly, TGAS offers the opportunity to perform a full-sky scientific validation of the *Gaia* instrument, calibration, and data processing at sub-mas level much earlier than previously anticipated. For this reason alone, we believe TGAS should be attempted as soon as *Gaia* has collected sufficient data for such a solution, which could be in early 2015.

Acknowledgements. TGAS originated from discussions with Thierry Forveille and Claus Fabricius during the review phase of the HTPM paper. We are grateful to Ulrich Bastian, Anthony Brown, Jos de Bruijne, José Hernández, Sergei Klioner, Uwe Lammers, Paul McMillan, and the referee Floor van Leeuwen, for providing many supportive comments, questions, and feedback on the manuscript. The DAM data were kindly provided by Daniel Risquez. We gratefully acknowledge support from the Swedish National Space Board and the Royal Physiographic Society in Lund.

References

de Bruijne, J. H. J. 2012, Ap&SS, 341, 31
Høg, E., Fabricius, C., Makarov, V. V., et al. 2000a, A&A, 357, 367
Høg, E., Fabricius, C., Makarov, V. V., et al. 2000b, A&A, 355, L27
Holl, B., Lindegren, L., & Hobbs, D. 2012, A&A, 543, A15
Kohley, R., Garé, P., Vétel, C., Marchais, D., & Chassat, F. 2012, in SPIE Conf. Ser., 8442
Lindegren, L., Lammers, U., Hobbs, D., et al. 2012, A&A, 538, A78
Michalik, D., Lindegren, L., Hobbs, D., & Lammers, U. 2014, A&A, 571, A85
Mignard, F. 2009, The Hundred Thousand Proper Motions Project, Gaia Data Processing and Analysis Consortium (DPAC) Technical Note GAIA-C3-TN-OCA-FM-040, http://www.cosmos.esa.int/web/gaia/public-dpac-documents
Perryman, M. A. C., & ESA 1997, The HIPPARCOS and TYCHO catalogues. Astrometric and photometric star catalogues derived from the ESA HIPPARCOS Space Astrometry Mission, ESA SP, 1200
Perryman, M. A. C., de Boer, K. S., Gilmore, G., et al. 2001, A&A, 369, 339
Risquez, D., van Leeuwen, F., & Brown, A. G. A. 2013, A&A, 551, A19
van Leeuwen, F. 2007, HIPPARCOS, The New Reduction of the Raw Data, Astrophys. Space Sci. Lib. (Springer), 350

Conference poster in Appendix A.3

Paper V

A&A 583, A68 (2015)
DOI: 10.1051/0004-6361/201526936

Astronomy & Astrophysics

Gaia astrometry for stars with too few observations. A Bayesian approach

Daniel Michalik[1], Lennart Lindegren[1], David Hobbs[1], and Alexey G. Butkevich[2]

[1] Lund Observatory, Department of Astronomy and Theoretical Physics, Lund University, Box 43, 22100 Lund, Sweden
e-mail: [daniel.michalik; lennart; david]@astro.lu.se
[2] Lohrmann Observatory, Technische Universität Dresden, 01062 Dresden, Germany
e-mail: alexey.butkevich@tu-dresden.de

Received 10 July 2015 / Accepted 21 August 2015

ABSTRACT

Context. The astrometric solution for *Gaia* aims to determine at least five parameters for each star, representing its position, parallax, and proper motion, together with appropriate estimates of their uncertainties and correlations. This requires at least five distinct observations per star. In the early data reductions the number of observations may be insufficient for a five-parameter solution, and even after the full mission many stars will remain under-observed, including faint stars at the detection limit and transient objects. In such cases it is reasonable to determine only the two position parameters. The formal uncertainties of such a two-parameter solution would however grossly underestimate the actual errors in position, due to the neglected parallax and proper motion.
Aims. We aim to develop a recipe to calculate sensible formal uncertainties that can be used in all cases of under-observed stars.
Methods. Prior information about the typical ranges of stellar parallaxes and proper motions is incorporated in the astrometric solution by means of Bayes' rule. Numerical simulations based on the *Gaia* Universe Model Snapshot (GUMS) are used to investigate how the prior influences the actual errors and formal uncertainties when different amounts of *Gaia* observations are available. We develop a criterion for the optimum choice of priors, apply it to a wide range of cases, and derive a global approximation of the optimum prior as a function of magnitude and galactic coordinates.
Results. The feasibility of the Bayesian approach is demonstrated through global astrometric solutions of simulated *Gaia* observations. With an appropriate prior it is possible to derive sensible positions with realistic error estimates for any number of available observations. Even though this recipe works also for well-observed stars it should not be used where a good five-parameter astrometric solution can be obtained without a prior. Parallaxes and proper motions from a solution using priors are always biased and should not be used.

Key words. astrometry – methods: data analysis – methods: numerical – parallaxes – proper motions – space vehicles: instruments

1. Motivation for this study

The ESA science mission *Gaia*, launched in December 2013, aims to determine accurate astrometry (positions, parallaxes, and proper motions) and complementary spectrophotometry for about one billion stars (Perryman et al. 2001; de Bruijne 2012). The astrometric parameters of a given star are calculated from the transits of the star's image across the CCDs in the focal plane of *Gaia*. Each such field-of-view transit is essentially an instantaneous, one-dimensional measurement of the stellar position in a certain scan direction (the "along-scan coordinate"). The perpendicular ("across-scan") coordinate is also measured, but to a lower accuracy, and does not contribute significantly to the final astrometric parameters.

The path of a star on the celestial sphere, as seen from *Gaia*, is in the simplest case modelled by five astrometric parameters representing its position (α, δ), parallax (ϖ), and proper motion ($\mu_{\alpha*}$, μ_δ) at some chosen reference epoch. To determine all five parameters one needs at least five observations suitably distributed in time, and different scan directions are needed to derive the two-dimensional positions from the one-dimensional scans. Due to the one-year periodicity of parallax, the observations must span at least a whole year in order to reliably disentangle parallax from proper motion. The *Gaia* scanning law ensures that these conditions are met for stars anywhere in the sky, if the scanning lasts long enough. The nominal mission length of five years provides an ample number of observation opportunities, with an average of some 70 field-of-view transits per star. This high redundancy factor is needed to determine a large number of nuisance parameters (attitude and instrument calibration) in addition to the astrometric parameters, for judging the quality of the data, and for detecting cases (such as binaries) where the simple five-parameter model is not adequate.

However, there are inevitably many situations where a star is insufficiently observed to solve all of its five astrometric parameters. These situations include:

- Transient objects, for example extragalactic supernovae, galactic dwarf novae, and large-amplitude (Mira type) variables: these may be visible for just a few months, possibly reoccurring at a much later date.
- Faint stars near the detection limit of *Gaia*: nominally, all point sources brighter than 20th magnitude are detected and observed. However, since the on-board magnitude estimation has some uncertainty, stars at the detection limit may not always be observed when they transit the focal plane. Because the detection probability decreases gradually with magnitude, large numbers of faint stars will have strongly diluted observation histories.

– The first release of astrometric results, based mainly on observations collected during the first year of the mission, where most stars will be insufficiently observed.

If there are not enough observations for a given star, a simple remedy is to solve only its position (α, δ) at the mean epoch of observation. This is always possible: even in the case of a single field-of-view transit, an approximate position can be calculated by combining the along-scan and across-scan measurements.

Solving only for the two position parameters α and δ is equivalent to assuming that the true parallax and proper motion of the object are equal to zero[1]. If this assumption is correct (as may effectively be the case e.g. for quasars), the resulting position estimate will be unbiased with a formal uncertainty reflecting the actual errors. However, if the true parallax and proper motion are non-zero, the estimated position will in general be biased. Its formal uncertainty (which does not depend on the parallax and proper motion value) will remain small, since the error calculus only takes into account the small observational noise of *Gaia*. As a result, the bias will often be many times larger than the formal uncertainty.

The solution proposed in this paper is to estimate all five parameters, while incorporating the prior information that the parallax and proper motion are typically small but non-zero quantities. Formally, this can be achieved by means of Bayes' rule. This paper tries to answer the question how to optimally choose the prior when there are not enough *Gaia* observations for a regular five-parameter astrometric solution. We use numerical experiments, based on simulated observations of stars in a galactic model, to investigate the influence of the prior under different scenarios. We show that with a suitable choice of prior the solution provides sensible results in terms of both the estimated position and its calculated uncertainty.

The first release of astrometric results from the *Gaia* mission is expected[2] in the summer of 2016. Due to the limited time interval covered by the early data, this release will, for the majority of stars, only contain mean positions and single-band (G) magnitudes. Exceptions are the HIPPARCOS stars, for which improved proper motions and possibly also parallaxes can be derived based on the HTPM project (Mignard 2009; Michalik et al. 2014). A similar joint reduction is possible for the *Tycho*-2 stars (the TGAS project; Michalik et al. 2015).

The method developed in this paper could be applied to the estimation of the positional uncertainties in the first release, but more generally to any situation where the number and distribution of observations is insufficient for a full five-parameters solution. It should be emphasised that the use of prior information in the astrometric solution always leads to biased estimates of the parameters. The proposed recipe should therefore only be used when actually needed, e.g. in the previously mentioned cases, and then only in order to obtain positions with realistic estimates of their uncertainties. These positions are valuable, e.g. for identification purposes and as a reference for ground-based observations. The resulting parallaxes and proper motions should however not be used.

[1] We do not consider the possibility of solving three or four astrometric parameters per star, for example (α, δ, ϖ) or (α, δ, $\mu_{\alpha*}$, μ_δ). This would mean that proper motion is neglected compared to parallax, or vice versa. This makes little sense because, for most stars, the observable effect of the neglected parameter will be of a similar size as that of the retained parameter. This follows from the speed of the Earth's motion around the Sun, about 30 km s^{-1}, being of a similar magnitude as the peculiar motions of stars, including that of the Sun itself. Consequently we only consider solutions with either two or five astrometric parameters per star.

[2] See http://www.cosmos.esa.int/web/gaia/release

2. Theory

In this section we first formulate the estimation of the astrometric parameters as a classical least-squares problem, which provides a connection to the description of the overall *Gaia* astrometric solution (Lindegren et al. 2012). We then show how a Gaussian prior can be introduced using Bayes' rule. Finally we discuss the relevance and interpretation of the Gaussian prior and posterior probability densities in this context.

We use the term uncertainty for any quantitative measure of the expected degree of deviation of an estimated quantity from its true value, and reserve the term (actual) error for the signed, and in general unknown, deviation itself. In the Gaussian context the natural measure of uncertainty is the standard deviation, but as we are here dealing with strongly non-Gaussian distributions (e.g. of the true parallax values) we instead use measures based on the size of a confidence region.

2.1. Least-squares estimation of the astrometric parameters

The *Gaia* astrometric solution is calculated by a series of updating processes as described in Sect. 5 of Lindegren et al. (2012). In the "astrometric updating" the satellite attitude and geometric calibration are assumed to be known, in which case the linearised least-squares problem for an individual star can be written in matrix form as

$$\boldsymbol{A}\boldsymbol{x} \simeq \boldsymbol{h}, \tag{1}$$

where $\boldsymbol{x}$ is a column matrix containing differential corrections to the five astrometric parameters, $\boldsymbol{h}$ is a column matrix containing the n pre-adjustment observation residuals of the star, normalized by their formal uncertainties, and $\boldsymbol{A}$ is the $n \times 5$ design matrix, i.e., the partial derivative matrix row-wise normalized by the observational uncertainties. (The $\simeq$ is used in Eq. (1) because the system of equations is in general overdetermined and cannot be exactly satisfied.)

The astrometric parameters α, δ, ϖ, $\mu_{\alpha*} \equiv \mu_\alpha \cos\delta$ and μ_δ refer to some chosen reference epoch $t_{\rm ep}$, which in this paper is always taken to be the mean epoch of observation. In particular, (α, δ) is the barycentric direction to the star at time $t_{\rm ep}$. The differential corrections in $\boldsymbol{x}$ should be interpreted as $\Delta\alpha* \equiv \Delta\alpha\cos\delta$, $\Delta\delta$, $\Delta\varpi$, $\Delta\mu_{\alpha*}$, and $\Delta\mu_\delta$, or more rigorously using the "scaled modelling of kinematics" formalism in Appendix A of Michalik et al. (2014)[3].

The least-squares estimate of $\boldsymbol{x}$ minimizes the χ^2 goodness-of-fit, i.e., the squared norm of the post-fit residuals $\boldsymbol{h} - \boldsymbol{A}\boldsymbol{x}$,

$$\begin{aligned} Q_0(\boldsymbol{x}) &= \|\boldsymbol{h} - \boldsymbol{A}\boldsymbol{x}\|^2 = (\boldsymbol{h} - \boldsymbol{A}\boldsymbol{x})'(\boldsymbol{h} - \boldsymbol{A}\boldsymbol{x}) \\ &= \boldsymbol{h}'\boldsymbol{h} - 2\boldsymbol{x}'\boldsymbol{b}_0 + \boldsymbol{x}'\boldsymbol{N}_0\boldsymbol{x}, \end{aligned} \tag{2}$$

where $\boldsymbol{b}_0 = \boldsymbol{A}'\boldsymbol{h}$ and $\boldsymbol{N}_0 = \boldsymbol{A}'\boldsymbol{A}$. Putting $\partial Q_0/\partial \boldsymbol{x} = \boldsymbol{0}$ gives a linear system of equations,

$$\boldsymbol{N}_0\boldsymbol{x}_0 = \boldsymbol{b}_0, \tag{3}$$

[3] The rigorous treatment includes the radial proper motion μ_r as the sixth astrometric parameter. Even for nearby high-velocity stars the perspective effect in position, which is proportional to μ_r, is negligible over five years. In the present problem μ_r can therefore be ignored.

known as the normal equations, from which the least-squares estimate $\boldsymbol{x}_0$ can be calculated. For arbitrary $\boldsymbol{x}$ the goodness-of-fit can be written as

$$Q_0(\boldsymbol{x}) = Q_0(\boldsymbol{x}_0) + (\boldsymbol{x} - \boldsymbol{x}_0)' \boldsymbol{N}_0 (\boldsymbol{x} - \boldsymbol{x}_0). \quad (4)$$

For badly observed stars the normal matrix $\boldsymbol{N}_0$ will be either ill-conditioned or singular. If it is ill-conditioned (e.g., due to a small number of nearly collinear observations), then a solution can formally be obtained. It will however have large formal uncertainties and be vulnerable to outliers, which cannot be reliably detected. The situation is different if $\boldsymbol{N}_0$ is strictly singular, e.g., if there are fewer observations than the number of unknowns. From a mathematical point of view, the singular problem possesses an infinite number of solutions, while algorithmically it may not be possible to determine any of them, depending on implementation choices. A remedy to both singular and ill-conditioned situations is to incorporate prior information (Sect. 2.3), which always results in a unique and well-defined, albeit biased, solution.

2.2. The likelihood function

For a clean data set, with outliers filtered out or downweighted, it is reasonable to model the observational errors as independent normal random variables. For a properly calibrated instrument, the errors have mean (expected) values equal to zero and known standard deviations equal to the formal uncertainties of the observations. $\boldsymbol{h}$ is then an n-dimensional Gaussian, with mean value $\boldsymbol{A}\boldsymbol{x}_{\rm true}$ and unit covariance; its probability density function (PDF) is

$$f(\boldsymbol{h}|\boldsymbol{x}) = (2\pi)^{-n/2} \exp\left[-\frac{1}{2}\|\boldsymbol{h} - \boldsymbol{A}\boldsymbol{x}\|^2\right] \propto \exp\left[-\frac{1}{2}Q_0(\boldsymbol{x})\right], \quad (5)$$

evaluated for $\boldsymbol{x} = \boldsymbol{x}_{\rm true}$. Naturally, this PDF cannot be computed as $\boldsymbol{x}_{\rm true}$ is unknown. Regarded as a function of $\boldsymbol{x}$, for the given $\boldsymbol{h}$, it is known as the likelihood of the data, designated $L(\boldsymbol{x}|\boldsymbol{h})$. Maximizing this function with respect to $\boldsymbol{x}$ is clearly equivalent to minimizing $Q_0(\boldsymbol{x})$, showing that $\boldsymbol{x}_0$ is the maximum likelihood estimate of the astrometric parameters.

2.3. Incorporating a prior

Bayes' rule (e.g. Sivia & Skilling 2006, Sect. 3.5) expresses the posterior PDF of $\boldsymbol{x}$ as

$$f(\boldsymbol{x}|\boldsymbol{h}) \propto L(\boldsymbol{x}|\boldsymbol{h}) \times p(\boldsymbol{x}), \quad (6)$$

where $p(\boldsymbol{x})$ is the prior PDF and $L(\boldsymbol{x}|\boldsymbol{h}) \equiv f(\boldsymbol{h}|\boldsymbol{x})$ is the likelihood of the data. The constant of proportionality is left out as it is independent of $\boldsymbol{x}$, but can be determined from the normalization constraint $\int f(\boldsymbol{x}|\boldsymbol{h})\,\mathrm{d}\boldsymbol{x} = 1$. For example, a flat (uninformative) prior $p_0(\boldsymbol{x}) = \text{const}$ yields, by means of Eqs. (4), (5), the posterior PDF

$$f_0(\boldsymbol{x}|\boldsymbol{h}) = (2\pi)^{-5/2} \det(\boldsymbol{N}_0)^{1/2} \exp\left[-\frac{1}{2}Q_0(\boldsymbol{x})\right]. \quad (7)$$

This is a 5-dimensional Gaussian with mean value $\boldsymbol{x}_0$ and covariance $\boldsymbol{C}_0 = \boldsymbol{N}_0^{-1}$, which reflects our knowledge of $\boldsymbol{x}$ based on the data only.

In principle, the prior PDF $p(\boldsymbol{x})$ should quantify our prior knowledge of the astrometric parameters. For example, it could be strictly zero for $\varpi < 0$, while declining as a power law for large values of ϖ, reflecting the prior knowledge that parallaxes are generally positive, small quantities. However, in this paper we only consider Gaussian priors. This has two important advantages: (a) if both the prior PDF and the likelihood function are Gaussian, the posterior PDF is also Gaussian, which greatly simplifies its interpretation; (b) the incorporation of a Gaussian prior in the astrometric solution is straightforward, as will be shown in the following. The disadvantage is of course that a Gaussian prior is not very realistic, at least for the parallaxes; but with the interpretation proposed in Sect. 2.4 it is adequate for the present purpose.

Assuming a Gaussian prior with mean value $\boldsymbol{x}_{\rm p}$ and covariance $\boldsymbol{C}_{\rm p}$ we define

$$Q_{\rm p}(\boldsymbol{x}) = (\boldsymbol{x} - \boldsymbol{x}_{\rm p})' \boldsymbol{N}_{\rm p} (\boldsymbol{x} - \boldsymbol{x}_{\rm p}), \quad (8)$$

where $\boldsymbol{N}_{\rm p} = \boldsymbol{C}_{\rm p}^{-1}$. The prior probability density function is then

$$p(\boldsymbol{x}) \propto \exp\left[-\frac{1}{2}Q_{\rm p}(\boldsymbol{x})\right]. \quad (9)$$

Inserting Eqs. (5) and (9) into Eq. (6) yields the posterior PDF

$$f(\boldsymbol{x}|\boldsymbol{h}) \propto \exp\left[-\frac{1}{2}Q_0(\boldsymbol{x}) - \frac{1}{2}Q_{\rm p}(\boldsymbol{x})\right]. \quad (10)$$

Being the product of two Gaussian distributions, $f(\boldsymbol{x}|\boldsymbol{h})$ is clearly also Gaussian. The expected value of $\boldsymbol{x}$ can therefore be obtained by minimizing $Q(\boldsymbol{x}) = Q_0(\boldsymbol{x}) + Q_{\rm p}(\boldsymbol{x})$, i.e., by solving

$$\partial Q(\boldsymbol{x})/\partial \boldsymbol{x} = 2N_0(\boldsymbol{x} - \boldsymbol{x}_0) + 2N_{\rm p}(\boldsymbol{x} - \boldsymbol{x}_{\rm p}) = 0, \quad (11)$$

or

$$(\boldsymbol{N}_0 + \boldsymbol{N}_{\rm p})\boldsymbol{x} = \boldsymbol{b}_0 + \boldsymbol{b}_{\rm p}, \quad (12)$$

where

$$\boldsymbol{b}_{\rm p} = \boldsymbol{N}_{\rm p}\boldsymbol{x}_{\rm p}. \quad (13)$$

It is readily shown that the covariance of the posterior estimate is given by

$$\boldsymbol{C} = (\boldsymbol{N}_0 + \boldsymbol{N}_{\rm p})^{-1}. \quad (14)$$

Equations (12)–(14) are the theoretical basis for the "joint solution" scheme of incorporating HIPPARCOS and *Tycho*-2 priors in the *Gaia* data processing, developed for the HTPM and TGAS projects (Michalik et al. 2014, 2015). In the following the prior is not derived from earlier catalogues but from our expectation of the distributions of parallaxes and proper motions.

2.4. Interpretation of the Gaussian probability densities

In the following it is assumed that the prior distribution of parallaxes is Gaussian with mean value $\varpi_{\rm p} = 0$ and standard deviation $\sigma_{\varpi,{\rm p}}$ equal to the square root of the corresponding (third) diagonal element of $\boldsymbol{C}_{\rm p}$. (Similar assumptions are made concerning the prior distributions of the proper motion components.) Clearly this is not very realistic, as it implies that, a priori, there is a 50% probability that the parallax is negative. However, the same Gaussian prior also means that there is a 90% probability that the true parallax is less than $1.28\sigma_{\varpi,{\rm p}}$, and a 99% probability that it is less than $2.33\sigma_{\varpi,{\rm p}}$. These latter statements are obviously meaningful, and provide a useful quantification of the expected *smallness* of the parallax, even though the distribution of true parallaxes is far from Gaussian.

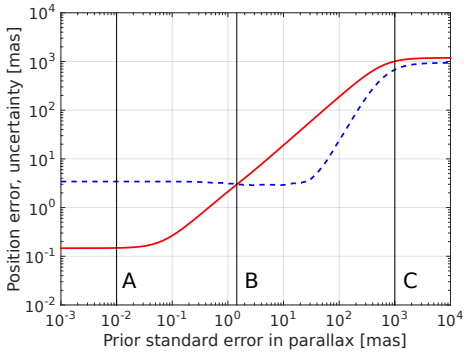

Fig. 1. Behaviour of the Bayesian position estimate as a function of the parallax prior uncertainty $\sigma_{\varpi,\mathrm{p}}$, for stars within one direction and magnitude bin (Table 1). Blue dashed curve: 90th percentile of the actual position errors. Red solid curve: semi-major axis of the 90% confidence ellipse. The priors labeled A, B, and C refer to the panels in Fig. 2.

A similar interpretation can be made of the Gaussian posterior PDF in Eq. (10). Although the actual error distribution of the Bayesian solution may be strongly non-Gaussian, this PDF can still be used to construct sensible confidence regions. In this work we are primarily interested in the positions and ignore the estimated parallaxes and proper motions. As the position uncertainty may be quite anisotropic, it should not be given as a single value but as a confidence region, for example a confidence ellipse, such that the true value is contained within that region with a certain degree of confidence P.

In this work we choose to work with a confidence level of 90% ($P = 0.9$). This means that the (Gaussian) posterior covariance should be such that a 90% confidence ellipse constructed from it will, in 90% of the cases, contain the true position. The choice of $P = 0.9$ is arbitrary, and a different value (e.g., 0.8, 0.95, or 0.99) would in general require a different covariance matrix in order to correctly characterise the errors at that P-value. Only in the case of Gaussian posterior errors would a single covariance matrix correctly describe the error distribution for different values of P.

The confidence ellipse can be constructed from the positional covariance (the 2×2 submatrix of $\boldsymbol{C}$) as described in Press et al. (2007). In particular, for $P = 0.9$ the semi-axes of the ellipse are $\sqrt{-2\ln(1-P)} \simeq 2.146$ times the square roots of the singular values of the positional covariance matrix. Inside the ellipse we have $Q(\boldsymbol{x}) - Q_{\min} < -2\ln(1-P) \simeq 4.605$.

A good astrometric solution should not only be as accurate as possible but also have formal uncertainties that characterize the actual errors correctly. Thus our general approach is to optimise the prior PDF for both goals. The formal uncertainties (positional covariance matrix) of the resulting posterior estimate should be such that the 90% confidence ellipse, computed as described above, contains the true position with 90% probability.

3. Prior in an astrometric solution

3.1. Framework and basic assumptions

In order to systematically evaluate the effect of the prior on the astrometric performance we have developed Matlab scripts which compute the Bayesian position estimates for a set of simulated stars. The true stellar parameters are taken from the *Gaia* Universe Model Snapshot (GUMS; Robin et al. 2012). *Gaia* observations are simulated using the *Gaia* Nominal Scanning Law (de Bruijne et al. 2010) with initial precession and scan phase

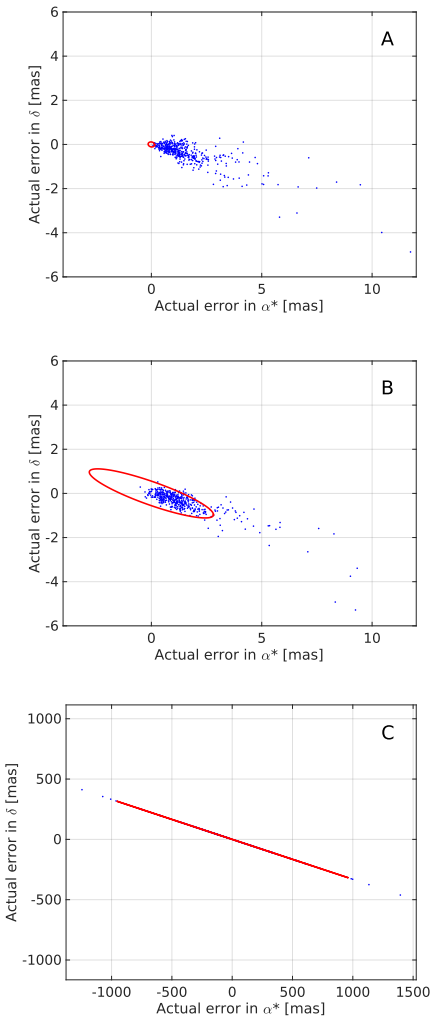

Fig. 2. Distribution of position errors for the three cases A, B, and C in Fig. 1. Blue dots: individual astrometric errors. Red curve: 90% confidence ellipse. Prior A is too tight and essentially gives a two-parameter solution. Prior B at the intersection of the curves in Fig. 1 (semi-major axis of the 90% confidence ellipse equals the 90th percentile of the actual errors) produces sensible error estimates. Prior C is too loose and yields a degenerate solution – although not visible in the diagram, 90% of the points are contained in the extremely elongated ellipse.

conditions consistent with the real mission from October 2014 until the end of 2015. The astrometric parameters are estimated as described in Sect. 2. For the initial analysis it is assumed that the spacecraft attitude and instrument calibration are known, so that the solution only involves the five astrometric parameters of each star. The posterior covariance and astrometric parameters are computed and compared for different combinations of magnitude range, position on the sky, as well as number of observations and their temporal distribution.

We then experiment with varying priors for parallax and proper motion in the different scenarios. Applying such prior knowledge aids the astrometric solution by constraining parallax and proper motion to small values, without forcing them to be strictly zero. In the present experiments the prior parallax

Table 1. Parameters of the single direction experiments reported in Figs. 1–3.

Celestial coordinates		
Equatorial:	$\alpha = 157.5°$	$\delta = 0.0°$
Ecliptic:	$\lambda = 159.2°$	$\beta = -8.8°$
Galactic:	$l = 245.7°$	$b = +46.5°$
Pencil beam parameters		
Radius of beam:		1°
Magnitude range:		$G = 15 \pm 0.5$ mag
Number of stars in GUMS:		458
Observations according to *Gaia*'s Nominal Scanning Law		
Date and time (UTC)	FOV	pos. angle #
2014-Oct-30 17.0h	P	230° 1
2014-Oct-30 18.8h	F	230° 1
2014-Nov-20 17.0h	P	156° 2
2014-Nov-20 18.8h	F	156° 2
2014-Dec-19 16.6h	P	247° 3
2014-Dec-19 18.4h	F	247° 3
2015-Apr-29 05.2h	P	341° 4
2015-Apr-29 07.0h	F	342° 4
2015-May-23 18.9h	F	65° 5
2015-Jun-21 04.9h	P	344° 6
2015-Jun-21 06.7h	F	344° 6
2015-Nov-09 06.1h	P	238° 7
2015-Nov-09 07.9h	F	238° 7
2015-Dec-29 11.8h	P	243° 8
2015-Dec-29 13.6h	F	244° 8

Notes. The P and F in the list of observations stand for preceding and following field of view (FOV). The position angle (third column) is the direction in which the FOV scans across the star, with 0° towards local North and 90° towards local East. The last column (#) is a sequential numbering of transit groups that are distinct in time and/or direction.

and proper motion are centred on zero with Gaussian uncertainties $\sigma_{\varpi,\mathrm{p}}$ and $\sigma_{\mu,\mathrm{p}}$, respectively. The largest known stellar parallax is 768 mas but typical parallaxes are much smaller than that. $\sigma_{\varpi,\mathrm{p}}$ is therefore in the few mas regime. The proper motion depends on the parallax through the expression for the transverse space velocity $v_T = A\mu/\varpi$, where $A \simeq 4.74$ km s^{-1} yr. Linear velocities in the Galaxy are of the order of 30–300 km s^{-1} and we therefore typically expect $\mu/\varpi \simeq 6$–60 yr^{-1}. At magnitude 15 the median ratio in GUMS is 10 yr^{-1}. For the ratio $\mathcal{R} = \sigma_{\mu,\mathrm{p}}/\sigma_{\varpi,\mathrm{p}}$ we have experimented with values in the range 1–60 yr^{-1} and found the results to be relatively insensitive to this choice. Using a value of $\mathcal{R} = 10$ yr^{-1} provides reasonable results in all cases, and we adopt this value in the rest of this paper.

3.2. Behaviour of the solution as a function of the prior

For an initial understanding of how the astrometric results depend on the choice of prior we show a representative example from our experiments. For one particular position on the sky we took stars from GUMS of a certain apparent G magnitude in a one degree pencil beam (Table 1). The framework described in Sect. 3.1 was used to simulate shorter or longer observation intervals of *Gaia*. Using one to eight distinct transits (Table 1, bottom section), we obtain the actual errors and formal uncertainties of the resulting position parameters for each observation interval as a function of prior size $\sigma_{\varpi,\mathrm{p}}$.

Figures 1 and 2 give the detailed results for an observation interval containing two transits that are distinct in time and angle (#1 and #2 in Table 1). Figure 1 summarizes how the actual errors and formal uncertainties vary as functions of $\sigma_{\varpi,\mathrm{p}}$. The sigmoid shape of the red curve describing the formal uncertainties is analytically explained in Appendix A.

Let us first look at the behaviour of the solution when a very tight prior is applied, e.g. $\sigma_{\varpi,\mathrm{p}} = 0.01$ mas as indicated by the vertical line at A in Fig. 1. The resulting solution (both with regard to the actual position errors and their formal uncertainties) is practically equivalent to solving only for the two position parameters, where the parallax and proper motion are implicitly assumed to be zero. In this regime the actual errors (dashed curve) are much larger than the formal position uncertainties (solid curve) due to the neglected parallax and proper motion. This is further illustrated by the top panel (prior A) in Fig. 2, where the 90% confidence ellipse (red) only contains a small fraction of the actual errors (blue dots).

Moving from tight to looser priors (increasing x-axis values in Fig. 1), the solution becomes less constrained and the formal uncertainties necessarily increase. For $\sigma_{\varpi,\mathrm{p}} \geq 30$ mas the size of the actual errors increases, since with two distinct transits the *Gaia* data alone are insufficient to determine all five parameters in the solution. Using a very loose prior, for example prior C illustrated in the bottom panel of Fig. 2, the astrometric solution becomes almost degenerate, though the formal uncertainties still correctly describe the actual errors. The intersection point marked with letter B in Fig. 1 would be a reasonable compromise, where the solution is as precise as permitted by the available data, while the formal uncertainties correctly characterize the actual position errors. This is illustrated in the middle panel (prior B) of Fig. 2, where most of the actual error points lie within the confidence ellipse.

The actual position errors in panels A and B in Fig. 2 are skewed in a direction depending on the position of the satellite in its orbit around the Sun. The offset of the error cloud from the origin depends on the sizes of the parallaxes and proper motions.

3.3. Criterion for the optimum prior uncertainties

The two quantities represented by the dashed and solid curves in Fig. 1 are not exactly comparable: one is the radius of the circle, centred on zero, that contains 90% of the actual errors; the other is the semi-major axis of the confidence ellipse. Using their point of intersection to optimise the prior, as suggested in the previous section, is therefore slightly illogical. We have instead adopted a different and much simpler criterion based on the confidence ellipse: the optimum prior should be such that 90% of the actual position errors are contained by the 90% confidence ellipse as calculated from the covariance matrix. The smallest $\sigma_{\varpi,\mathrm{p}}$ fulfilling this condition is in the following called $\sigma_{\varpi,\mathrm{F90}}$ and is illustrated in the second row of Fig. 3. The left diagram replicates the curves for two distinct transits previously shown in Fig. 1. The right diagram shows the corresponding fraction of actual errors contained in the 90% confidence ellipse. The prior choice $\sigma_{\varpi,\mathrm{F90}}$, marked by the solid vertical line and replicated in all panels of the figure, is in fact quite close to the intersection of the two curves in the left diagram.

So far we have limited our discussion to a scenario with two distinct transits. This is the case where the prior information is expected to be most critical: two distinct along-scan observations may suffice to determine a sensible position, but are always insufficient for a full five-parameter solution; on the other hand, three distinct transits in principle already allow a five parameter solution if both along- and across-scan information is used. We adopt $\sigma_{\varpi,\mathrm{F90}}$ based on the two-transit case and use it also in other scenarios with more or less observations. That the

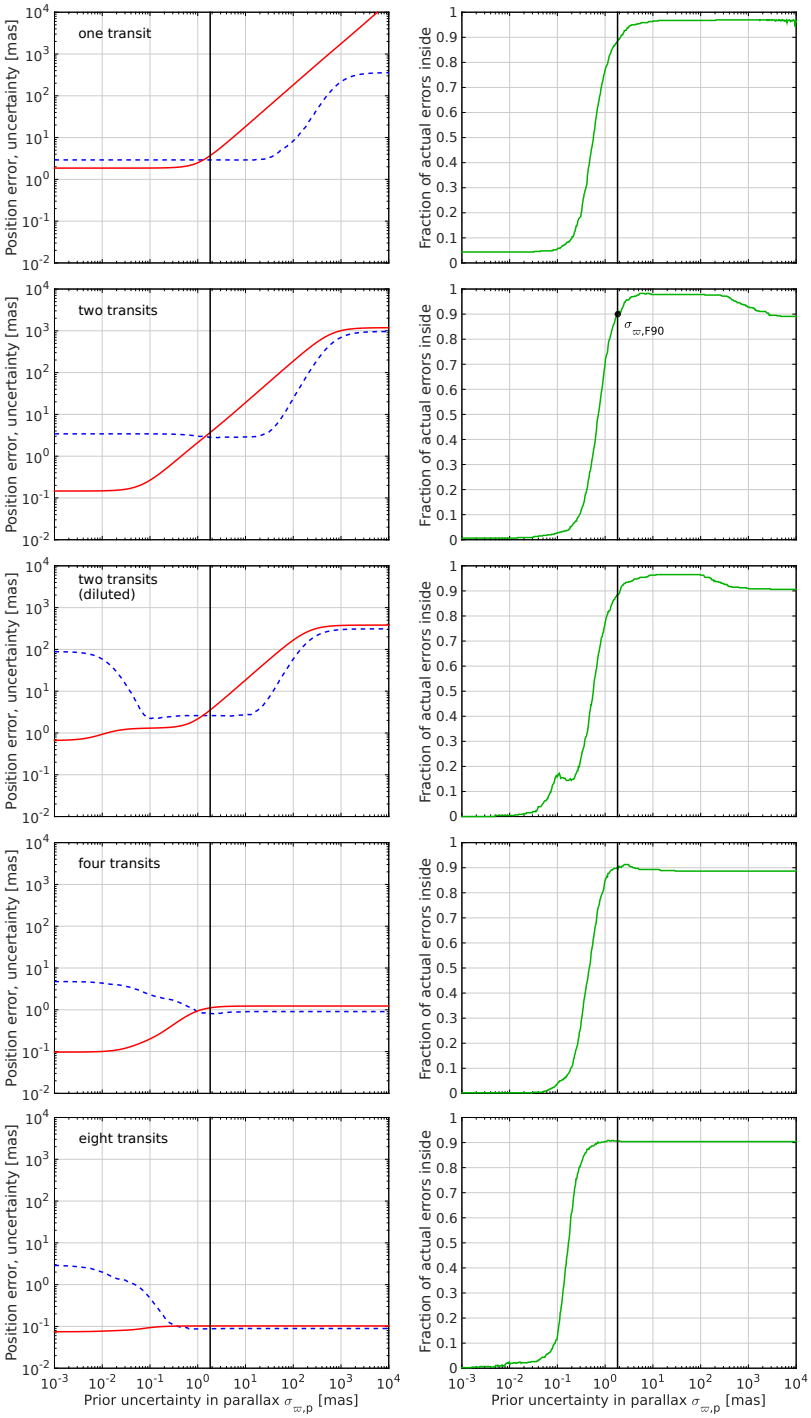

Fig. 3. Behaviour of the position error and uncertainty with varying priors, for stars in the direction and magnitude bin specified in Table 1. The rows display the behaviour for different numbers of distinct transits: one, two, two (diluted), four, and eight distinct transits. The diluted case uses the first and last transit from Table 1 instead of the first two transits. *Left column*: size of actual position errors (blue dashed) and their formal uncertainties (red solid), for stars in the same direction and magnitude bin, as a function of the prior uncertainty. *Right column*: fraction of actual errors contained by the formal error ellipse. The optimum prior $\sigma_{\varpi,\mathrm{F90}}$ is chosen based on the observation interval containing two distinct consecutive transits (second row). This prior is replicated in all other panels.

same prior works in these cases has been verified through simulations. Examples are given in Fig. 3, where the different rows show the behaviour of the astrometric solution for observation intervals containing one, two, four, and eight distinct transits, including one diluted case of two transits separated by 14 months. The prior $\sigma_{\varpi,\mathrm{F90}}$ determined from the two-transit scenario, and indicated by the solid vertical line in all panels, yields in all cases a solution where the size of the actual position errors (as measured by the 90th percentile) is close to its minimum, together with a realistic 90% confidence ellipse.

It is also evident that $\sigma_{\varpi,\mathrm{F90}}$ is a lower limit for a suitable prior. Increasing $\sigma_{\varpi,\mathrm{p}}$ by up to a factor ∼10 keeps the actual position errors at the same level while providing the same or a more conservative formal uncertainty estimate, whereas using a

smaller prior would underestimate the errors. In Appendix A we briefly address the effect of the prior uncertainty on the posterior error estimate from an analytical point of view.

3.4. Prior uncertainty as function of magnitude and direction

In Sect. 3.3 we described the determination of an optimum value of $\sigma_{\varpi,\mathrm{p}}$, called $\sigma_{\varpi,\mathrm{F90}}$, for one particular direction and magnitude interval. We repeated this experiment for different directions and magnitude bins (G = 6–20, in steps of 1 mag). We find that 48 directions uniformly distributed on the sky are sufficient to sample the large-scale structures of the underlying Galaxy model. As expected, $\sigma_{\varpi,\mathrm{F90}}$ is a strong function of magnitude (fainter stars being on average more distant), and to a lesser extent dependent on direction (because of extinction and the spatial distribution of stars in our Galaxy)[4]. For a given magnitude bin we find that a reasonable fit to the individual data points is provided by

$$\log_{10}\sigma_{\varpi,\mathrm{F90}} = s_0 + s_1|\sin b| + s_2\cos b\cos l \tag{15}$$

(see the left panel of Fig. 4). The variations of the coefficients s_0, s_1, and s_2 with G magnitude bins are shown in the middle panel of Fig. 4. They are well approximated by simple polynomials in G:

$$s_0(G) = 2.187 - 0.2547G + 0.006382G^2 \tag{16}$$

$$s_1(G) = 0.114 - 0.0579G + 0.01369G^2 - 0.000506G^3 \tag{17}$$

$$s_2(G) = 0.031 - 0.0062G. \tag{18}$$

The size of the fitted $\sigma_{\varpi,\mathrm{F90}}$ prior is illustrated in the right panel of Fig. 4. For the astrometric solution of an arbitrary star of magnitude G at galactic coordinates (l, b) the prior normal matrix to be used in Eqs. (12), (13) is then

$$\boldsymbol{N}_\mathrm{p} = \mathrm{diag}\left(0,\ 0,\ \sigma^{-2}_{\varpi,\mathrm{F90}},\ \sigma^{-2}_{\mu,F90},\ \sigma^{-2}_{\mu,F90}\right), \tag{19}$$

where $\sigma_{\varpi,\mathrm{F90}}(l, b, G)$ is given by Eqs. (15)–(18), and $\sigma_{\mu,F90} = \mathcal{R}\sigma_{\varpi,\mathrm{F90}}$, where $\mathcal{R}$ = 10 yr^{-1}.

An extension of $\sigma_{\varpi,\mathrm{F90}}(l, b, G)$ to fainter stars is non-trivial, since GUMS is only complete to G = 20. For fainter stars the value at G = 20 should be used since it provides a conservative (over)estimate. For stars brighter than G = 6 it might be preferable to make solutions directly using priors from the HIPPARCOS and *Tycho*-2 catalogues.

In principle more sophisticated priors could be considered, which take into account photometric, spectroscopic, or other auxiliary information. For example, blue stars have on average smaller parallaxes than red stars, and for identified extragalactic objects the prior uncertainty could be much smaller. However, such information may be unavailable precisely in the cases where a prior is needed. On the other hand, a direction and an approximate magnitude are always available, and allow us to define a general prior.

4. Simulation of potential application scenarios

In this section we demonstrate the feasibility of the proposed method based on simulations of potential applications. We used GUMS to provide simulated "true" parameters for a large catalogue of stars of different magnitude classes, where we include the 5×10^5 brightest stars fainter than each of the magnitudes G = 11, 15, and 19, respectively. The software package AGISLab (Holl et al. 2012; Bombrun et al. 2012) was used to simulate *Gaia* observations and to perform a global astrometric solution.

In Sect. 1 we described three situations where the Bayesian approach might be useful: transient objects, faints stars at the detection limit, and the processing of short stretches of *Gaia* data. The first two situations are similar to the diluted case presented in Sect. 3.3. When solving the astrometric parameters we can assume that an accurate satellite attitude is known from a previous solution of well-observed stars. The third situation applies to the first release of *Gaia* data, where the spacecraft attitude must be obtained together with the astrometric parameters from the same (insufficient) data, and therefore is much less accurate than in the previous scenario. We therefore performed two distinct sets of simulations described hereafter.

4.1. Stars with very diluted observation histories

Here we use an attitude determined by a five year solution of simulated *Gaia* data without prior. We then compute the astrometric parameters without changes to the attitude (a so-called secondary solution) for stars with a highly diluted observation history. The dilution is simulated by assigning each field of view transit a 95% probability of being removed from the solution. The average number of retained transits per star is ≃4.4.

We made a solution using the optimum prior according to Sect. 3.4. Additionally we experimented with a very tight prior ($\sigma_{\varpi,\mathrm{p}}$ = 0.01 mas, analogous to case A in Fig. 2) and a very loose prior ($\sigma_{\varpi,\mathrm{p}}$ = 1000 mas, analogous to case C in Fig. 2) to check the behaviour of the solution in these extreme cases. For comparison we also made two runs without any prior, one in which only the two position parameters were determined, and one with all five astrometric parameters. In the latter case it was not possible to determine a unique astrometric solution for all stars, as explained at the end of Sect. 2.1.

Table 2 summarizes our results. Only the results for the position estimates are shown. When using a very tight prior the results are very similar to a two parameter solution. The formal uncertainties computed in this solution grossly underestimate the actual errors. Using the optimum prior $\sigma_{\varpi,\mathrm{F90}}$ (or ten times its value) instead yields sensible estimates of the uncertainties. The use of this prior not only provides improved uncertainties, but also reduces the actual errors compared with a two-parameter solution (or a very tight prior). This somewhat surprising behaviour can be understood from the three bottom left panels in Fig. 3: using a non-zero prior uncertainty provides the necessary freedom for the solution to accommodate non-zero parallaxes and proper motions and hence to reduce the actual position errors.

With a very loose prior of one arc-second the Bayesian approach still results in a numerically stable astrometric solution (which is not true for solutions without any prior), including realistic estimates of the positional uncertainties. However the actual errors are up to a factor two larger than when using a well-chosen prior.

4.2. The first data release

Another possible application of the proposed method is for the planned first release of intermediate *Gaia* data. As this may be

[4] Statistically, $\sigma_{\varpi,\mathrm{F90}}$ is closely related to the distribution of parallaxes in GUMS. Inspection of the distribution shows that, for any given magnitude and direction, it is roughly equal to 0.5–0.8 times the 90th percentile of the parallaxes.

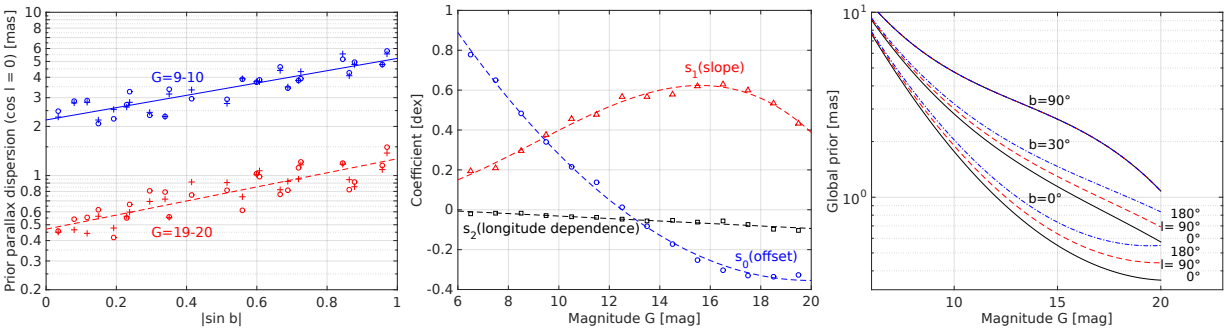

Fig. 4. Illustrations of the all-sky approximation to the parallax prior $\sigma_{\varpi,\mathrm{F90}}$. *Left*: representative example of the linear fit in Eq. (15) of the logarithm of the parallax prior $\sigma_{\varpi,\mathrm{F90}}$ as a function of galactic latitude b, for two magnitude ranges $G = 9{-}10$ (blue), and $G = 19{-}20$ (red). The small dependence on galactic longitude (the third term in Eq. (15)) has been subtracted leaving no systematic dependence on galactic longitude l, as shown by the different symbols ($\circ$ for $\cos l > 0$, + for $\cos l < 0$). *Middle*: variations of the coefficients s_0, s_1, and s_2 with G magnitude, and polynomial fits according to Eqs. (16)–(18). *Right*: the prior $\sigma_{\varpi,\mathrm{F90}}$ in Eq. (15) as a function of magnitude, for different latitudes (lowest to highest group: $b = 0°$, 30°, and 90°) and different longitudes (black solid $l = 0°$, red dashed 90°, blue dotted-dashed 180°).

Table 2. Simulation results for stars with 95% diluted five year observation histories, where the spacecraft attitude was determined by a separate solution from well-observed stars.

Prior $\sigma_{\varpi,\mathrm{p}}$	Fraction in 90% conf. ellipse			Actual position errors [mas]		
	$G \simeq 11$	$G \simeq 15$	$G \simeq 19$	$G \simeq 11$	$G \simeq 15$	$G \simeq 19$
Subset of stars with ≤4 field-of-view transits						
none (2 parameters)	0.5%	1.8%	13.5%	33.0	16.3	15.2
0.01 mas	1.5%	3.5%	14.3%	21.8	12.1	14.8
$\sigma_{\varpi,\mathrm{F90}}$	90.1%	91.4%	91.2%	7.6	4.3	7.6
$10\sigma_{\varpi,\mathrm{F90}}$	92.7%	93.3%	94.4%	8.4	5.2	10.5
1000 mas	92.5%	93.0%	93.3%	8.6	7.4	15.5
Subset of stars with >4 field-of-view transits						
none (2 parameters)	0.3%	0.8%	8.6%	21.0	11.3	9.7
0.01 mas	3.1%	5.4%	10.4%	6.7	5.0	8.9
$\sigma_{\varpi,\mathrm{F90}}$	89.4%	89.9%	90.3%	0.2	0.3	1.6
$10\sigma_{\varpi,\mathrm{F90}}$	89.5%	89.8%	90.5%	0.2	0.3	2.0
1000 mas	89.5%	89.8%	90.0%	0.2	0.3	2.2

Notes. A prior uncertainty $\geq\sigma_{\varpi,F90}$ provides a sensible solution for all stars. Column 1: prior uncertainty used in the solution. Columns 2–4: fractions of actual position errors contained in the 90% confidence ellipses calculated from the formal covariances; ideally, these values should be around 90%. Columns 5–7: 90th percentile values of the actual position errors (estimated minus true value) in mas; these should be as small as possible. For comparison: two parameter solution (position only) without a prior.

based on too short a stretch of data for a reliable five-parameter solution, the release is targeted[5] to give only positions and mean G. We propose the use of a prior to ensure that the one year global solution provides a sensible formal position uncertainty for all stars. This scenario is different compared to Sect. 4.1, since the attitude must now be determined from the same observations as the astrometric parameters, a so-called primary solution[6]. We simulate this through a global solution assuming one year of *Gaia* observations with 20% of dead time, and using priors of varying size.

Table 3 summarizes our results. Contrary to Sect. 4.1 and Table 2 we now find that the prior $\sigma_{\varpi,\mathrm{F90}}$ constrains the solution too much. It appears that the prior uncertainty needs to be increased to account for the larger attitude errors caused by the unknown parallax and proper motion contributions. Empirically we find that a ten fold increase of the prior uncertainty provides the necessary relaxation of the constraint and allows the solution to fulfill the criteria for a sensible astrometric result.

5. Conclusions

In this paper we discuss the astrometric solutions for stars with an insufficient number of *Gaia* observations. This will be the case for the majority of stars in the first data release of *Gaia* data, but is also an important issue during later stages of the mission, e.g. for transient objects that are only observed in their bright phases, and stars close to the detection limit. In all these cases one can still obtain very valuable position estimates, either by solving only for the position parameters or through the use of priors for the remaining parameters. In fact, solving only for the position parameters is equivalent to assuming that the parallax and proper motion are exactly zero, in other words to the use of a prior value equal to zero with infinite weight. Using a more carefully selected prior improves the quality of the astrometric solution for these stars. Very specifically, it provides an elegant way to ensure that the position estimates obtain formal uncertainties that correctly characterize the actual errors.

[5] A tentative release schedule is given by ESA on http://www.cosmos.esa.int/web/gaia/release

[6] It could also be considered to use the attitude from a potential *Tycho–Gaia* Astrometric Solution (Michalik et al. 2015).

Table 3. Global astrometric solutions using 12 months of simulated *Gaia* data, where the attitude is determined as part of the solution.

Prior $\sigma_{\varpi,\mathrm{p}}$	Fraction in 90% conf. ellipse			Actual position errors [mas]		
	$G \simeq 11$	$G \simeq 15$	$G \simeq 19$	$G \simeq 11$	$G \simeq 15$	$G \simeq 19$
Subset of stars with ≤4 field-of-view transits						
$\sigma_{\varpi,\mathrm{F90}}$	76.5%	86.8%	92.4%	1.2	0.7	2.0
$10\sigma_{\varpi,\mathrm{F90}}$	89.1%	90.4%	94.3%	1.4	1.1	4.2
1000 mas	89.7%	89.8%	90.6%	3.8	3.4	17.7
Subset of stars with >4 field-of-view transits						
$\sigma_{\varpi,\mathrm{F90}}$	32.3%	53.3%	88.0%	0.2	0.2	0.8
$10\sigma_{\varpi,\mathrm{F90}}$	88.6%	89.3%	90.4%	0.1	0.2	1.0
1000 mas	88.7%	89.4%	90.0%	0.1	0.2	1.1

Notes. The prior uncertainty needs to be relaxed to $10\sigma_{\varpi,F90}$ to obtain a sensible solution. Columns as in Table 2.

Prior information is incorporated in the astrometric solution using Bayes' rule. For practical reasons the prior probability distributions are taken to be Gaussian. Moreover, they are always centred on zero, since any other choice would necessarily involve additional assumptions and thus be even more arbitrary. For objects with negligible parallax, such as quasars, it is a conservative choice.

We analyse the influence of different priors on the astrometric solutions, based on numerical experiments with realistic distributions of stellar parameters from the *Gaia* Universe Model Snapshot (GUMS). To optimize the prior we require that 90% of the actual position errors are included in the 90% confidence region calculated from the (Gaussian) posterior probability density, i.e. from the formal covariance matrix. Using the resulting prior ($\varpi_\mathrm{p} = 0 \pm \sigma_{\varpi,\mathrm{F90}}$) we find that non-singular five-parameter astrometric solutions can be obtained, with reasonable estimates of the position uncertainties, for any star that is observed in at least one field-of-view transit. Using this prior slightly reduces the actual position errors, compared with a two-parameter solution. The solution is robust to using a larger prior uncertainty than $\sigma_{\varpi,\mathrm{F90}}$, and in some cases (depending on the attitude estimation) a ten fold increase is motivated (Sect. 4.2).

The choice of a 90% confidence level for the position errors is arbitrary and it would be possible to optimize the prior for any other desired percentage. The 10% stars falling outside the confidence ellipse cannot easily be identified from the data and could be considered outliers. In statistical uses of the data, 90% provides a good compromise between keeping a reasonably small fraction of outliers and maintaining a good characterization of the positional uncertainties for most stars. A higher confidence level would decrease the fraction of outliers, but at the expense of a rapidly growing confidence region due to the non-Gaussian nature of the actual position errors.

Like any solution using a prior, the resulting astrometric parameters are in general biased. Using a reference epoch centred on the observations, the position bias is of the order of the neglected parallax, or at most a few mas in typical cases. As discussed below this is acceptable. In order to obtain realistic uncertainties of the positions, it is necessary to introduce the parallax and proper motion as formal parameters in the solution. This means that posterior estimates are also provided for these. However, the resulting parallaxes and proper motions are in general so strongly biased by the prior that they become physically meaningless, and they should therefore not be used.

For the first release of *Gaia* data, consisting mainly of position information and G magnitudes, small biases in the resulting position estimates are fully acceptable and unavoidable. For future releases however, where a full solution can be determined for most of the stars, it is important to determine attitude and geometric calibration parameters as part of the primary solution, by using only the stars with a sufficient amount of observations. For all of these it is mandatory that no prior is used. Any star with insufficient observations, which requires the use of a prior for the solution, must be part of a separate (secondary) update, in which the attitude and calibration are not modified. For the secondary stars with insufficient data, the $\varpi_\mathrm{p} = 0 \pm \sigma_{\varpi,\mathrm{F90}}$ prior will however allow us to obtain sensible position estimates with well-characterized formal uncertainties.

Acknowledgements. We thank Uwe Lammers, who contributed to the idea and progress of this study, and its funding under ESA Contract No. 4000108677/13/NL/CB. We are grateful to Ulrich Bastian, Alex Bombrun, Anthony Brown, Sergei Klioner, Uwe Lammers, Paul McMillan, Mercedes Ramos-Lerate, and the referee, Floor van Leeuwen, for their helpful feedback to our manuscript. This work was supported by the Gaia Data Processing and Analysis Consortium (DPAC) and uses the AGIS/AGISLab and GaiaTools software packages; special thanks to their maintainers and developers. We gratefully acknowledge financial support from the Swedish National Space Board and the Royal Physiographic Society in Lund.

Appendix A: Analytical illustration

To analytically study how the prior affects the posterior position uncertainty, we consider a simplified case where the solution includes only two astrometric parameters: one component of position (e.g. δ) and the parallax (ϖ). The normal matrix incorporating the prior $\boldsymbol{N}_\mathrm{p} = \mathrm{diag}(0, \sigma_{\varpi,\mathrm{p}}^{-2})$, similar to Eq. (19), then takes the form

$$\boldsymbol{N}_0 + \boldsymbol{N}_\mathrm{p} = \frac{1}{1-\rho^2}\begin{pmatrix} \sigma_\delta^{-2} & \dfrac{-\rho}{\sigma_\delta \sigma_\varpi} \\ \dfrac{-\rho}{\sigma_\delta \sigma_\varpi} & \sigma_\varpi^{-2} + \left(1-\rho^2\right)\sigma_{\varpi,\mathrm{p}}^{-2} \end{pmatrix}, \tag{A.1}$$

where σ_δ and σ_ϖ are the standard errors of the position and parallax, respectively, and ρ is the correlation coefficient; all these quantities are based on the data only. Calculating the posterior covariance matrix using Eq. (14) we find the position uncertainty

$$\sigma_{\delta,\,\mathrm{posterior}} = \sigma_\delta \sqrt{1 - \frac{\rho^2}{1 + \left(\sigma_{\varpi,\mathrm{p}}/\sigma_\varpi\right)^2}}. \tag{A.2}$$

This formula agrees with our numerical experiments. In particular it reproduces the behaviour of the position uncertainty shown

in Figs. 1 and 3, featuring a monotonically increasing $\sigma_{\delta,\,\mathrm{posterior}}$ between two asymptotic values, $\sigma_\delta\sqrt{1-\rho^2}$ and σ_δ, as the prior goes from very tight to very loose. Equation (A.2) implies that the improvement in the positional uncertainty gained by using the parallax prior depends only on the correlation coefficient ρ and the ratio of the parallax prior to the formal uncertainty without prior, $\sigma_{\varpi,\mathrm{p}}/\sigma_\varpi$. For uncorrelated data, no improvement is possible, as $\sigma_{\delta,\,\mathrm{posterior}} = \sigma_\delta$ for $\rho = 0$.

Similar arguments hold for the general five-parameter solution, except that they cannot be demonstrated so easily.

References

Bombrun, A., Lindegren, L., Hobbs, D., et al. 2012, A&A, 538, A77
de Bruijne, J. H. J. 2012, Ap&SS, 341, 31
de Bruijne, J., Siddiqui, H., Lammers, U., et al. 2010, in Relativity in Fundamental Astronomy: Dynamics, Reference Frames, and Data Analysis, ed. S. A. Klioner, P. K. Seidelmann, & M. H. Soffel, IAU Symp., 261, 331
Holl, B., Lindegren, L., & Hobbs, D. 2012, A&A, 543, A15
Lindegren, L., Lammers, U., Hobbs, D., et al. 2012, A&A, 538, A78
Michalik, D., Lindegren, L., Hobbs, D., & Lammers, U. 2014, A&A, 571, A85
Michalik, D., Lindegren, L., & Hobbs, D. 2015, A&A, 574, A115
Mignard, F. 2009, The Hundred Thousand Proper Motions Project, Gaia Data Processing and Analysis Consortium (DPAC) technical note GAIA-C3-TN-OCA-FM-040, http://www.cosmos.esa.int/web/gaia/public-dpac-documents
Perryman, M. A. C., de Boer, K. S., Gilmore, G., et al. 2001, A&A, 369, 339
Press, W. H., Teukolsky, S. A., Vetterling, W. T., & Flannery, B. P. 2007, Numerical Recipes, The Art of Scientific Computing, 3rd edn. (New York: Cambridge University Press)
Robin, A. C., Luri, X., Reylé, C., et al. 2012, A&A, 543, A100
Sivia, D. S. & Skilling, J. 2006, Data analysis: a Bayesian tutorial, Oxford science publications (Oxford: Oxford University Press)

Paper VI

Astronomy & Astrophysics manuscript no. quasarsInTGAS
October 26, 2015

Quasars can be used to verify the parallax zero-point of the Tycho–Gaia Astrometric Solution

Daniel Michalik and Lennart Lindegren

Lund Observatory, Department of Astronomy and Theoretical Physics, Lund University, Box 43, 22100 Lund, Sweden
e-mail: [daniel.michalik; lennart]@astro.lu.se

Received 24 September 2015 / Accepted 25 October 2015

ABSTRACT

Context. The Gaia project will determine positions, proper motions, and parallaxes for more than one billion stars in our Galaxy. It is known that Gaia's two telescopes are affected by a small but significant variation of the basic angle between them. Unless this variation is taken into account during data processing, e.g. using on-board metrology, it causes systematic errors in the astrometric parameters, in particular a shift of the parallax zero-point. Previously, we suggested an early reduction of Gaia data for the subset of Tycho-2 stars (Tycho-Gaia Astrometric Solution; TGAS).
Aims. We aim to investigate whether quasars can be used to independently verify the parallax zero-point already in early data reductions. This is not trivially possible as the observation interval is too short to disentangle parallax and proper motion for the quasar subset.
Methods. We repeat TGAS simulations but additionally include simulated Gaia observations of quasars from ground-based surveys. All observations are simulated with basic angle variations. To obtain a full astrometric solution for the quasars in TGAS we explore the use of prior information for their proper motions.
Results. It is possible to determine the parallax zero-point for the quasars with a few μas uncertainty, and it agrees to a similar precision with the zero-point for the Tycho-2 stars. The proposed strategy is robust even for quasars exhibiting significant fictitious proper motion due to a variable source structure, or when the quasar subset is contaminated with stars misidentified as quasars.
Conclusions. Using prior information about quasar proper motions we could provide an independent verification of the parallax zero-point in early solutions based on less than one year of Gaia data.

Key words. astrometry – methods: data analysis – parallaxes – proper motions – quasars: general – space vehicles: instruments

1. Introduction

Gaia is a European space mission determining astrometry, photometry, and spectroscopy for more than one billion sources[1] (Perryman et al. 2001; de Bruijne 2012). Important features of Gaia's astrometric measurements are

- the uniform scanning that ensures a relatively homogeneous all-sky performance;
- the high accuracy of the final astrometric data, at tens of μas level for $G = 15$;
- the relatively faint $G \simeq 20$ magnitude limit, which makes it possible to observe a large number of quasars, necessary for determination of the reference frame and as an independent check of the parallax zero-point;
- and the capability to measure absolute parallaxes by combining simultaneous measurements of different objects separated by a large angle on the sky.

For the last point Gaia's design includes two viewing directions, separated by a large basic angle, which needs to be either perfectly stable, or independently monitored. Gaia's basic angle was designed to be very stable while at the same time being measured on-board with high accuracy through an interferometric device called the basic angle monitor (BAM; Mora et al. 2014).

[1] The word source refers to any point-like object observed by Gaia, this includes stars, quasars, supernovae, etc.

Verification of the stability of the basic angle and of the quality of the on-board metrology can only partially be done through the analysis of the post-fit residuals of the astrometric solution, but a full verification requires the use of external data. Quasars provide a clean and self-consistent approach, as they are so far away that their true parallaxes can safely be assumed to be zero. It is thus possible to determine the zero point of the parallaxes measured by Gaia simply by taking the median of the resulting parallax distribution in a quasar subset and comparing it to the expected zero value. The width of this distribution gives an indication for the uncertainty of the obtained median value.

For a full five-parameter solution of the astrometric parameters (position, parallax, and proper motion), at least five distinct observations of each source are necessary, unless prior knowledge can be used to complement the observational data (Michalik et al. 2015b). A full five-parameter data reduction with less than one year of Gaia data is possible for example for the Tycho-2 (Tycho–Gaia Astrometric Solution; TGAS; Michalik et al. 2015a) and the Hipparcos stars (Hundred Thousand Proper Motions project; HTPM; Mignard 2009; Michalik et al. 2014). The Tycho-2 and Hipparcos catalogues contain extremely few extragalactic objects, which are not sufficient for an independent verification of the basic angle. Adding quasars to such early solutions requires prior information to overcome the ambiguity of parallax and proper motion. In this paper we explore which prior information can be used, and demonstrate the feasibility of

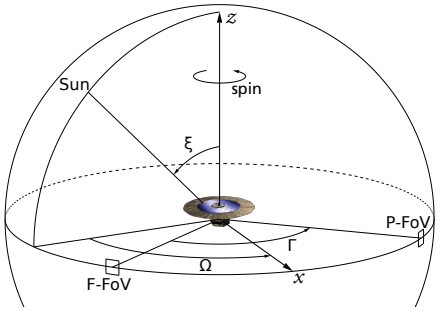

Fig. 1. Solar-aspect angle ξ and spin phase Ω define the orientation of the spacecraft relative to the Sun. $\boldsymbol{x}$ and $\boldsymbol{z}$ are axes fixed in the spacecraft reference system. The basic angle Γ separates the preceding and following fields of view (FoV), with $\boldsymbol{x}$ half-way between them.

adding quasars to the TGAS project for verification of the parallax zero-point in the light of basic angle variations.

2. Basic Angle Variations and Metrology

The two viewing directions of Gaia are separated by a basic angle $\Gamma = 106.5$ deg. Basic angle variations are harmful to the resulting astrometry unless they are modelled as part of the data processing or corrected by means of data from the on-board metrology device BAM. The BAM deploys a laser beam to create an interferometric pattern in each field-of-view (FoV). Variations in the basic angle cause a change in the relative phases of the fringes, which are measured by a dedicated BAM CCD adjacent to the main astrometric field of Gaia. It is desirable to verify that these measurements correctly characterize the variations for the entire focal plane. This can be done by comparing the BAM data with the variations determined from the astrometric observations themselves.

Gaia's scanning requires a constant tilt $\xi = 45$ deg of the spacecraft spin axis with respect to the Sun (de Bruijne 2012). The phase of the spacecraft relative to the Sun is therefore completely described by the angle $\Omega(t)$ giving the pointing of the satellite within its six hour spin period (Fig. 1). Mora et al. (2014) reported an early analysis of BAM measurements finding stable periodic variations depending on Ω with an amplitude of about 1 mas. This is much larger than expected from the design of the spacecraft; however the effects on the astrometric results can be largely eliminated if the basic angle variations are determined with sufficient accuracy. The basic angle variations can be described by a Fourier expansion in terms of $\cos k\Omega$ and $\sin k\Omega$ where $k = 1, 2, \ldots$ is the order of the harmonics.

Dedicated simulations have shown that all but the $\cos\Omega$ term can be solved with high accuracy from Gaia data alone, even with less than one year of observations. They are thus neglected throughout the rest of this article. However, the first cosine harmonic is virtually indistinguishable from a constant shift of the parallax zero-point (Lindegren et al. 1992, Sect. 6.1) and therefore impossible[2] to determine from Gaia data alone. Lindegren (2004) relates the parallax zero-point $\Delta\varpi$ to the amplitude a_1 of the $\cos\Omega$ term and the spacecraft distance R (in au) from the Sun as

$$\Delta\varpi = \frac{a_1}{2R\sin\xi\sin(\Gamma/2)}. \quad (1)$$

[2] It has been suggested that the finite size of the FoV and other design details of Gaia may allow to determine even the $\cos\Omega$ term purely from the observational data (S. Klioner, private communication).

In this paper we limit the further analysis to the first cosine term assuming a fixed amplitude $a_1 = 1$ mas. For the observation interval used in the following simulations R evolves such that the expected average $\Delta\varpi \simeq 871.9$ μas.

3. Quasar parallaxes in early solutions

We first repeat simulations of the TGAS scenario as described in Michalik et al. (2015a, Sect. 3), but perturb the observations by a periodic basic angle variation proportional to $\cos\Omega$ with an amplitude of 1 mas. Otherwise we follow the same assumptions as before, i.e., we simulate half a year of Gaia observations of the Hipparcos and Tycho-2 stars, and process them using the Hipparcos positions and proper motions and the Tycho-2 positions at 1991.25 as priors. As expected, the resulting parallax solution is strongly biased with a median parallax error (estimated minus true value) consistent with Eq. (1). This zero-point shift cannot be easily determined from the stellar observations themselves, and the recovery of absolute parallaxes in such a solution must instead rely on the correctness of BAM metrology, which can be verified using external information.

Thus, it is desirable to include an additional subset of quasars. The true quasar parallaxes are known to be virtually zero. Therefore, the median of the quasar subset can be used to estimate the parallax zero-point of the astrometric solution. For our simulations the quasar subset is taken from the Gaia Initial Quasar Catalogue (GIQC; Andrei et al. 2014). GIQC is a list of quasars produced in preparation for the Gaia mission, based mainly on the Large Quasar Astrometric Catalogue (LQAC; Souchay et al. 2012), itself based on the Sloan Digital Sky Survey (SDSS; Abazajian et al. 2009) and other ground-based surveys. It contains positions and approximate magnitudes for over one million objects. The source distribution is strongly inhomogeneous and shows the survey footprint. We use the ∼190 000 entries flagged as "defining", i.e., objects with high level of certainty to be quasars within the magnitude limits of Gaia, based on their observational history and spectroscopic properties.

To account for the possibility that early Gaia solutions might not include observations for all of them, 150 000 (∼80%) of the quasars listed in GIQC are randomly selected and the rest discarded. From GIQC we use the position and magnitude to define the simulated 'true' quasar sources. The true values of parallax and proper motion are initially set to zero.

To allow us to obtain a sensible five-parameter solution with as short a stretch of data as present in a half year TGAS solution, we need some prior information for the quasars. One could consider using the precisely known radio positions of VLBI quasars. Approximately 2500 ICRF sources with optical counterparts are expected to be bright enough to be detected by Gaia. However this number of sources is too small to provide a statistically meaningful result. For the much larger number of GIQC quasars no reliable position information exists at a level that makes it usable as prior information. Even though we know that quasar parallaxes are supposed to be zero, we do not want to use this as prior information in the solution either, since we want to determine the parallax values freely from the Gaia data in order to verify the parallax zero-point. Instead, we suggest to make use of the fact that quasars have negligible proper motions[3] due to

[3] Fictitious proper motions caused by intrinsic variations in the quasars are discussed in Sect. 3.2. Additionally, the expected proper motion of the Galactocentric acceleration must be taken into account in the real data. This effect is a few μas yr^{-1} (Bastian 1995; Kovalevsky 2003) and does not affect the principle shown in this paper.

Table 1. Simulation results of three different experiments, comparing the parallax median between the stellar subset and the quasars.

	Parallax selection			
	90% best		all	
Subset	Median [μas]	RSE [μas]	Median [μas]	RSE [μas]
Experiment 1: clean quasar sample				
Stars	872.1 ± 0.2	441.9	872.1 ± 0.2	613.5
Quasars	876.4 ± 2.0	1336.6	876.7 ± 2.5	2324.7
Experiment 2: with fictitious proper motions				
Stars	872.0 ± 0.2	442.0	872.0 ± 0.2	613.4
Quasars	876.7 ± 2.9	1644.7	877.7 ± 3.4	2676.3
Experiment 3: with 5% contamination				
Stars	872.1 ± 0.2	441.9	872.0 ± 0.2	613.5
Quasars	871.7 ± 2.2	1429.2	872.0 ± 2.4	2452.9

Notes. "Stars" refers to the combined subset of Hipparcos and Tycho-2 sources. In each subset, statistics are given for the selection of the 90% sources with the smallest individual formal uncertainties and for all sources together. The values given are the median (and its uncertainty from the bootstrap method) and the RSE dispersion of the parallax errors (estimated minus true).

their cosmological distances. Incorporating this information as a prior in the early Gaia astrometric solutions will lift the degeneracy to the parallax and is sufficient to obtain a good astrometric solution for the quasar subset.

We demonstrate the feasibility of the method through three different simulations. First we use a clean quasar sample with zero true proper motions and parallaxes. Then we relax these assumptions and introduce quasar structure variations, as well as contamination of the dataset with stellar sources. Table 1 shows the results of the three experiments, with further explanations below.

3.1. Clean quasar sample

In the first experiment the simulated 'true' parallaxes and proper motions in the quasar subset are strictly zero. To allow a full five-parameter astrometric solution we apply a prior of 0 ± 10 μas yr^{-1} to each proper motion component. The prior uncertainty of 10 μas yr^{-1} is somewhat arbitrary, but provides enough weight to constrain the proper motions to negligible values without causing numerical difficulties. We incorporate the prior using Bayes' rule as described in Michalik et al. (2015b).

We evaluate the resulting parallaxes separately for the stellar subset (Hipparcos and Tycho-2 stars) and the quasars. Table 1, experiment 1, presents the median value of the parallax errors (estimated minus true), the uncertainty of the median calculated using the bootstrap method, and the RSE[4] dispersion of the parallax errors for each of the subsets. The different columns give statistics for selections based on the individual formal standard uncertainties of the parallaxes. The median obtained for the quasar subset agrees with the corresponding stellar value to within a few μas, independent of the selection of sources.

[4] The "Robust Scatter Estimate" (RSE) is defined as 0.390152 times the difference between the 90th and 10th percentiles of the distribution of the variable. For a Gaussian distribution it equals the standard deviation. Within the Gaia core processing community the RSE is used as a standardized, robust measure of dispersion (Lindegren et al. 2012).

3.2. Fictitious proper motion from variable source structure

Variation in the source structure of quasars can lead to shifts of their photocentres up to the milli-arcsecond level (e.g., Popović et al. 2012; Porcas 2009; Taris et al. 2011). Linear trends of these shifts might lead to fictitious proper motions measured for quasars and stable over years to decades. Titov et al. (2011) fitted long term proper motions for 555 quasars from VLBI observations. We find that the total proper motion $\mu = \sqrt{\mu_{\alpha*}^2 + \mu_\delta^2}$ in μas yr^{-1} in their catalogue is well-described by a log-normal distribution with mean 1.9 dex and standard deviation 0.61 dex. It is impossible to say whether these measurements give an optimistic or conservative characterization of fictitious quasar proper motions on the much shorter time baselines of our simulations. Additionally, the morphology of the host galaxy might lead to a statistical increase in the centroiding error, and photometric variability of the nucleus together with the stable photocentre of the host galaxy might lead to a similar effect as "variability-induced movers" in binaries (Wielen 1996). Physically all of these effects are expected to be random and therefore should only increase the dispersion of the results but not the median values themselves.

We use the statistical properties of the results by Titov et al. (2011) as basis for simulations, but apply a factor 10 to provide a conservative assumption on the total fictitious motion. The individual components of the proper motion are computed as

$$\mu_{\alpha*} = \mu \sin\theta, \quad \mu_\delta = \mu \cos\theta, \tag{2}$$

where θ is a random position angle and $\log_{10}\mu$ is taken from a normal distribution with mean value 2.9 dex and standard deviation 0.61 dex. The median value of the resulting μ is about 800 μas yr^{-1}. While this fictitious proper motion increases the RSE of the solution for the quasar subset, the agreement of median parallax between the quasars and the stellar subset remains at the previous level (see Table 1, experiment 2). This shows that significant fictitious proper motions due to photocentre variability do not harm the proposed strategy.

3.3. Contamination through misidentification

One potential problem with the use of quasars for the zero-point verification will be the identification of quasars in the Gaia observations. It is possible that a small fraction will be misclassified. Stars mistaken for quasars may have a noticeable parallax and proper motion which could contaminate the results obtained for the presumed quasar subset. To characterize the deterioration caused by misclassification we replace 5% of the quasars by stellar sources. We assume that misclassification will be most prevalent for faint sources where no good spectra exist, and obtain true position, parallaxes, and proper motions for contaminating stars from the Gaia Universe Model Snapshot (GUMS; Robin et al. 2012). We use the 7500 brightest stars fainter than magnitude 19. The results for experiment 3 in Table 1 present the combined evaluation of the quasar subset including the contaminating stars. Even with the contamination the median parallaxes of the quasar subset still agree to within a few μas with the values found for the other subsets.

4. Conclusions

We present a strategy to verify the parallax zero-point in a TGAS solution in the presence of basic angle variations. It uses quasars which however can be included in the solution only if prior information is applied. In the absence of accurate prior position information – available only for a small number of VLBI quasars –

we propose to constrain their proper motions. Simulations show that this allows us to recover the parallax zero-point in a solution with half a year of Gaia data to within a few μas. This is true even if the quasars exhibit considerable variability in their photocentres, provided the resulting fictitious proper motions are random from source to source. Furthermore, the scheme is robust to the quasar subset being contaminated by a significant fraction of stellar sources misclassified as quasars. In all cases the zero-point determined from the quasars agrees well with the theoretically expected parallax shift from the basic angle perturbations applied in the simulations.

Practical difficulties using quasars may arise from the colour calibration of the point spread function, which is based on stellar sources. Quasars however have very different spectra, which may require a separate calibration (U. Bastian, private communication). Whether this can be overcome in practice remains to be seen.

Acknowledgements. Uli Bastian, Anthony Brown, Jos de Bruijne, David Hobbs, Sergei Klioner, Timo Prusti, and an anonymous referee gave helpful comments on the draft manuscript, for which we are grateful. Thanks to Alexandre Andrei for providing the GIQC data and information about its content. This work was supported by the Gaia Data Processing and Analysis Consortium (DPAC) and uses the AGIS/AGISLab and GaiaTools software packages; special thanks to their maintainers and developers. We gratefully acknowledge financial support from the Swedish National Space Board, the Royal Physiographic Society in Lund, and from the European Space Agency (contract no. 4000108677/13/NL/CB). Quasar proper motion data were obtained through VizieR.

References

Abazajian K.N., Adelman-McCarthy J.K., Agüeros M.A., et al., Jun. 2009, ApJS, 182, 543
Andrei H., Antón S., Taris F., et al., Dec. 2014, In: Capitaine N. (ed.) Journées 2013 "Systèmes de référence spatio-temporels", 84–87
Bastian U., 1995, In: Perryman M.A.C., van Leeuwen F. (eds.) Future Possibilities for bstrometry in Space, vol. 379 of ESA Special Publication, 99
de Bruijne J.H.J., Sep. 2012, Ap&SS, 341, 31
Kovalevsky J., Jun. 2003, A&A, 404, 743
Lindegren L., December 2004, Scientific requirements for basic angle stability monitoring, Gaia Data Processing and Analysis Consortium (DPAC) technical note GAIALL057, `http://www.cosmos.esa.int/web/gaia/public-dpac-documents`
Lindegren L., Hog E., van Leeuwen F., et al., May 1992, A&A, 258, 18
Lindegren L., Lammers U., Hobbs D., et al., Feb. 2012, A&A, 538, A78
Michalik D., Lindegren L., Hobbs D., Lammers U., Nov. 2014, A&A, 571, A85
Michalik D., Lindegren L., Hobbs D., Feb. 2015a, A&A, 574, A115
Michalik D., Lindegren L., Hobbs D., Butkevich A.G., Jul. 2015b, ArXiv e-prints
Mignard F., October 2009, The Hundred Thousand Proper Motions Project, Gaia Data Processing and Analysis Consortium (DPAC) technical note GAIA-C3-TN-OCA-FM-040, `http://www.cosmos.esa.int/web/gaia/public-dpac-documents`
Mora A., Biermann M., Brown A.G.A., et al., Aug. 2014, vol. 9143 of Society of Photo-Optical Instrumentation Engineers (SPIE) Conference Series
Perryman M.A.C., de Boer K.S., Gilmore G., et al., Apr. 2001, A&A, 369, 339
Popović L.Č., Jovanović P., Stalevski M., et al., Feb. 2012, A&A, 538, A107
Porcas R.W., Oct. 2009, A&A, 505, L1
Robin A.C., Luri X., Reylé C., et al., Jul. 2012, A&A, 543, A100
Souchay J., Andrei A.H., Barache C., et al., Jan. 2012, A&A, 537, A99
Taris F., Souchay J., Andrei A.H., et al., Feb. 2011, A&A, 526, A25
Titov O., Lambert S.B., Gontier A.M., May 2011, A&A, 529, A91
Wielen R., Oct. 1996, A&A, 314, 679

Appendix

Appendix A: Conference posters

Poster 1: Combining and Comparing Astrometric Data from Different Epochs: A Case Study with Hipparcos and Nano-JASMINE

Presented 2011 at the *Astronomical Data Analysis Software and Systems* (ADASS) conference in Paris, France. For further details refer to Paper I and Sect. 4.1.

Poster 2: Improving distance estimates to nearby bright stars: Combining astrometric data from Hipparcos, Nano-JASMINE and Gaia

Presented 2012 at the General Assembly of the International Astronomical Union, Symposium 289, *Advancing the Physics of Cosmic Distances*, in Beijing, China. For further details refer to Paper II and Sect. 4.1.

Poster 3: Gaia astrometry for stars with too few observations

Presented 2014 at the ESA SRE *Science Workshop* in Volendam, the Netherlands. This poster presents an early stage of the work detailed in Paper V and Sect. 4.4.

Combining and comparing astrometric data from different epochs

A case study with Hipparcos and Nano-JASMINE

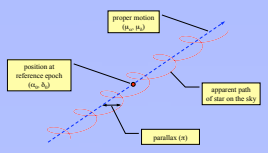

Introduction

Astrometry is the accurate determination of positions, distances (through parallaxes) and proper motions of stars. The data reduction of space based astrometry missions is done using a least-square solution to determine the stellar parameters from the observation data. In the future we will have access to several independent astrometric catalogues, produced by different space projects. Improved proper motions can be computed by comparing the positions in catalogues at different epochs.

Daniel Michalik[1], Lennart Lindegren[1], David Hobbs[1], Uwe Lammers[2] and Yoshiyuki Yamada[3]

[1] Lund Observatory, Lund University
[2] European Space Agency/ESAC
[3] Department of Physics, Kyoto University

E-mail: Daniel.Michalik@astro.lu.se

Theory

A natural extension of the least-squares approach is to make a **joint solution** of the data from two or more missions. This allows to obtain good results even when each data set alone is insufficient for an accurate reduction. We developed a method to combine information from different sets of astrometric data in a statistically optimal way by making a joint astrometric solution. This is now part of the Astrometric Global Iterative Solution which will be used for the data reduction of two upcoming space missions, Gaia and Nano-JASMINE. Solving for astrometric parameters is done by forming a set of normal equations from observation equations to which we can now add the normal equations of the older mission (e.g. from Hipparcos) before solving for the unknowns. This requires that both sets of data use the same reference epoch.

Conventional catalogue combination

In the conventional approach, catalogues are reduced independently and the combination is done a posteriori.

$$\left.\begin{array}{rcl} \boldsymbol{N}_1\boldsymbol{x} = \boldsymbol{b}_1 & \rightarrow & \boldsymbol{x}_1 \\ \boldsymbol{N}_2\boldsymbol{x} = \boldsymbol{b}_2 & \rightarrow & \boldsymbol{x}_2 \end{array}\right\} \Rightarrow \hat{\boldsymbol{x}}$$

Positions and parallaxes: $\sigma^{-2} = \sigma_1^{-2} + \sigma_2^{-2}$

Proper motions: $\sigma = \dfrac{\sqrt{\sigma^2_{position1} + \sigma^2_{position2}}}{\Delta T}$

Joint least-squares solution

In our proposed approach the normal equations from the two missions are combined before the solution:

$$(\boldsymbol{N}_1 + \boldsymbol{N}_2)\boldsymbol{x} = \boldsymbol{b}_1 + \boldsymbol{b}_2 \Rightarrow \hat{\boldsymbol{x}}_{\text{joint}}$$

Performs better by taking correlations between the parameters into account, see Results!

Hipparcos and Nano-JASMINE

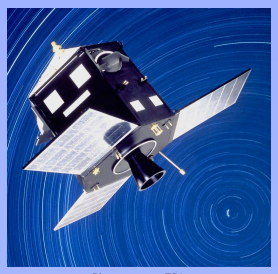

Picture courtesy ESA

The Hipparcos mission was launched by ESA in 1989 as the first space astrometry mission. It surveyed ~118,000 bright stars with ~1 mas accuracy. The catalogue is still the main source of fundamental data for stars in our neighbourhood. The accuracies (Robust Scatter Estimate) of the astrometric parameters of its fifteen thousand brightest stars are

$$\sigma_{position} \sim 0.6 \text{ mas}$$
$$\sigma_{parallax} \sim 0.8 \text{ mas}$$
$$\sigma_{proper\ motion} \sim 0.7 \text{ mas/yr}$$

Nano-JASMINE is the first space astrometry satellite mission in JAPAN and a technical demonstrator for the future JASMINE mission. It is scheduled for launch in November 2013. Simulations are based on the original version of its scanning law. For the fifteen thousand brightest Hipparcos stars we expect accuracies (RSE) of

$$\sigma_{position} \sim 2.5 \text{ mas}$$
$$\sigma_{parallax} \sim 3 \text{ mas}$$
$$\sigma_{proper\ motion} \sim 4.5 \text{ mas/yr}$$

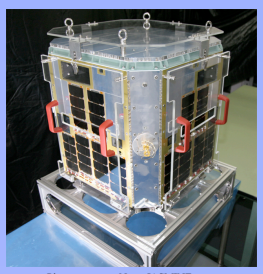

Picture courtesy Nano-JASMINE team

The epoch difference between Nano-JASMINE and Hipparcos is ΔT = 23.75 years. Combining the two data sets gives a big improvement of the proper motions and a significant improvement in position and parallaxes.

Simulations

Simulations are carried out using AGISLab, a software package aiding the development of algorithms for the data reduction of Gaia, developed at Lund Observatory.

Catalogues

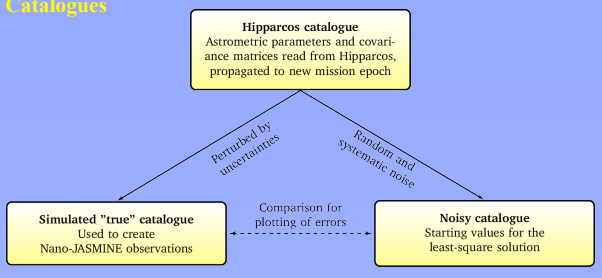

To simulate observations we need to know the true values of the astrometric parameters, which are of course not known. We therefore simulate a "true" catalogue by perturbing the Hipparcos catalogue with an error distribution $\boldsymbol{e}$ consistent with Hipparcos uncertainties. We use 5 Gaussian random variates $\boldsymbol{g}$ scaled by the square root $\boldsymbol{L}$ of the covariance matrix $\boldsymbol{C}$ to introduce the correct correlations between the errors $\boldsymbol{e}$ in each parameter.

$$\boldsymbol{C} = \boldsymbol{L}\boldsymbol{L}^T \quad \text{(Cholesky)}$$
$$\boldsymbol{e} = \boldsymbol{L}\boldsymbol{g}$$

$$\alpha = \alpha_0 + e_{\alpha\star} \sec\delta_0$$
$$\delta = \delta_0 + e_\delta$$
$$\pi = \pi_0 + e_\pi$$
$$\mu_{\alpha\star} = \mu_{\alpha\star 0} + e_{\mu_{\alpha\star}}$$
$$\mu_\delta = \mu_{\delta 0} + e_{\mu_\delta}$$

Reconstruction of the Hipparcos normal equations

N is taken as the covariance inverse: $\boldsymbol{N}_{\text{HIP}} = \boldsymbol{C}^{-1}$

$\boldsymbol{b}_{\text{HIP}}$ is chosen so that solving for Hipparcos only the update $\boldsymbol{x_d}$ would recover the original source values. The vector $\boldsymbol{x_d}$ is the difference between the original Hipparcos and the current noisy values.

$$\boldsymbol{b}_{\text{HIP}} = \boldsymbol{N}_{\text{HIP}}\boldsymbol{x_d} = \boldsymbol{N}_{\text{HIP}} \begin{pmatrix} (\alpha_o - \alpha_c)\cos\delta_o \\ \delta_o - \delta_c \\ \pi_o - \pi_c \\ \mu_{\alpha\star o} - \mu_{\alpha\star c} \\ \mu_{\delta o} - \mu_{\delta c} \end{pmatrix}$$

Results

The tables below show first results of simulation runs. As expected the combination of Hipparcos and Nano-JASMINE gives a great improvement in proper motions. Additionally we show that our proposed joint solution performs significantly better than the conventional catalogue combination method. This can be understood as follows.The astrometric parameters in the Hipparcos (or Nano-JASMINE) catalogue are not uncorrelated. The huge improvement of the proper motions therefore brings some improvement also to the other parameters, provided that the correlations are properly taken into account. This is the case for the joint solution, but not for the conventional combination.

The position values from Hipparcos have been propagated to the Nano-JASMINE mid-mission epoch J2015. Simulations of Nano-JASMINE are based on a conservative observation performance model and an optimal scanning law.

		Position @J2015 [mas]		Parallax [mas]	Proper motions [mas/year]	
		α	δ	π	$\mu_{\alpha\star}$	μ_δ
mag < 7.5 ~15 000 stars	Hipparcos only (Hip)	18.19	14.84	0.77	0.63	0.80
	Nano-JASMINE only (NJ)	2.56	2.54	4.65	4.50	3.05
	Conventional combination Hip + NJ	2.54	2.51	0.111	0.110	0.77
	Joint solution Hip + NJ	**2.41**	**2.4**	**0.108**	**0.105**	**0.75**
	Improvement of joint solution	5.2%	4.4%	3.2%	4.4%	3.5%
mag < 11.5 ~117 000 stars	Hipparcos only (Hip)	27.06	22.35	1.18	1.14	0.94
	Nano-JASMINE only (NJ)	4.57	4.53	5.43	8.38	8.02
	Conventional combination Hip + NJ	4.51	4.44	1.15	0.197	0.194
	Joint solution Hip + NJ	**4.43**	**4.26**	**1.11**	**0.188**	**0.185**
	Improvement of joint solution	1.8%	3.9%	4.0%	4.5%	4.5%

Lund Observatory

Design consultant: Helene Jönsson

Improving distances to nearby bright stars

Combining astrometric data from Hipparcos, Nano-JASMINE and Gaia

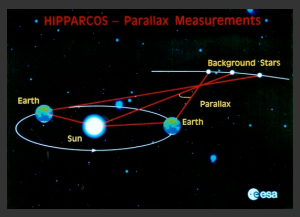

Introduction

The distance to a star can most directly be deduced from its trigonometric parallax. In the coming years Gaia will provide millions of stellar parallaxes of unprecedented accuracy. However, the brightest ~5000 stars (mag < 6) are not observed by Gaia, and for these Hipparcos will continue to be a main source of distance information. Stars brighter than 10th magnitude will however be re-observed with the Japanese Nano-JASMINE satellite, and we explore how the combination of data from all three missions (Hipparcos, Nano-JASMINE, Gaia) can lead to an overall improvement in trigonometric distance determination.

Authors

Daniel Michalik[1], Lennart Lindegren[1], David Hobbs[1], Uwe Lammers[2] and Yoshiyuki Yamada[3]

[1] Lund Observatory, Lund University
[2] European Space Agency/ESAC
[3] Department of Physics, Kyoto University

E-mail:
Daniel.Michalik@astro.lu.se

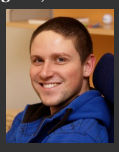

The idea

Nano-JASMINE and Gaia overlap in the magnitude range 6 to 10. The calibration of Nano-JASMINE's attitude and CCD is enhanced by processing its data together with preliminary Gaia results for the stars seen by both missions. This improves the astrometric results also for the bright stars observed only by Nano-JASMINE, tying them securely to Gaia's reference frame and parallax scale.

Combining with Hipparcos data gives additional improvements from the combined weight of the parallaxes and long temporal baseline between the missions. Optimum combination of data from different missions is discussed by Michalik et al. (2012, arXiv:1201.2849).

Nano-JASMINE

Nano-JASMINE is the first space astrometry mission in Japan and a technical demonstrator for the future missions in the JASMINE series. It is scheduled for launch in November 2013.

Picture courtesy Nano-JASMINE team

Hipparcos

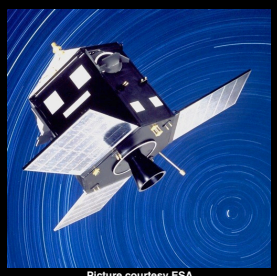

Picture courtesy ESA

The Hipparcos satellite was launched by ESA in 1989 as the first space astrometry mission. It surveyed ~118 000 bright stars with ~1 milli-arcsecond [mas] accuracy. The catalogue is still the main source of fundamental data for stars in the solar neighbourhood.

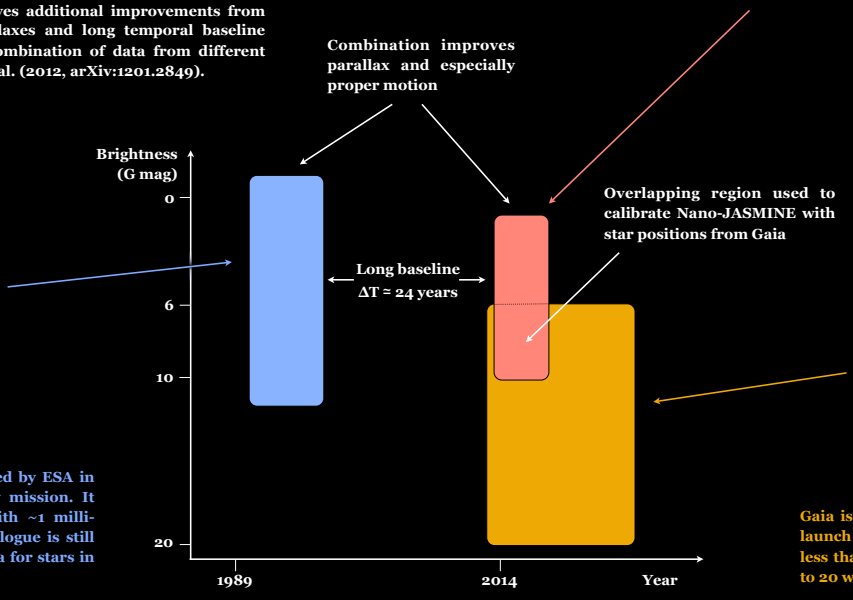

Gaia

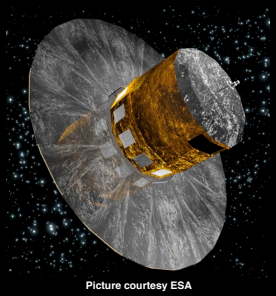

Picture courtesy ESA

Gaia is an ESA cornerstone mission due for launch in September 2013. It will observe not less than one billion stars from magnitude 6 to 20 with unprecedented accuracy.

Simulations

Simulations are carried out using AGISLab, a software package developed at Lund Observatory to aid the development of algorithms for the Gaia data processing. Nano-JASMINE simulations are based on the most realistic scanning law featuring a triangular spin axis precession motion. The observation accuracy model assumes a (somewhat optimistic) centroiding uncertainty of 1/300th of a pixel (~7 mas) for stars brighter than magnitude 7, with additional photon noise for fainter stars (~30 mas at magnitude 10).

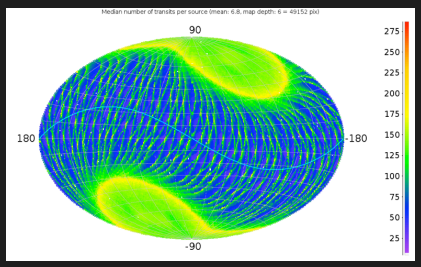

Number of observations per star (equatorial skymap), after simulating two years of the baseline Nano-JASMINE scanning law

In the simulation dataset there are 5026 bright Hipparcos stars (mag < 6) with their astrometric parameters and uncertainties taken from the Hipparcos catalogue. To this we add 330 000 randomly distributed stars of magnitude 10. For the latter we simulate the astrometric parameters with Gaia accuracy and fold the Gaia covariances into the Nano-JASMINE data processing.

Results

We compare four cases of the bright star astrometric uncertainties. Current knowledge is represented by the Hipparcos catalogue (HIP). The results of the Nano-JASMINE (NJ) observations alone are less precise, but combined with Hipparcos they give a significant improvement over current knowledge. Including provisional Gaia results brings a further improvement thanks to the enhanced calibration of the geometry and attitude of Nano-JASMINE.

Average uncertainties of 5026 Hipparcos stars between magnitude 1 and 6

	Parallax [μas]	Proper motion [μas/year]
Current knowledge (HIP)	740	673
NJ only	1282	1844
NJ + HIP	595	50
NJ + HIP + Gaia	**588**	**43**

Conclusions

Nano-JASMINE offers an opportunity to significantly improve the Hipparcos parallaxes and proper motions of the brightest 5000 stars which will not be observed by Gaia. A combined solution with Gaia data ensures that the results are on the same reference frame as the Gaia catalogue and that the parallaxes are absolute.

Lund Observatory

Design consultant: Helene Jönsson

Gaia astrometry for stars with too few observations

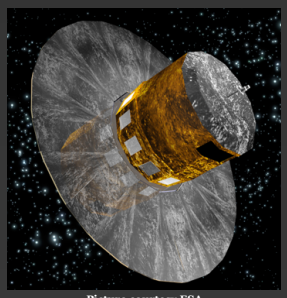

Picture courtesy ESA

Summary

The astrometric solution for Gaia needs to determine at least five parameters for each star, representing its position, parallax, and proper motion. This requires at least five distinct observations per star. In the early data reductions the number of observations may be insufficient, and even after the full mission there will be some stars (e.g. variables, supernovae) that could be under-observed.

We provide a general recipe to handle under-observed stars in the Gaia astrometric solution. It allows all five astrometric parameters to be determined with sensible formal error estimates. The recipe uses Bayes' rule to incorporate prior knowledge about the distribution of parallaxes and proper motions in the solution. The prior information is derived from the Gaia Universe Model Snapshot (GUMS, Robin et al. A&A 432, A100, 2012), which simulates the stellar content in the Milky Way as seen by Gaia.

Authors

Daniel Michalik, Lennart Lindegren, David Hobbs (Lund University, Sweden) and Uwe Lammers (ESA/ESAC)

Email: daniel.michalik@astro.lu.se

Experiment with different priors for one patch in the sky

The use of prior information on parallax and proper motion, when estimating the position, is illustrated by simulating a few scans across a small patch in the sky.

```
Equatorial coordinates (centre of patch): ( 45.00, +66.44) deg
Galactic coordinates:                     (135.29,  +6.71) deg
Radius of patch:                          1 deg
Magnitude range:                          15 ± 0.5 mag
Number of stars in GUMS:                  4406
90th percentile parallax/proper motion:   1.23 mas / 9.88 mas/yr
Observations within 3 months of Nominal Scanning Law:
- 2014 Aug 11, 00:47:27 UTC in preceding FoV at position angle 212.51 deg
- 2014 Aug 11, 02:34:06 UTC in following FoV at position angle 212.38 deg
- 2014 Sep 14, 00:14:59 UTC in preceding FoV at position angle 100.41 deg
- 2014 Sep 14, 02:01:38 UTC in following FoV at position angle 100.45 deg
```

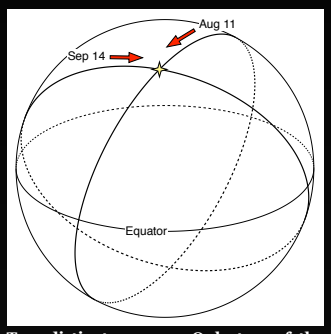

Two distinct scans ⇒ Only two of the five astrometric parameters can be determined, e.g. position (α, δ). Otherwise additional prior information is necessary.

Strong prior

$\sigma_\varpi = 0 \pm 0.01$ mas, $\sigma_\mu = 0 \pm 0.1$ mas/yr

Signifies the assumption of zero parallax and proper motion, essentially a position-only solution. The formal 90% confidence region (blue) grossly under-estimates the actual errors in position (red).

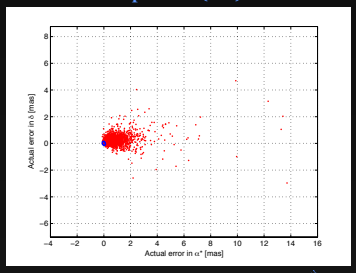

Intermediate prior

$\sigma_\varpi = 0 \pm 1.35$ mas, $\sigma_\mu = 0 \pm 13.5$ mas/yr

Value computed from equation (1) below. Signifies that parallaxes and proper motions are small but finite. The formal 90% confidence region (blue) contains ~95% of the actual errors in position (red).

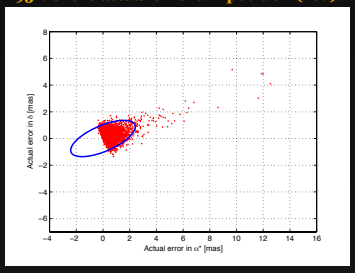

Weak prior

$\sigma_\varpi = 0 \pm 1$ arcsec, $\sigma_\mu = 0 \pm 10$ arcsec/yr

Signifies no constraint on parallax and proper motion. Results in a degenerate solution in this case, where not enough distinct observations are available.

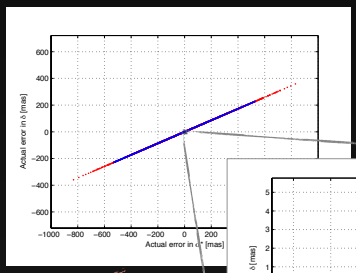

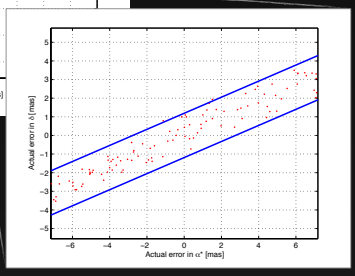

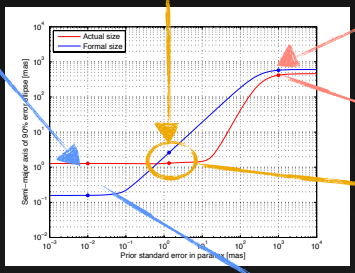

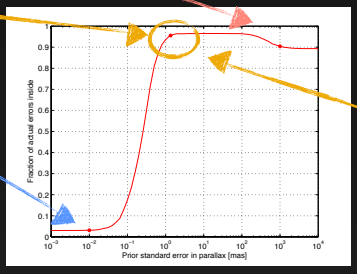

The intermediate prior provides a good astrometric solution with appropriate formal error estimates. The solution is robust to changes in the prior by a factor two. We can therefore use a Galactic model to estimate a suitable prior.

Reverend Bayes' stamp of approval

Estimating a suitable prior from a Galactic model

Empirically we find that a good parallax prior is the 90th percentile of the parallax values. Analysing GUMS we derive an approximation as an analytical function of magnitude and Galactic coordinate.

$$\log_{10}\varpi_{90}(G,\ell,b) = (+0.175 - 0.449\cos\ell\cos b + 0.119|\sin b|) + (-0.048 - 0.048\cos\ell\cos b - 0.016|\sin b|)\left(\frac{G-13}{5}\right) + (+0.526 + 0.159\cos\ell\cos b - 0.091|\sin b|)\left(\frac{G-13}{5}\right)^2. \quad (1)$$

The prior in annual proper motion is ten times the prior in parallax.

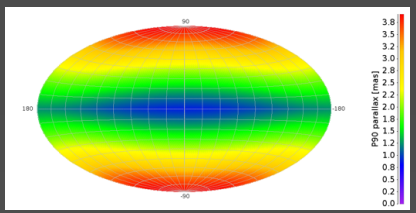

Estimated prior for magnitude 15. The all-sky map shows the dependency to the Galactic direction.

Global astrometric solution with prior

We successfully used this prior in a global astrometric solution based on six months of simulated Gaia observations. We were able to determine all five astrometric parameters with sensible formal errors, demonstrating that this scheme could indeed be used for the early Gaia data releases.

Design consultant: Helene Jönsson

Printed by Media-Tryck, Lund University 2015

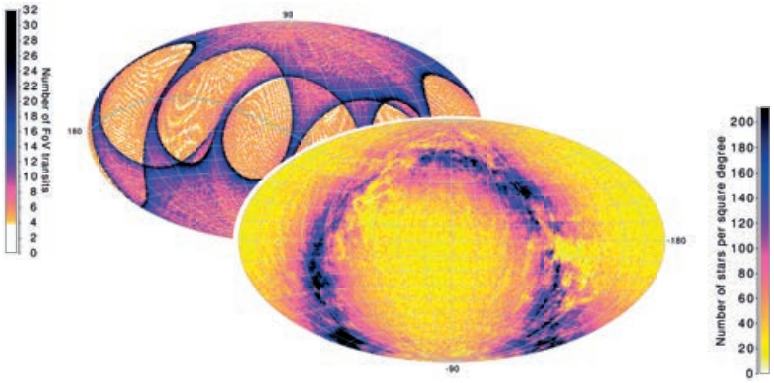

Tycho-Gaia and beyond describes the incorporation of prior knowledge in the data analysis of astrometry satellites, demonstrated through detailed simulations. The aim of the study is an improved understanding of Gaia data early in the mission.

Daniel Michalik studied computer science and astronomy at Friedrich-Alexander University Erlangen-Nuremberg in Germany. He has been part of the Gaia Data Processing and Analysis Consortium since 2009 and works on combining astrometry data from space missions.

LUND UNIVERSITY

Faculty of Science
Department of Astronomy
and Theoretical Physics

ISBN 978-91-7623-546-1